DOTTORATO DI RICERCA IN SCIENZE BIOMEDICHE

CICLO XXXV

COORDINATORE Prof. Chiti Fabrizio

Experimental studies in the colon of rodents

MORPHOLOGICAL AND FUNCTIONAL STUDY OF THE MICE AND RAT COLON AFTER EXPOSURE TO CHEMOTHERAPEUTICS OR PSYCHOSOCIAL STRESS AND TREATMENT WITH PREBIOTICS OR OTILONIUM BROMIDE

Settore Scientifico Disciplinare BIOS-13/A Istologia e Embriologia Umana

Dottoranda

Dott.ssa Cristina Biagioni

Supervisore

Prof.ssa Maria Giuliana Vannucchi

Coordinatore

Prof. Chiti Fabrizio

Anni 2019 – 2023

INDEX

ABSTRACT

GENERALITY

The digestive tract is formed by organs that are responsible for the collection of food, its mechanical and chemical reduction into absorbable molecules and the elimination of residual food waste. The director of the gut is the enteric nervous system (ENS). The ENS is a complex circuit that alone, together with the interstitial cells of Cajal (ICC) or in concert with extrinsic parasympathetic and sympathetic innervation controls not only bowel movements/motility but local blood flow, immune responses and transmucosal movement of fluids. Therefore, assaults to the ENS endanger gut health and normal physiology, prompting to severe GI comorbidities. The present doctoral thesis addresses two particular assaults to the gut and two possible helpers/strategies that can reduce the local damage. Both studies were conducted using rodents as animal models and colon was the main focus of the morphological and functional studies.

In particular the first study, conducted in mice, shows the effect of the chronic administration of the antimitotic and antibiotic agent, cisplatin, in combination with the administration of a diet enriched in non-digestible fibres (prebiotics) to sustain the resident microbiome.

The second study, conducted in rats, shows how a chronic psychosocial stress in an animal model causes colonic signs and symptoms similar to those of Irritable Bowel Syndrome (IBS) and how, the spasmolytic drug, Otilonium Bromide (OB), is able to counteract most of those effects.

RESEARCH STUDY 1 – EXTENDED ABSTRACT

Background. Cisplatin, an antimitotic agent, is known to cause both acute and chronic gastrointestinal side effects. Acute effects primarily consist in a mucositis, while chronic effects are due to neuropathy. Additionally, cisplatin has antibiotic properties that disrupt the microbiota, leading to dysbiosis, which intensifies inflammation and exacerbates local tissue damage. A strategy to protect the microbiota could potentially reduce the toxicity associated with chemotherapy. Furthermore, as a healthy microbiota may enhance the effectiveness of chemotherapeutic agents, prebiotics could also improve cisplatin's therapeutic outcomes.

Aim and methodology. In this study, we explored whether chronic cisplatin administration leads to morphological and functional changes in the proximal colon of mice, and whether a prebiotic-enriched diet could provide protective benefits.

Results. Our findings revealed that cisplatin administration resulted in poor weight gain, increased kaolin consumption, and reduced stool production and mucus secretion. Prebiotics effectively mitigated the increase in kaolin intake and the alterations in stool production and mucus secretion, although they did not impact weight gain. Moreover, cisplatin reduced the amplitude of spontaneous colonic muscle contractions and decreased Connexin (Cx)43 expression in ICC, changes that were partially prevented by prebiotic supplementation.

Conclusions. our study demonstrates that daily prebiotic administration, likely through the protection of the microbiota, prevents most cisplatin-induced colonic changes.

RESEARCH STUDY 2 - EXTENDED ABSTRACT

Background. Irritable Bowel Syndrome (IBS) is a prevalent gastrointestinal disorder primarily affecting the large intestine. Among its risk factors, psychosocial stress is the most recognized. The repeated water avoidance stress (rWAS) model is widely used to simulate psychosocial stress in animals and is considered an effective model for IBS. Otilonium bromide (OB), an orally administered medication, accumulates in the large bowel and effectively controls many IBS symptoms in humans. OB is known to have various mechanisms of action and multiple cellular targets.

Aim and methodology. In this study, we examined whether rWAS in rats induced morphological and functional changes in cholinergic neurotransmission in the distal colon, and whether OB could prevent these alterations.

Results. Our results showed that rWAS impairs cholinergic neurotransmission, leading to increased acid mucin secretion, heightened electrically evoked contractile responses (which were abolished by atropine), and an increased number of myenteric neurons expressing choline acetyltransferase. OB effectively countered these changes and exhibited an intrinsic antimuscarinic effect on postsynaptic muscular receptors.

Conclusions. We hypothesize that the alterations in the cholinergic system following rWAS are mediated by the activation of corticotrophin-releasing factor-1 (CRF1) receptors by the hypothalamic CRF hormone. OB appears to avoid this CRF/CRF1 activation, thus preventing the cascade of events responsible for the changes observed in the rWAS rat colon.

INTRODUCTION

1 THE LARGE BOWEL

1.1 ANATOMY

The digestive tract is formed by organs that are responsible for the collection of food, its mechanical and chemical reduction into absorbable molecules and the elimination of residual food waste. It can be represented as a long tube that starts from the oral cavity and ends with the rectus. It is anatomically divided in the oral cavity, part of the pharynx, oesophagus, stomach and intestine. At this tube are associated two fundamental full organs such as the liver with the gallbladder and the pancreas

The intestine differentiates in two parts, each of which is divided in portions:

- the small intestine: composed by duodenum, jejunum and ileum
- the large intestine: constituted by cecum, colon and rectum.

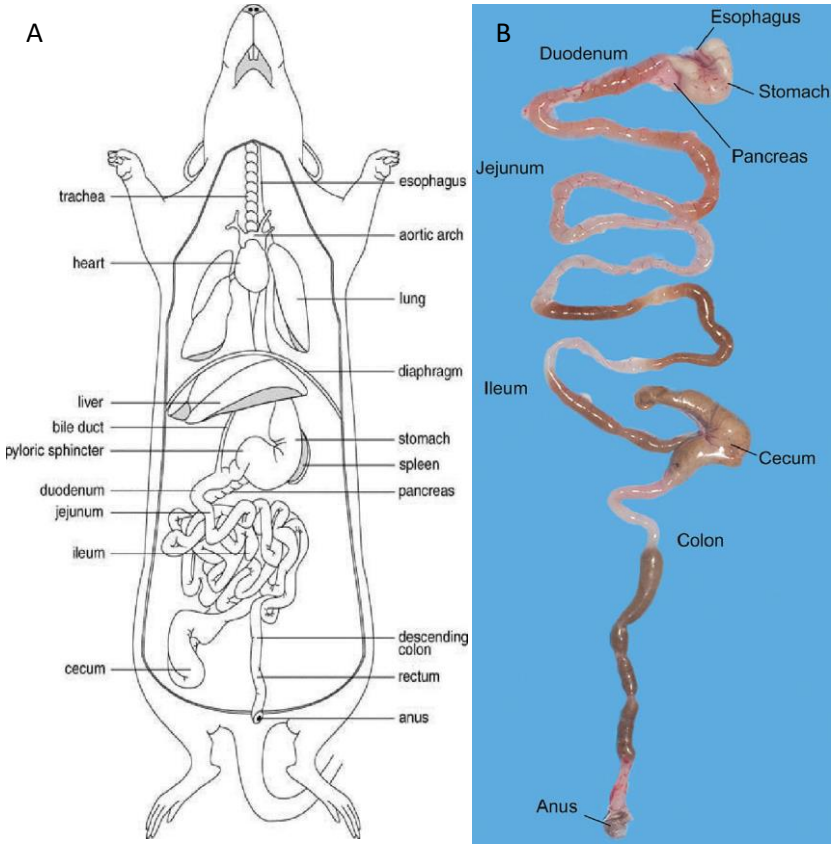

Figure 1. A) ***Scheme of rodent's gut****. B)* ***Photograph of the GI tract after removal of the mesentery****. The approximate regions of the GI tract are indicated. Modified from[1].*

The present research is focused on the study of the colon of two rodent species that are the most commonly used as models for gut investigations, rat and mouse. Presently, they are: male Wistar rats (*Rattus norvegicus albinus*) were used as a model for studying modifications caused by stress conditions; male C57BL/6JolaHsd mice (*Mus musculus*) were used as a model for studying the modifications of the colonic wall during chemotherapy. In both studies targeted drugs were tested.

As all the investigations were done in the colon, from now on, only the large intestine will be described.

The large intestine consists of the cecum, colon and rectum (Fig. 1). In mice the entire segment measures 10-12 centimetres (cm), while in rats it is up to 25 cm. The main function of the large intestine is to receive, from the small intestine, a bolus that contains undigestible substances but also water and electrolytes. The large intestine absorbs water, electrolytes (like sodium) and other small molecules, and leaves the waste products forming the faeces that pass through the rectum and are expelled from the anus. The total transit time is between 6 and 7 hours (h)[2]. Since these two rodents are omnivores, with a diet rich in plants, and the digestive enzymes of mammals are not able to digest the walls of plant cells, the latter require a fermentation that occurs in the cecum. In fact, the cecum functions as a microbial fermentation sac. Note that the cecum represents about a third of the large intestine in both mice (that is 3-4 cm long) and rats (i.e. 3-7 cm long)[3]. Microorganisms living in the cecum perform the first digestion of plant fibres, splitting them into smaller nutrients (e.g. vitamins) that can be absorbed as they move through the colon. In addition, these microorganisms, thanks to their metabolic activity, independently produce vitamins and other nutrients that are beneficial to the host. The location and shape of the cecum may vary, depending on the species; in mice it is localized in the right part [4] (Fig.1), caudal to the stomach greater curvature, filling the space between the stomach and liver lobes cranially and the reproductive organs caudally. In rats, cecum has a more variable topographical arrangement, lying either ventrolateral to the right or midventral, filling up the ventral abdominal space from the liver cranially to the mid-lower fourth of the abdomen. The mouse cecum is kidney-shaped and bent or curved onto itself (flexura) while the rat cecum has the form of a comma. The entry of the ileum in the colon is located in the *ampulla ceci*, i.e. in the ileal-cecum junction. In both rodents the entry of the ileum is dorsal and covered by the cecum; the colon starts ventrally and has a conical

shape, with the tip corresponding to the origin of the ascending colon, at the cecocolic junction[5]. The colon in adult rats is approximately 20 cm long, while adult mice colon is up to 6 cm[6]. The colon is divided into three sections: ascending, transverse and descending, separated by two tube direction changes or flexures. Their vascularization distinguishes the three parts mentioned above. In fact, the cranial mesenteric artery vascularises the ascending colon, the caudal mesenteric artery vascularises the descending colon and both arteries reach the transverse colon, which is located in front of the root of the mesentery. The ascending colon is in continuity with the cecum therefore, it is in the same part of the abdominal cavity, then the transverse colon crosses the cavity from one half to the other (from left to right or vice versa, depending on the species), in front of the cranial mesenteric artery; the descending colon begins at the abdominal roof and advances caudally to enter the pelvic cavity where it continues with the rectum. The rectum runs dorsally in the pelvis along the median sagittal plane to the anus, located at the root of the tail.

The entire gut structure is very movable in the abdominal cavity and hangs together via the *radix mesenterii*. This radix itself is bound to the dorsal abdominal wall in the upper abdominal area under the stomach. The greater portion of the small intestine and proximal and transverse portions of the colon are attached to the radix, while the descending colon is attached to the dorsal wall by a separate mesentery. The extensions of the *radix mesenteri* runs along the end of the ileum, on one side, onto the cecum and down to the apex, carrying the vessels. On the other side of the ileum, the mesentery stretches out over the *ampulla ceci* onto the proximal colon. Thanks to this support, the cecum is free to move.

The ascending colon absorbs the remaining water in the intestinal contents so that the waste begins to consolidate, becoming faecal balls in the transverse colon. Rats and mice excrete a single type of faeces in the form of faecal pellets that they eat in part, either their own or that of another individual, taken from the ground.

During the embryogenesis, between day 9 and day 11 and 1/2 of gestation, the primitive intestine is formed [7]. It is a small tube that goes from the oropharyngeal membrane to the cloacal membrane and is divided into three portions; the anterior, middle and posterior intestine.

1.2 HISTOLOGY

The colonic wall is made up of four layers: the serosa, the *tunica muscularis*; the submucosa and the mucosa (Fig. 2). The latter two are separated by a thin layer of smooth muscle cell called *muscularis mucosa*. All layers are innervated by the enteric nervous system (ENS) that controls absorption, secretions and motility of the intestine independently from the central nervous system (CNS). Defecation is the only exception, in fact, the defecation centres are located in the lumbosacral spinal cord thus under the control of the CNS[8].

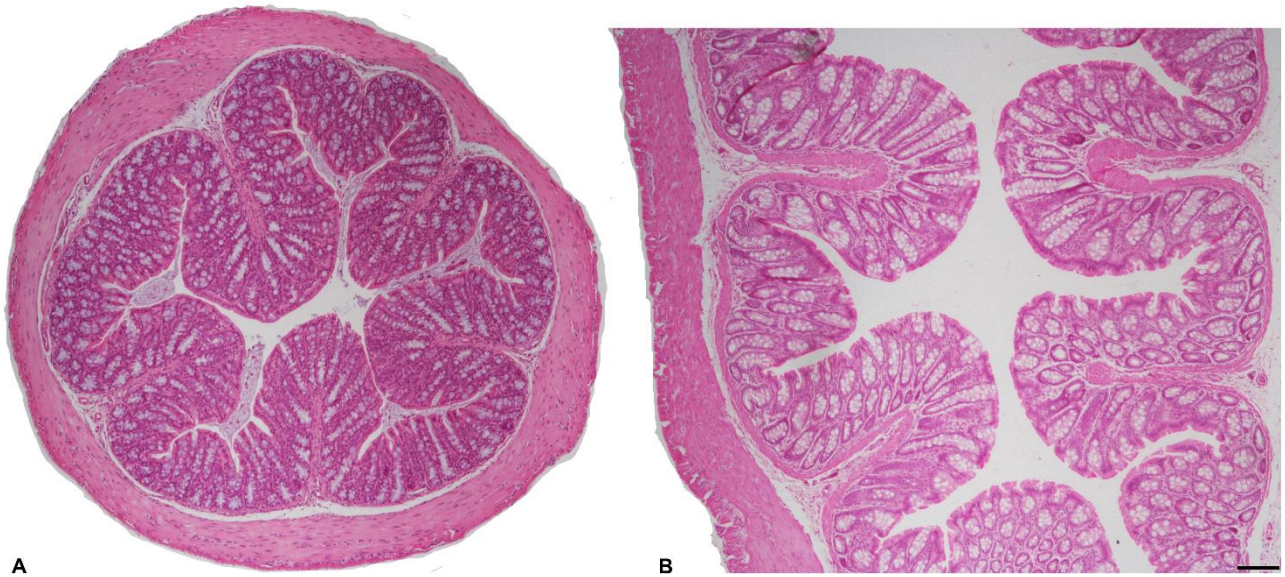

***Figure 2**. Paraffin embedded section stained with Haematoxylin & Eosin (A) Section of mouse ascending colon; (B)Section of rat descending colon (4x). Bar=200µm.*

The *serosa*, continuous with the peritoneum in the abdominal cavity, is made up of a simple squamous epithelium, the mesothelium. It functions as an organ envelope and secretes aqueous fluid, filtered from the blood, to lubricate the surface of the organs, preventing friction between them. The serosa derives from the mesoderm and surrounds the *tunica muscularis*.

The *tunica muscularis* is composed by two layers of smooth muscle cells (SMCs) called circular and longitudinal muscle layers. The outer longitudinal layer is thinner than the inner circular layer, they are both derived from the splanchnic mesoderm surrounding the primitive gut and forming two different layers of SMCs with longitudinal or circumferential orientation in response to mechanical forces. This proper alignment of muscle layers is crucial for normal function as this *tunica* is the engine of the gut that with its

relaxation and subsequent contraction, permits food and dross storage, mixture and progression. The SMCs have an elongated shape with tapered ends. In the intestine, SMCs have actin and myosin proteins but, at variance with skeletal muscle fibres, do not present sarcomeres or striations, this explains their homogenous staining with eosin of the cytoplasm. The nucleus is located at the centre of the cell and, in longitudinal section, if the cell is contracted, the nucleus has a corkscrew shape, while in non-contracted cells it appears as an elongated structure with tapered ends. In transversal section the nucleus appears circular and, when the section is made at one of the ends of the cell, no nuclei are visible. SMCs are interlinked by gap junctions (GJs) through which ions and small molecule can pass from one cell to another, ensuring the communications that regulate the contraction of the entire bundle or layer. GJs connect also the *interstitial cells of Cajal* (ICCs) to the SMCs. ICCs are the pacemaker cells of the tunica and, with their spontaneous depolarization, they allow the maintenance of the spontaneous contraction of the muscle wall. The contraction is initiated by depolarization of an ICC and the subsequent depolarization, via GJs, of an SMC membrane followed by the opening of calcium channels that increase of calcium ions (Ca^{2+}) in the cytoplasm(i) with the activation of the Ca^{2+}-calmodulin-myosin system. There are two major mechanisms by which $[Ca^{2+}]_i$ is raised in smooth muscle: (1) entry of Ca^{2+} from the extracellular space, and (2) release of Ca^{2+} from intracellular stores. Influx of extracellular Ca2+ is mediated by ion channels in the plasmalemma, the most prominent of which are the voltage-dependent Ca2+ channels (VDCC). Other important pathways for extracellular Ca2+ entry in SMCs are nonselective cation channels, such as transient receptor potential (TRP) channels and ionotropic purinergic (P2X) receptors. Many intracellular organelles take up and release Ca^{2+} but the biggest store of this ion is the sarcoplasmic reticulum. This organelle releases Ca^{2+} in the cytoplasm in response to ryanodine receptors (RyR) and inositol trisphosphate receptors (IP3Rs) stimuli[9,10].

The *tunica muscularis* contains the myenteric plexus or Auerbach plexus. This plexus is situated between the circular and the longitudinal muscular layer and it is part of the ENS, (further explanations can be found in chapter 2).

The *submucosa* adheres to the *tunica muscularis* and it is a loose connective tissue rich of blood vessels, numerous cells and nerve fibre. It supports the mucosal layer and contains the second component of the ENS: the submucosal plexus or Meissner plexus (an in-depth analysis is described in chapter 2). The vessels

of the submucosal layer send branches to the mucosa. In this layer, different stromal cells hold the ganglia structure together. The extended nervous net in the submucosal layer includes visceral sensitive fibres, mostly of sympathetic origin, parasympathetic ganglia, parasympathetic preganglionic and postganglionic nerve fibres.

The *muscularis mucosae* surrounds the mucosa and it is made up of a few rows of smooth muscle cells, disposed parallel and transversally to the colon major axis. The contraction of the *muscularis mucosae* produces the movement of the mucosa forming folds and depressions that facilitate absorption and secretion. Mucosal movements are independent from the peristalsis. This muscle layer is a bit more prominent in rats than it is in mice and, in both species, it separates the submucosa from the lamina propria of the mucosa.

The *mucosa* is made by the lamina propria, and, on the luminal side, by a simple cylindrical epithelium formed by enterocytes alternate with goblet cells. The epithelium gives rise to highly repetitive invaginations, which represent the basic functional units of the large intestine and they are called colonic crypts or crypts of Lieberkühn.

The Lieberkühn crypts are simple tubular glands that extend from the *muscularis mucosae* and open in the luminal surface of the intestine. These glands consist of a simple columnar epithelium in continuity with the colonic epithelium.

The *lamina propria* adheres to the *muscularis mucosae*, surrounds the intestinal glands and it is formed by loose connective tissue containing: a peri-cryptal cellular sheath, the gut-associated lymphoid tissue (GALT) and small lymphatic vasa at the gland basis. The loose connective tissue contains also elastin fibres, collagen and proteoglycans to help the carrying of electrolytes from the intracellular compartment of the epithelium to the absorbing fenestrated venous capillaries. The GALT is represented by diffuse lymphatic tissue and lymphatic nodules. The cells are lymphocytes, macrophages, mastocytes, plasma cells and eosinophil granulocytes. The GALT works as an integrated immunologic barrier that protects against pathogens and other antigens that could enter from the intestinal lumen through the mucosa. The colonic GALT extends also to the submucosal layer and aggregates in greater nodules called Payer patches generally localised at the opposite side of the mesentery insertion.

The *colonic epithelium* contains several different cell types that are located in the Lieberkühn crypts or in the surfaces of the colonic epithelium. These cell types are:

1. Enterocytes (also named colonocytes[11]), which are columnar absorbing cells that take up electrolytes and water.
2. Goblet cells are unicellular glands that release mucus and they alternate between enterocytes.
3. Paneth cells that have the function of maintaining the innate immune system, releasing bactericide substances (they are very few).
4. Enteroendocrine cells that release endocrine and paracrine hormones.
5. M cells that are specialized cells on the epithelium which covers the lymphatic nodules of the lamina propria.
6. Staminal cells, located in the deepest part of the crypts.

In the epithelium, several types of junctional complexes join enterocytes, goblet cells, enteroendocrine cells and other types of cells to one another.

Enterocytes are tall columnar cells with the nucleus at the base. On the apical surface there is a striated border formed by microvilli that increase the absorptive surface by 600 times. Enterocytes absorb electrolytes and water from the dross. These cells are bound one another by tight junctions to avoid unselective absorption, as solutes can pass through the barrier only by active transport (that will be described in 1.3). The lateral membrane of enterocytes has folds that increase the membrane surface area and contains transport enzymes. These folds reduce during active absorption, increasing the intracellular compartment. Mitochondria inside the enterocyte give the energy for the transport and they are concentrated in the apical cytoplasm between the terminal web and the nucleus, while the tubules and cisterns of the smooth endoplasmic reticulum are located in the apical cytoplasm under the terminal web and allow the absorption of fatty acids and glycerol[12]. Enterocytes have a high turnover rate, living only five days, and their progenitors come from the intestinal stem cells. The stem cells are located at the base of the crypts and they present the surface marker leucine-rich repeat-containing G protein-coupled receptor 5 (LGR5+) and CD44+. LGR5+ cells fuel the constant replenishment of the intestinal epithelium migrating from the bottom to the top of the crypt during their differentiation. LGR5+ cells generate not only enterocytes but also goblet cells or enteroendocrine cells. LGR5+ cells are very sensitive to insults such as irradiation and chemotherapeutic agents. Depletion of LGR5+ cells after such an insult blocks regeneration[13]. At the end of their life cycle,

mature cells are shed from the tip of the crypt into the lumen between two glands for disposal[11,14]. Goblet cells live around 6 days, while enteroendocrine cells live about 4 weeks.

Goblet cells are unicellular glands and produce and release the intestinal lubricant, called mucus[12]. In conventional histological preparations the water-soluble mucinogen is lost and the cellular vesicles appear empty. The name "goblet" is due to its form as the apex of the cell contains a large accumulation of mucin vesicles surrounded by a cup of an extensive set flattened Golgi cisternae. The basal portion resembles a thin stem and it is intensely basophilic as it is occupied by a heterochromatic nucleus, a rough endoplasmic reticulum (RER) and free ribosomes. The goblet cells form few microvilli at the thin rhyme of the upper portion (the theca); microvilli are more visible in immature goblet cells situated in the bottom of the Lieberkühn crypt.

Paneth cells are in small number in a healthy colon. They are located at the base of the glands, and have a basophilic cytoplasm, a supranuclear Golgi apparatus and large, refractory and intensely acidophilic apical secretory vesicles. These vesicles contain antimicrobial enzymes, like lysozyme and α-defensins, and also other glycoproteins among which a protein rich in arginine and zinc. These cells help with the maintenance of the intestinal microflora.

Enteroendocrine cells secrete their products in the *lamina propria* and in the underlying blood vessels. There are two different types of enteroendocrine cells in the gut. Most of them are "closed" endocrine cells as they are small and lean on the basal lamina without reaching the intestinal lumen; some of them are "open" enteroendocrine cells as they have a small cytoplasmatic extension exposed to the lumen. The "open" ones have a primary chemoreceptor function as they test the lumen content and release hormones depending on the information obtained from these samplings. Unfortunately, the enteroendocrine cells are difficult to observe with haematoxylin and eosin staining as their cytoplasm appears clear due to a lack of sufficient sustainable material. The enteroendocrine cells can be distinguished through immunohistochemical staining for the hormones they produce: histamine, somatostatin or neuroendocrine-acting hormones like the vasoactive intestinal peptide (VIP). Another way to distinguish them is through the transmission electron microscope (TEM) based on their shape, dimension and density of their secretory vesicles.

The M cells cover the Payer patches and the greater lymphatic nodules and they are antigen presenting cells. Each cell develops a deep pocket-like recess connected to the extracellular space where dendritic cells, macrophages, B and T lymphocytes are located. The apical membrane presents microfolds and a smooth layer of glycocalyx with abundance of glycoprotein 2 (Gp2) receptors that bind Gram-negative bacteria (like *Escherichia coli*). The substrates bound to Gp2 receptor are incorporated in endocytosis vesicles and transported to the basolateral membrane of the alcove with pocket form. The content of vesicles is released inside the pocket and transferred to the immune cells that are in that space. With this system, antigens from the intestinal lumen are conveyed intact to the epithelial barrier.

1.3 FUNCTIONS

There are 3 primary functions of the large bowel. The main is to absorb water and electrolytes from undigested food, the second is to produce and absorb vitamins and the third is to form, collect and propel faeces toward the rectum to be expelled[15]. Dross progression is due to the contraction of the smooth muscle cells of the circular and the longitudinal muscular layers, while the mucus functions as lubricant to avoid friction between dross and mucosa.

Absorption

Enterocytes (Fig. 3[16,17]) use osmosis to collect water: sodium (Na^+) in the lumen is absorbed through electroneutral NaCl transport, mediated by epithelial sodium channels (ENaC)[18] and by members of the SLC9 family (NH2, NH3 and NH8) that exchange Na^+/H^+ and act in parallel with SCL26A6 a Cl^-/HCO_3^- exchanger[19], both situated in the apical membrane[20]. On the lateral membrane the Na^+/K^+ ATPase pumps transport Na^+ in the extracellular matrix under the tight junctions (that are situated in the lateral membrane close to the intestinal lumen). The high Na^+ concentration in the intercellular space, pulls water (H_2O) from the cytoplasm to the intercellular space, the cytoplasmic Na^+ and H_2O concentration drops, taking H_2O and Na^+ inside the cell from the intestinal lumen (apical surface). There is an increase in osmolarity in the intracellular space that pumps H_2O and Na^+ through the basal lamina to the connective tissue.

Through this mechanism the indigested food material is deprived of the remaining water in ascending colon and the dross is solidified to form stool. The descending colon is a faeces storage until the sigmoid colon

contracts to increase the pressure inside the colon, so stool moves to the rectum. Finally, elimination occurs through the rectum by defecation[18]. The neuronal regulation of this mechanisms will be described in chapter 2.

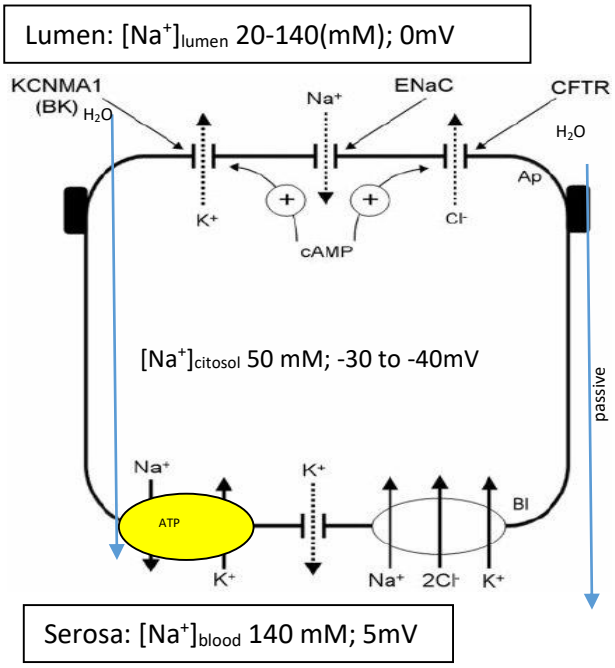

Figure 3. Cell model of an enterocyte (colonocyte) showing apical (Ap) localization of KCNMA (BK) channels (Ca(2+)-activated K(Ca)1.1 (BK, KCNMA) channel, that is the luminal secretory K(+) channel, with large conductance, and is the only functionally relevant luminal K(+) efflux pathway in mouse distal colon[15], cystic fibrosis transmembrane conductance regulator channel (CFTR) that allow Cl- colonic secretion and Na + channels (ENaC). The different Na+ concentration in the cell and the electric potential of -30/–40 mV, provides an electric, as well as a chemical, driving force that induces Na+ entry into the cell from either side of the cell. The Na+/K+ ATPase (sodium pump) on the basolateral membrane is essential for maintaining the electrochemical profile. The process induces an increase in osmolarity so water and solutes are pushed to cross the epithelium either around the cell (paracellular) or through the cell (transcellular). [Modified from[16]]

Motility

The colonic motility is necessary for absorption and transit of dross and subsequently for transit of faeces. It is mediated by the coordination among myogenic, neurogenic and chemical or mechanical stimuli[21]. In mammals, the coordination among them defines two distinct motor patterns that permit the formation and propulsion of faecal pellets (Fig. 4):

1) Spontaneous contraction (or slow phasic contractions) mediated by the pacemaker cells ICCs that depolarize artlessly changing the voltage of the adjacent SMCs through gap junctions, these movement appears as a slow wave. This type of contraction is not blocked by tetrodotoxin (TTX).
2) Colonic motor complexes (CMCs) or colonic migrating motor complexes (CMMCs), which regularly sweep the entire colon to initiate bouts of propulsion. CMCs and CMMCs are abolished by TTX, so they are under neuronal regulation. In mice colon, Costa M et al[21] registered three distinct neurally dependent motor patterns underlying formation and propulsion of faecal pellets, like herbivores:

   i) the proximal colonic separation of pellet-shaped boluses at the ceco-colonic junction by circular muscle contraction and slow propulsion of the newly formed boluses in the proximal colon;

   ii) complete CMMCs regularly sweeping the entire colon to initiate bouts of propulsion;

   iii) faster self-sustaining distal colonic propulsion, which reassemble the peristaltic movement.

   CMMCs are predominantly driven by two neurotransmitters: acetylcholine (Ach) and tachykinins (TK)[22–24].These neurotransmitters act directly on SMCs and indirectly through the ICCs network (the pacemaker cells of the gut, more details are discussed in chapter 2.3) in particular CMMCs is governed by neural stimulation of ICC of the myenteric ganglionated plexus (ICC-MP)[25].

Without these neurochemical stimuli, the muscular apparatus alone is not able to produce effective propulsive contractions. Thanks to the spontaneous depolarization of the ICCs, the SMCs also depolarize inducing spontaneous contractions of the *tunica muscularis*. SMCs membrane potential oscillations (slow waves) is driven by a syncytial network of ICCs that communicate with these SMCs via GJs. These junctions will be better described in chapter 3. The tunica is kept relaxed due to a permanent inhibitory influence, mediated by the inhibitory neurotransmitter nitric oxide (NO) released aboral by descending inhibitory fibres. NO acts on the NO-sensitive guanylyl cyclase (NO-GC) present in both ICCs and SMCs, as reported by Beck

and others [26]. NO regulates smooth muscle tone and slow phasic contractions. Keeping the aboral smooth muscle relaxed allows the proceeding of faeces as it counteracts the excitatory impulse given by Ach and TK. CMMCs start in the cecum and propagate to the proximal colon and can be complete or incomplete: there is an initial propulsion by an incomplete CMMC in the proximal colon, that pushes the content in the transverse colon, then it stops, and another incomplete CMMC starts in the proximal colon. When the pellet reaches the transition zone, propulsion becomes continuous to empty the proximal colon. A complete CMMC occurs in the final propulsive period and is triggered by a CMMC starting quasi simultaneously in the proximal colon and at the colonic transition zone. The generation of CMMC is determined by excitatory and inhibitory nerve fibers, and is blocked by TTX.

Other chemicals that are present in murine enteric neurons are calbindin, calcitonin gene related peptide (CGRP), calretinin, gamma-aminobutyric acid (GABA), 5-hydroxytryptamine (5-HT), neuropeptide Y (NPY) and vasoactive intestinal peptide (VIP). Further explanations about these neurotransmitters can be found in chapter 2.2.

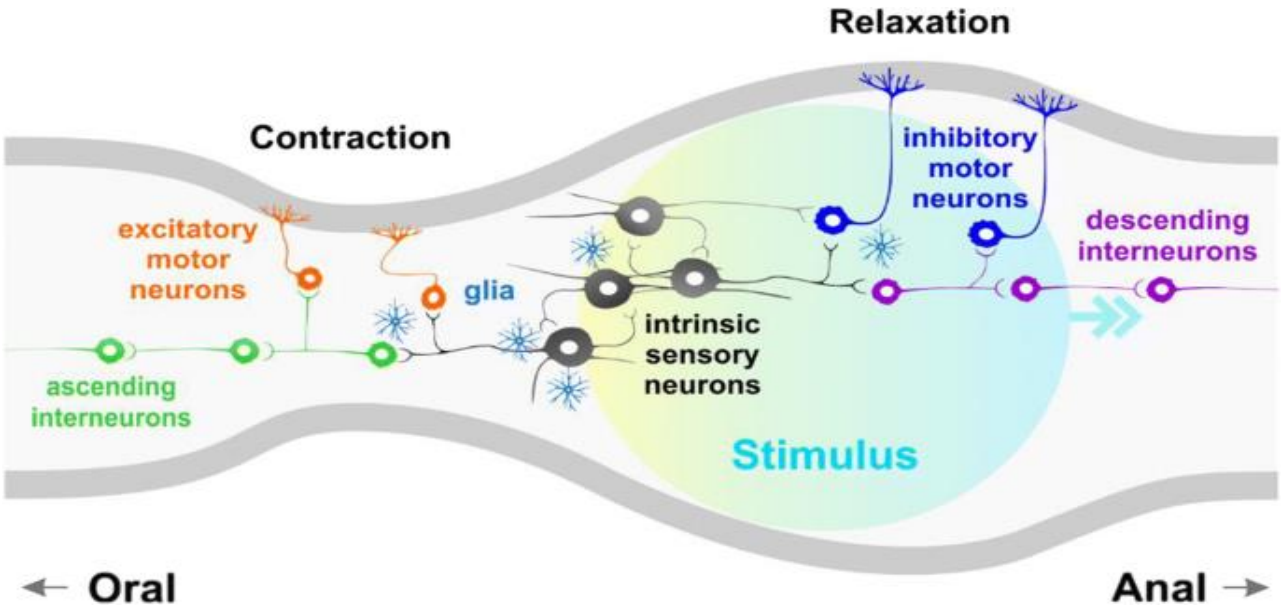

Figure 4. Schematic representation of the enteric circuitry underlying the peristaltic reflex. Intrinsic sensory neurons synapse with ascending and descending interneurons that form chains along the length of the intestine, as well as excitatory and inhibitory motor neurons. Interneurons also innervate motor neurons which in turn supply the circular and longitudinal muscle (musculature represented by grey lines; note that different muscle layers and their innervation are not defined). Upon detection of a luminal stimulus, the activation of ascending interneurons connected to excitatory motor neurons evoke a contraction orally, while the activation of descending interneurons connected to inhibitory motor neurons elicit a relaxation anally to propel the contents along. Enteric glia also plays an active role in regulating intestinal motility Adapted from[27]

2 THE ENTERIC NERVOUS SYSTEM

An autonomous nervous system called enteric nervous system (ENS) drives the neurogenic control of motility. This ENS, (recently reviewed by Spencer NJ and coll.[28]) is made of small ganglia that are continuous to each other through nerve strands. They form two different plexuses in different sites: the myenteric or Auerbach plexus located in between the longitudinal and circular muscle layer and the submucosal or Meissner plexus, located in the submucosa, proximally to the circular muscle.

The Auerbach plexus is made by ganglia containing neurons and supporting glial cells forming, along the entire gastrointestinal tract, a continuous network by interganglionic strands. The neurons are either excitatory, inhibitory or interneurons whose processes connect with other neurons. They innervate the ICCs and the SMCs to coordinate muscle movements underlying the propulsion of content. The Meissner plexus presents smaller ganglia and finer interconnecting strands [29] that are broadly involved in secretion and absorption.

The ENS is connected with the CNS by parasympathetic fibres. Fibres originate from the vagus nerve and enter through the mesentery in the intestine wall forming synapses with the neuronal cells of both plexuses. The sympathetic post synaptic nerve fibres also contribute to the ENS [12].

Embryologically, the ENS is derived from neural crest cells. The cells are mostly of vagal origin and migrate through the paraxial mesoderm to the digestive tract. From this point, they migrate in a rostrocaudal direction and end up colonizing almost the entire gut.

2.1 NEURONAL AND GLIAL CELL POPULATIONS

Dogiel, a Russian histologist, was the first author who described the morphology of the myenteric neurons, classifying them into three main groups: Dogiel types I, II, III [30]. Dogiel type I and II (Fig. 5) are the most common in many species of mammals, the type III is less common. All these neurons can be classified as multipolar neurons displaying one (long or short) axon and several dendrites.

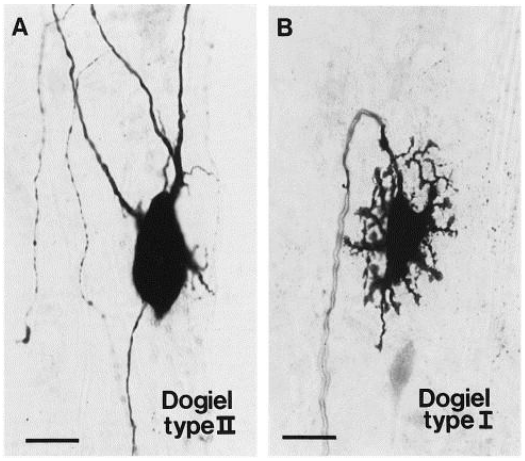

Figure 5. Dogiel type II and Dogiel type I neurons (B and A). (B) Dogiel type I neurons are characterized by many short and a single long procesess, whereas Dogiel type II (A) presents multipolar conformation with many long, smooth processes. Adapted from Clerc et al. [31]

Dogiel *type I* neurons (Fig. 5B) have a stellar shape body with one axon and up to twenty short dendrites with broad or lamellar endings. Their axons run through the adjacent ganglia and occasionally into the muscle coat. They are mechanosensitive interneurons and receive fast synaptic inputs; they also present fine processes in the circular muscle.

Dogiel *type II* neurons (Fig. 5A) have one axon and rarely more than ten dendrites. They are the primary afferent neurones and have large cell somas. Their multipolar processes ramify extensively within the plexuses. They have projections into the mucosa, in the muscle wall and, circumferentially or aborally, along the intestine. Mechanosensation might be a ubiquitous property of Dogiel type II neurons in the ENS of different species.

Dogiel *type III* neurons have one axon and 10 or more dendrites that are longer than those of Dogiel *type I* neurons. Their dendrides are ramified and differ also from *type II* neurons as they have tapering endings within the ganglion of origin, which is absent in *type II*.

Nurgali and coll.[32] described the morphology and the electrophysiological properties of neurons in mice observing cells with large, round or oval shape with several long processes that conform with Dogiel *type II* neurons morphology. This research group described also nerve cells with irregular lamellar dendrites corresponding to Dogiel *type I* neurons. Based on neuronal projection, they identified four types of neurons as building blocks of ganglia. The first three types are uniaxonal in mice with a Dogiel *type I* morphology:

1) **circular muscle motor neurons** that innervate the circular muscle with branches 50–200 μm wide, so one neuron may supply many muscle cells. Nurgali's group named these neurons as S neurons. S neurons are named thanks to their electrophysiological analysis. They show a monophasic action potential, the after hyperpolarizing potential (AHP) is not slow. No slow AHP means that the refractory period is short and they respond with fast excitatory postsynaptic potentials (EPSPs) to stimulation of presynaptic inputs.
2) **longitudinal muscle motor neurons**, which innervate the longitudinal muscle, have S-type electrophysiological properties and are traced to a plexus of nerve fibres that lies at the inner surface of this muscle layer and are called the tertiary component of the myenteric plexus.
3) **interneurons**: whose processes ran almost directly orally or anally for long distances before supplying innervation of other neurons, especially in the colon, these neurons traversed more than one or two ganglia, with no long circumferential projections in the plexus; some of them provide branches within myenteric ganglia. Depending on their direction they are defined as ascending or descending interneurons.

   In the mouse distal colon, the majority of the uniaxonal neurons had fast EPSPs, whose amplitude was substantially reduced or blocked by nAChR blockers in all S neurons, while purine receptor blocker PPADS could only reduce fast EPSPs amplitude but not block them. These findings suggested that ACh is the major fast neurotransmitter in synapses of the myenteric ganglia; ATP could also mediate a part of fast neurotransmission.

   Few uniaxonal neurons show AHP, which means a hump on the repolarizing phase of the action potential, usually have a slow AHPthat lasts for more than 2 sec with fast EPSPs.

Dogiel type II neurons constituted 20.6% of the morphologically identified nerve cells in the mouse distal colon; they show a smaller cell body than Dogiel type I neurons and several long processes. (usually from two

to five). Some Dogiel type II neurons are pseudounipolar, and the long process branched into two or more similar branches at a distance from the cell body; they provide numerous varicose terminals in the same ganglion and/or in nearby ganglia. Electrophysiological analysis of Dogiel type II neurons shows a duration of action potentials like those in uniaxonal neurons with a shoulder on the descending phase of the action potential that might be due to a component of the action potential carried by an inward Ca2 current, as mouse AHP neurons, action potential is not blocked by tetrodotoxin (TTX). The input capacitance of Dogiel type II neurons is similar to the one of uniaxonal neurons. The slow AHP that follows the action potential is present in 70% of Dogiel type II neurons in the mouse colon. Spontaneous neural activity was common in the myenteric ganglia, attached to the circular muscle. No Dogiel type II neurons exhibited fast EPSPs.

Nurgali supposed that these neurons were the fourth type of neuron:

4) **Intrinsic primary afferent neurons (IPANs)**, also called intrinsic sensory neurons: smooth surfaced neurons with several long processes that gave rise to networks of fibres within myenteric ganglia, they respond to luminal chemical stimuli, mechanical deformation of the mucosa, radial stretch and muscle tension. It seems that their neuronal terminals also respond to the serotonin produced by enterochromaffin cells, but not to 5-hydroxytryptamine. They are characterized by delayed and prolonged after hyperpolarizing potential, and for this reason, they are defined as AH neurons.

Apart from the neurons described by Nurgali and collaborators in 2004, other types of neurons reported in the ENS are:

5) **Secretomotor and vasomotor neurons** represent two small classes situated in the myenteric ganglia, projecting to the mucosa. They are cholinergic (acting on muscarinic receptors in the mucosal epithelium) or non-cholinergic (using VIP as mediator of the local reflex response)[33].
6) **Intestinofugal neurons:** with their cell bodies in the myenteric plexus, project out of the gut wall to sympathetic neurons in prevertebral ganglia. In the colon, these neurons respond primarily to changes in circumferential but not in longitudinal stretch, monitoring changes in intracolonic volume. These neurons decrease their firing during muscle contraction. The hypothesis is that they cause increased sympathetic inhibition of gut motility, via noradrenergic neurons in prevertebral ganglia.

In organ bath experiments, it has been showed that when one segment of colon is distended, extrinsic sympathetic reflex pathways can inhibit neighbouring isolated segments of colon [34–36].

Intermingled with the several type neurons are the enteric glial cells (EGC). 10 different types of enteric glial cells have been described within the layers of the gastrointestinal tract with different response signatures. EGC use glial fibrillary acid protein (GFAP), SOX10 and S100 calcium-binding protein β (S100 β) to communicate. Their morphological features, spatial distribution and genetic profile are not completely clarified, yet[37].

2.2 CHEMICAL CODING OF THE ENTERIC NEURONS

Pan-neuronal markers

Enteric neurons can be identified using pan-neuronal markers, besides, based on the immunoreactivity for one or more neurotransmitter, they can be classified as excitatory or inhibitory neurons.

Pan-neuronal markers mostly used are: NeuN, protein gene product (PGP) 9.5 and beta 3 Tubulin.

NeuN protein exists in two possible isoforms, one of 46 and the other of 48 kDa; they are localized in nuclei (NeuN 46kDa) and perinuclear cytoplasm (NeuN 48kDa) of most of the neurons in CNS and ENS of mammals. This protein was discovered in 1992, when the Smith team managed to obtain monoclonal antibodies (A60 clone) to this hitherto unknown nuclear protein [38]. NeuN emerges during early embryogenesis in postmitotic neuroblasts and remains in differentiating and terminally differentiated neurons. In vitro, observing the nucleus, NeuN is bound to the nuclear matrix in areas with low DNA packing, while is absent in high dense chromatin areas. In vivo this protein seems to be a permanent regulator of the neuronal phenotype, and is substituted by other functionally similar proteins in other cells like glial cells [39].

PGP 9.5 is neuron and neuroendocrine specific member of a gene family and its products hydrolyse ubiquitin protein conjugates and inactive polyubiquitin chains to generate free active monomeric ubiquitin. This enzyme is also known as UCH-L1. PGP 9.5 protein is 24-27 kDa and represents 1-2% of the soluble protein of a nerve cell. PGP 9.5 stains central and peripheral neurons but also cells of the diffuse neuroendocrine system. PGP 9.5 appears during neurons differentiation in both mice and rats[40].

Beta 3 Tubulin (β3Tub) is a member of the Beta tubulins that together with alpha tubulins form the two subunit proteins of microtubules. During the formation of microtubules, the 50-kDa α- and β-tubulins form heterodimers, which in turn constitute the building blocks of tubules. Microtubules allow the maintenance and changing of cell morphology [41]. β3Tub is encoded by a gene located at the chromosome 8 in mice and in the chromosome 19 in rats [42]. β3Tub protein has been considered a neuron-specific marker molecule as it plays a critical role in proper axon guidance and maintenance.

Neurotransmitters are chemical molecules synthesized and released endogenously by neurons to interact with each other or with targeted no-neuronal cells [43,44].

More than 20 distinct neurotransmitters have been identified in the ENS. Table 1 reports each type of neuron with its neurotransmitter [44].

2.2.2 EXCITATORY NEUROTRANSMITTERS

The principal excitatory neurotransmitter is ***Acetylcholine* (ACh)**, that is synthesized by the choline acetyltransferase (ChAT) enzyme; the neurons releasing Ach are defined cholinergic neurons. The receptors for acetylcholine are located on both neurons and SMCs [45].

Those on the SMCs belong to the muscarinic M_1, M_2, and M_3 receptor subtypes; the ACh binding induces Ca2+ entry and Ca2+ release form the intracellular stores, causing smooth muscle contraction.

Neurons express nicotinic receptor, to which ACh binds inducing fast synaptic neurotransmission.

The second most important excitatory molecule is ***Substance P***, that is the principal member of the tachykinin's family [Reviewed by Steinhoff MS et al. [46]. SP identifies enteric efferent neurons and NON-adrenergic NON-cholinergic neurons. SP is an undecapeptide that binds to the neurokinin receptors (NK) 1,2 and 3 with the highest affinity for the NK1 isoform, which are expressed by neurons and smooth muscle cells.

Glutamate is poorly expressed in the ENS but a recent study using calcium imaging from myenteric neurons in mice colon suggested that in neurons that express calbindin endogenous glutamate may mediate part of the slow EPSP [47].

2.2.3 INHIBITORY NEUROTRANSMITTERS

The main inhibitory neurotransmitters are ***nitric oxide (NO), carbon oxide (CO), sulfuric acid (H2S),*** **vasoactive** ***intestinal peptide (VIP), adenosine triphosphate (ATP)*** and ***pituitary adenylyl cyclase activating***

peptide (PACAP). Noradrenaline, a classical inhibitory neurotransmitter, does not participate as a post-synaptic inhibitory mediator in the gut, so it is not used in ENS classification.

NO is a gaseous neurotransmitter synthesized by NO synthase (NOS) from the amino acid L-arginine. NOS exists in three isoforms: two are constitutively expressed in neurons, named neuronal NOS (nNOS), and endothelial NOS (eNOS), and one named inducible NOS (iNOS). nNOS containing neurons are found throughout the gastrointestinal tract of most vertebrates. NO causes relaxation and hyperpolarization of SMCs due to inhibition of L-type Ca2+ channel, activation of cyclic guanosine 3'-5' cyclic monophosphate (cGMP) independent K+ channels and activation of the soluble guanylate cyclase (sGC) with an increase in cGMP that leads to cGMP dependent protein kinase (protein kinase G) activation of cGMP-dependent K+ channels. Neurons that release NO are defined nitrergic neurons. NO is released in a basal way as the smooth muscle must be kept relaxed. NO synthesis is blocked by L-nitroarginine (LNNA).

VIP is a polypeptide that interacts with its G-protein coupled receptors (predominantly VPAC-2 receptor) of smooth muscle cells to activate adenylate cyclase followed by an increase in cAMP levels and smooth muscle relaxation. The cAMP-mediated relaxation involves activation of K+ channels, including ATP-dependent K+ channels, large conductance Ca2+-activated K+ channels, delayed rectifying K+ channels, inwardly rectifying K+ channels and voltage-dependent K+ channels[48].

CO is a gas produced endogenously by NADPH-dependent oxidative degradation of heme (Fe protoporphyrin IX) catalysed by heme oxygenase (HO). There are two HO isoforms in the gut: an inducible (HO-1) and a constitutive enzyme (HO-2). HO-1 is expressed at very low levels except when induced by injury, inflammation or disease while HO-2 is expressed in enteric neurons in several species including mice and rats and has also been detected in the ICCs. CO modulates the cGMP-dependent delayed rectifier K+ current, inducing SMC hyperpolarization and subsequent relaxation. CO may also contribute to VIP neurotransmission [49].

PACAP is co-expressed with VIP in enteric inhibitory neurons and causes hyperpolarization and relaxation by increasing an apamin-sensitive small conductance Ca2+-dependent K+ outward current through PACAP type 1 (PACAP1) receptors present in SMCs. Hyperpolarization and activation of a small conductance Ca2+-dependent K+ outward current through PACAP1 receptors could be caused by phospholipase C activation

and 1,4,5-trisphosphate inositol accumulation which leads to increased Ca2+ release from intracellular stores.

ATP is reported to be both excitatory and inhibitory, depending on the area where it is released. When released at the neuromuscular junction in the GI, it hyperpolarizes and relaxes the smooth muscle. The relaxation occurs via adenylate cyclase enzyme activation and it increases in cAMP levels. *ATP* mediates the fast component of the inhibitory junction potential ('fast IJP') via purinergic (P2Y) G-protein-coupled receptor activation of small conductance Ca2+- activated potassium channels in mouse and rat intestine [50–52].

Somatostatin is a cyclic peptide, with a half-life of 3 minutes, also named growth hormone inhibiting hormone. It exists in two isoforms, one of 14 amino acids, typically expressed in the brain and one of 28 amino acids that operates in the GI tract. Its function is to inhibit colonic fluid secretion. Somatostatin also inhibits VIP. It binds to G protein coupled receptors (GPCR), inducing decrease in cyclic AMP and CA2+ and increment in K+ inward currents, bringing to decrease in secretion by the target cell [53].

Table 1:

Type of neuron	**Primary transmitter**	**Secondary transmitters, modulators**	**Other neurochemical markers**	**Referencees**
Enteric excitatory muscle motor neuron	ACh	Tachykinin, enkephalin (presynaptic inhibition)	Calretinin, γ-aminobutyric acid	Brookes *et al*. (1991)[54]; Holzer & Holzer Petsche (1997)[55]; Grider (2003)[56]
Enteric inhibitory muscle motor neuron	NO	VIP, ATP or ATP-like compound, carbon monoxide	PACAP, opioids	Fahrenkrug *et al*. (1978) [57]; Costa *et al*. (1992) [58]; Sanders & Ward (1992)[59]; Xue *et al*. (2000) [60]
Ascending interneuron	ACh	Tachykinin, ATP	Calretinin, enkephalin	Brookes *et al*. (1991) [61]
ChAT, NOS descending interneuron	ATP, ACh	ND	Nitric oxide, VIP	Young *et al*. (1995) [62]; Brookes (2001) [63]
ChAT, 5-HT descending interneuron	ACh	5-HT, ATP	ND	Furness & Costa (1982) [64]; Monro *et al*. (2002)[65]; Gwynne & Bornstein (2007)[66]

ChAT, somatostatin descending interneuron	ACh	ND	Somatostatin	Gwynne & Bornstein (2007) [66]; Portbury *et al*. (1995) [67]
Intrinsic sensory neuron	ACh, CGRP, tachykinin	ND	Calbindin, calretinin, IB4 binding	Grider (2003)[56]; Gwynne & Bornstein (2007)[66]; Li & Furness (1998)[68]; Johnson & Bornstein (2004) [69]
Interneurons supplying secretomotor neurons	ACh	ATP, 5-HT	ND	Suprenant (1984) [70]; Monro *et al*. (2004) [71]
Noncholinergic secretomotor neuron	VIP	PACAP	NPY (in most species)	Cassuto *et al*. (1981) [72]; Banks *et al*. (2005) [73]
Cholinergic secretomotor neuron	ACh	ND	Calretinin	Brookes *et al*. (1991) [61]; Keast *et al*. (1985) [74]
Motor neuron to gastrin cells	GRP, Ach	ND	NPY	Holst *et al*. (1987) [75]; Weiget *et al*. (1997) [76]
Motor neurons to parietal cells	ACh	Potentially VIP	ND	Nilsson *et al*. (1972)[77]; Feldman *et al*. (1979)[78]
Sympathetic neurons, motility inhibiting	Noradrenaline	ND	NPY in some species	Finkleman (1930)[79]; Macrae *et al*. (1986)[80]
Sympathetic neurons, secretion inhibiting	Noradrenaline	Somatostatin (in guinea pig)	ND	Costa & Furness (1984)[81]
Sympathetic neurons, vasoconstrictor	Noradrenaline, ATP	Potentially NPY	NPY	Dresel & Wallentin (1966)[82]; Furness (1971)[83]; Furness *et al*. (1983)[84]
Intestinofugal neurons to sympathetic ganglia	ACh	VIP	Opioid peptides, CCK, GRP	Crowcroft *et al*. (1971)[85]; Dalsgaard *et al*. (1983)[86]; Love & Szurszewski (1987)[87]

3 INTERSTITIAL CELLS OF CAJAL

Santiago Ramón y Cajal described these cells for the first time [88] as a particular cell type that appeared to function as an 'endostructure' of the intrinsic nervous system. Cajal, using staining techniques which specifically labelled neurons (e.g. methylene blue (Fig. 6) or silver impregnation), identified these cells in the *interstitium* between nerve endings and SMCs and he named them 'interstitial neurones'. Their functional and structural characteristics were defined later and they were named interstitial cells of Cajal (ICCs) [89].

ICCs differentiate from the mesenchymal lineage and start to differentiate together with enteric neurons and glia. This process has been demonstrated in vitro through the induction of pluripotent cells combined with cells derived from the neural crest, which migrate to the mesenchyme and form neuroglial structures and functional ICCs [90].

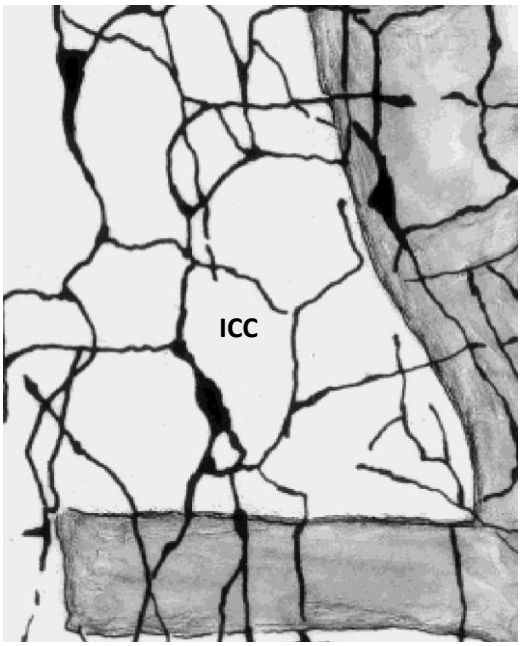

Figure 6. Drawing by Cajal of ICC-AP of rabbit intestine stained with methylene blue[88].

ICCs are thought to primarily serve as the pacemaker cells. Thuneberg et al. (1982)[91] postulated this hypothesis in the mouse small intestine. The signature of the ICC is its "slow wave" in membrane potential: ICC have a basal membrane potential of -50mV that spontaneously fluctuates between 10 or 20 mV (reaching -40 or -30mV) generating a rhythmic depolarization, Ca^{2+} entry and a slow-wave activity that is transmitted as a pacemaker activity via gap junctions to the smooth musculature. The transmission can be either ongoing or on-demand, in both cases it triggers slow-wave activity within smooth muscle cells, which then actively propagates throughout the muscle layer[92] thanks to the gap junctions (also called connexons) that allows the depolarization of all the intestine. ICCs are the ones that induce the basal electric rhythm of the intestine called peristalsis.

Embryologically ICCs originate from gut mesenchyme (Fig. 7) and not from the neural crest cells that colonize the gut. ICCs differentiation is a complex process where a significant role is played by the neuronal cells that

produce the stem cell factor binding to the c-kit receptor on the ICCs[93]. Animals without ICC have no spontaneous contractions but they can survive as the ENS is able to induce efficacious SMCs contraction, leading to peristalsis and *complete colonic motor complexes* (CMCs). On the opposite, without neurons ICCs pacemaker activity is not able to produce sufficient contractions of the muscle layer to propel content[92].

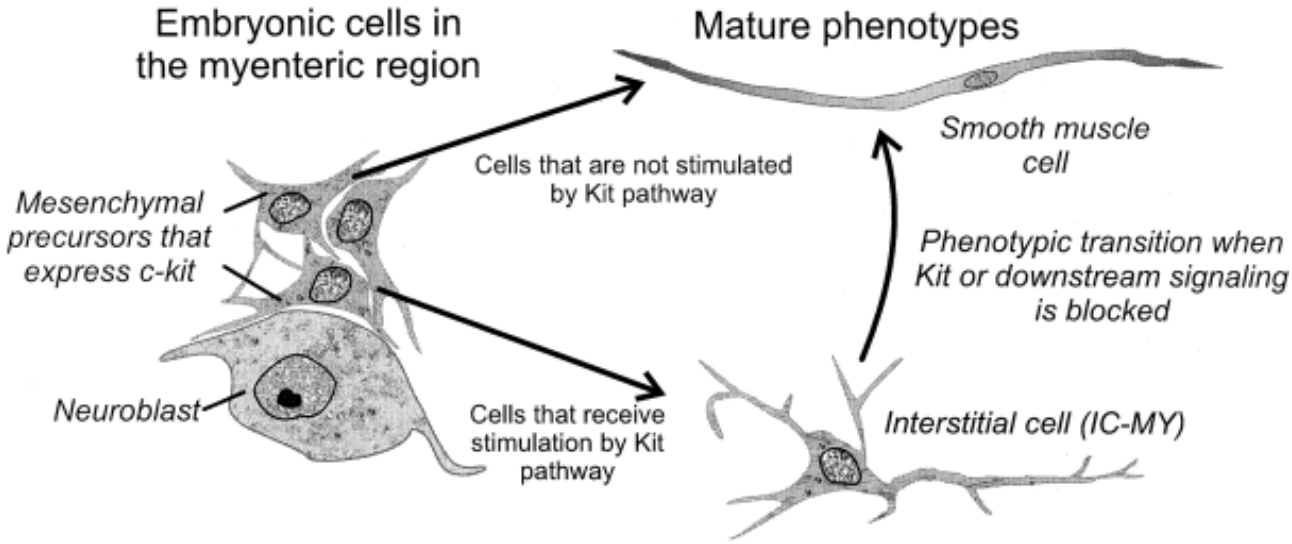

Figure 7. Development and plasticity of interstitial cells of Cajal: ICC and longitudinal smooth muscle cells develop from common mesenchymal precursors. Expression of c-kit appears at about E12.5 in mesenchymal cells around the periphery of the small intestine. At E15 these cells express both Kit and the smooth muscle marker, desmin. With normal Kit signaling some cells become ICC and some become longitudinal smooth muscle cells. This hypothesis was supported by in situ hybridization studies. Without proper Kit signaling (i.e. in W/WV and Sl/Sld mice) or when Kit is blocked with neutralizing antibody at E15 the longitudinal muscle layer still develops, but IC-MY fail to develop. These data suggest that Kit signaling is needed for the lineage decision to become an ICC or a smooth muscle cell and for subsequent development of ICC. The Kit pathway also appears to be important for maintenance of the ICC phenotype because, when Kit is blocked, well-developed, functional ICC re-differentiate and take on a smooth muscle phenotype [93,94].

Depending on their location, ICCs were named differently [89,95]. The ICCs located in between the circular and longitudinal muscle layers are called ICC-AP (Auerbach plexus) or ICC-MP (myenteric plexus); those located between the inner thin and outer thick sublayers of the circular smooth muscle of the small intestine are the ICC-DMP (deep muscular plexus); those located along the border of the circular muscle layer and the submucosa, in the stomach and colon, are the ICC-SMP (submucosal plexus); finally, ICCs are also present in the thickness of the circular muscle (ICC-CM) and longitudinal muscle (ICC-LM) layers (Fig. 8).

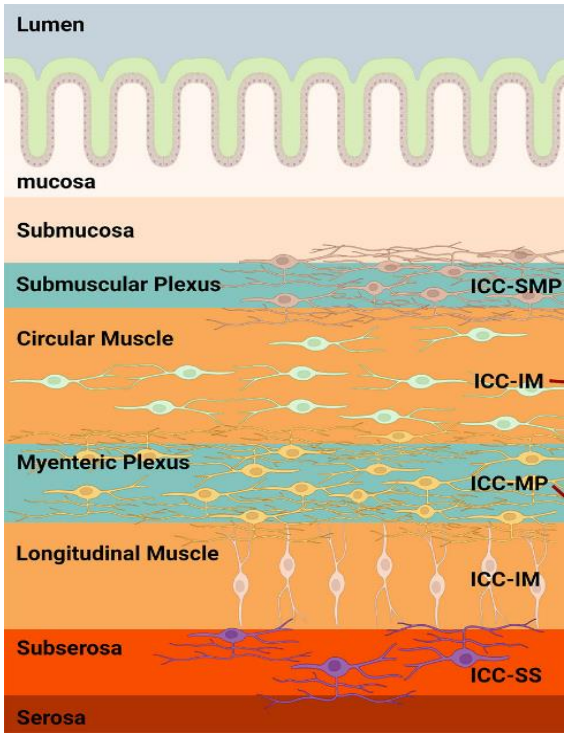

Figure 8. Modified from[95]. Schematic drawing of the ICC networks throughout the thickness of the colon wall. ICC-IM, intramuscular ICC; ICC-MP, ICC associated with the myenteric plexus; ICC-SMP, ICC associated with the submuscular plexus in the colon; ICC-SS, subserosal ICC.

Transmission electron microscopy is the best way to visualize ICCs. They have variable size and irregular profile in mammals but share common ultrastructural features, such as the presence of numerous mitochondria, abundant intermediate filaments, formation of gap junctions with other ICCs and with SMCs, their processes are narrow, rounded, or only slightly flattened structures. Furthermore, some subtypes of ICC show some typical SMCs characteristics like a basal lamina, caveolae, subsurface cisterns and dense bodies. In rodents ICCs share a slim, elongated cell body, and several cell processes of variable length. They are relatively few in comparison with muscle cells and they are mostly found at the periphery of muscle cell bundles or the muscle layers (Fig. 9 and Fig. 10).

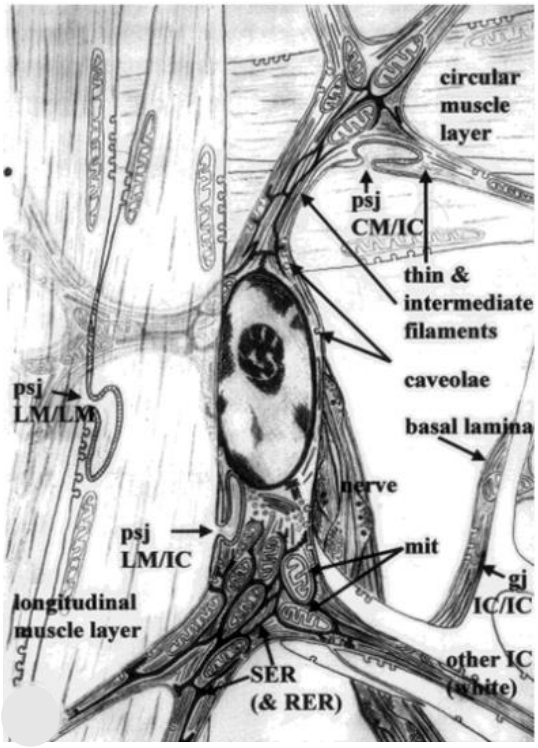

Figure 9. Drawing of ICC-MP. LM: longitudinal muscle layer; CM: circular muscle layer; gj: gap junction; psj: peg-and-socket junctions; mit: mitochondria; smooth (SER) and rough (RER)endoplasmic reticulum [96].

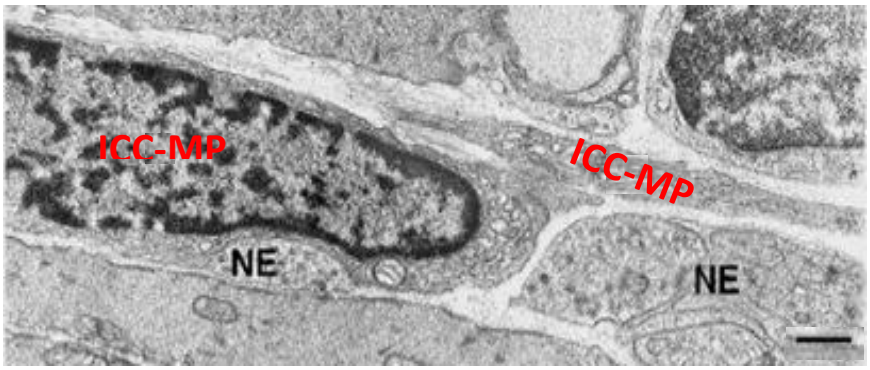

Figure 10. Modified from[97]. Two interstitial cells in the myenteric plexus of mouse colon [ICC-MP] with normal features. Note a nerve ending (NE) in close contact with one ICC. Bar = 0.2 µm.

A living stain method is the employment of neurobiotin which diffuses in ICCs through gap junctions (Fig. 11A). Immunohistochemistry is a more recent way to visualize ICCs distribution, as ICCs express two specific markers: the transmembrane protein tyrosine kinase receptor c-Kit, also named CD117 (Fig. 11B; 12; 13) [95,98] and the chloride channel Ano1 (Fig. 12; 13)[99].

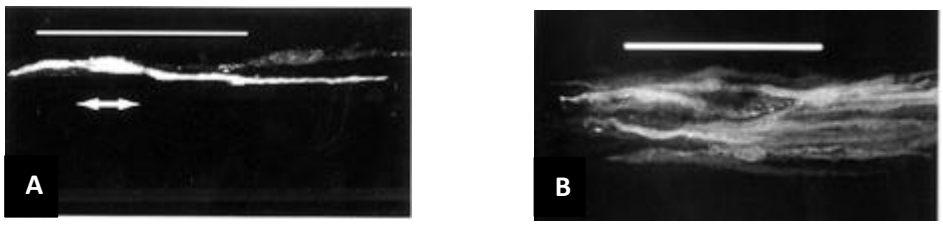

Figure 11. Neurobiotin-filled cells distributed in the submucosal layer of mouse proximal colon (A and B are from different pieces of proximal colon) Calibration bar / 100 µm. In A, the two-headed arrow indicates the length of the cell body[99].

The ***c-kit receptor*** (also known as CD117) is a transmembrane receptor tyrosine kinase which is widely expressed on the surface of ICCs. It is involved in cell signalling pathways that regulate cell growth, survival, and differentiation [59]. The c-kit antibody specifically marks the c-kit receptor on ICCs, enabling their visualization in tissue sections. In mice and rats colon, this antibody is used to immunostaining ICCs, providing detailed information about their distribution, density, and morphology within the wall [95]. The c-kit immunostaining is useful to investigate ICC role in gastrointestinal motility and the loss of c-kit expression is associated with motility disorders such as gastroparesis or chronic constipation [101]. The c-kit antibody

staining can also be utilized to study various colonic pathologies, such as inflammatory bowel disease (IBD), colorectal cancer, and Hirschsprung's disease. Chronic inflammation in conditions like inflammatory bowel disease (IBD), may change c-kit distribution as it affects ICCs; Veress and coll. [103] have shown that ICC density and distribution can be altered in IBD, possibly due to direct damage to the ICCs or their microenvironment.

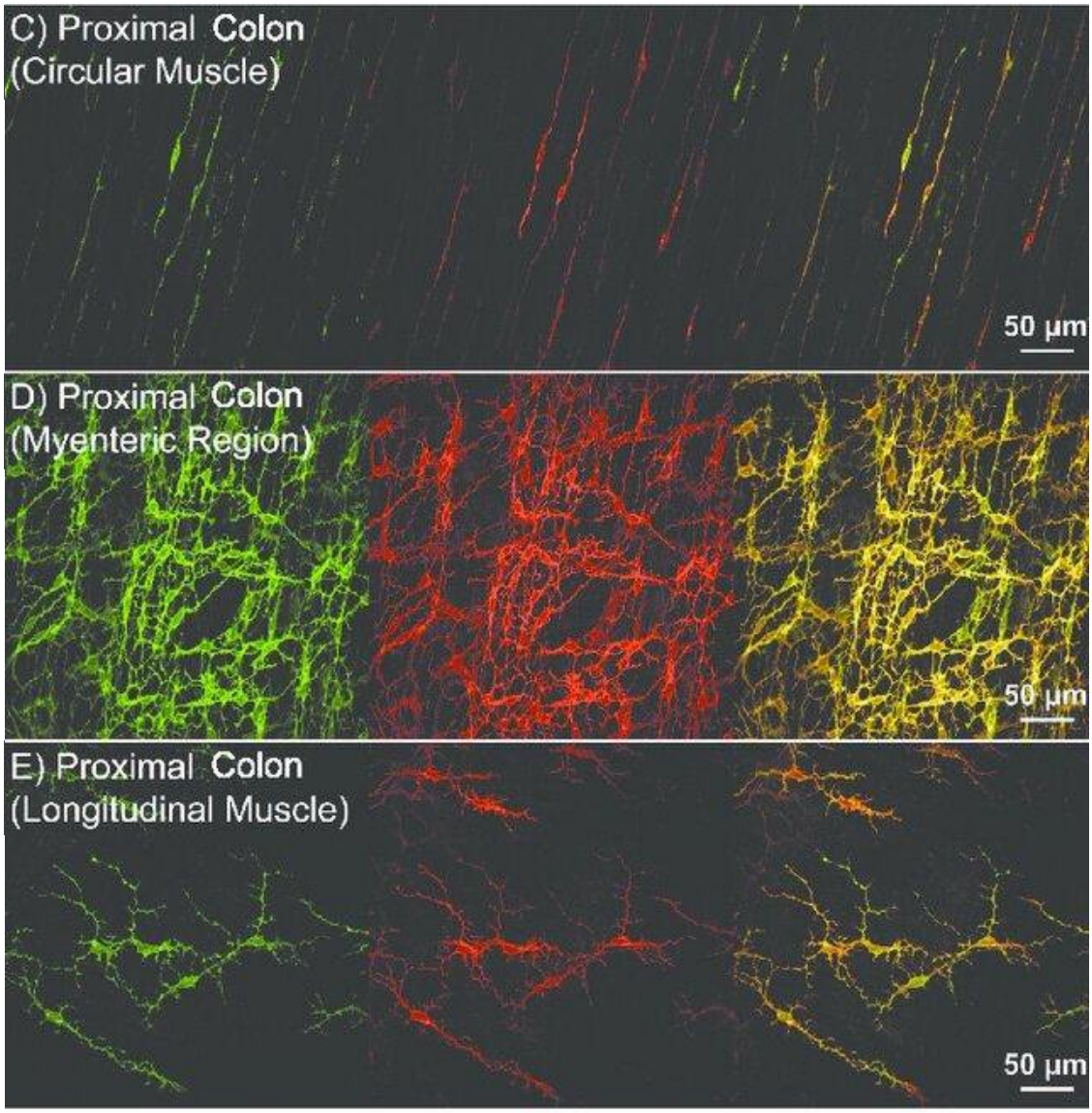

99

Figure 12. Ano1 antisera label ICC in adult murine proximal colon. Representative enface projection images of confocal stacks collected at 400 magnification from a whole mount incubated with rabbit anti-Ano1 antiserum (Abcam, green) and ACK2, a rat anti-Kit antibody (red). Merged images are on the right. A: ICC-IM from circular muscle of proximal colon. B: myenteric region ICC in proximal colon. C: subserosal ICC in proximal colon. [Modified from[100]]

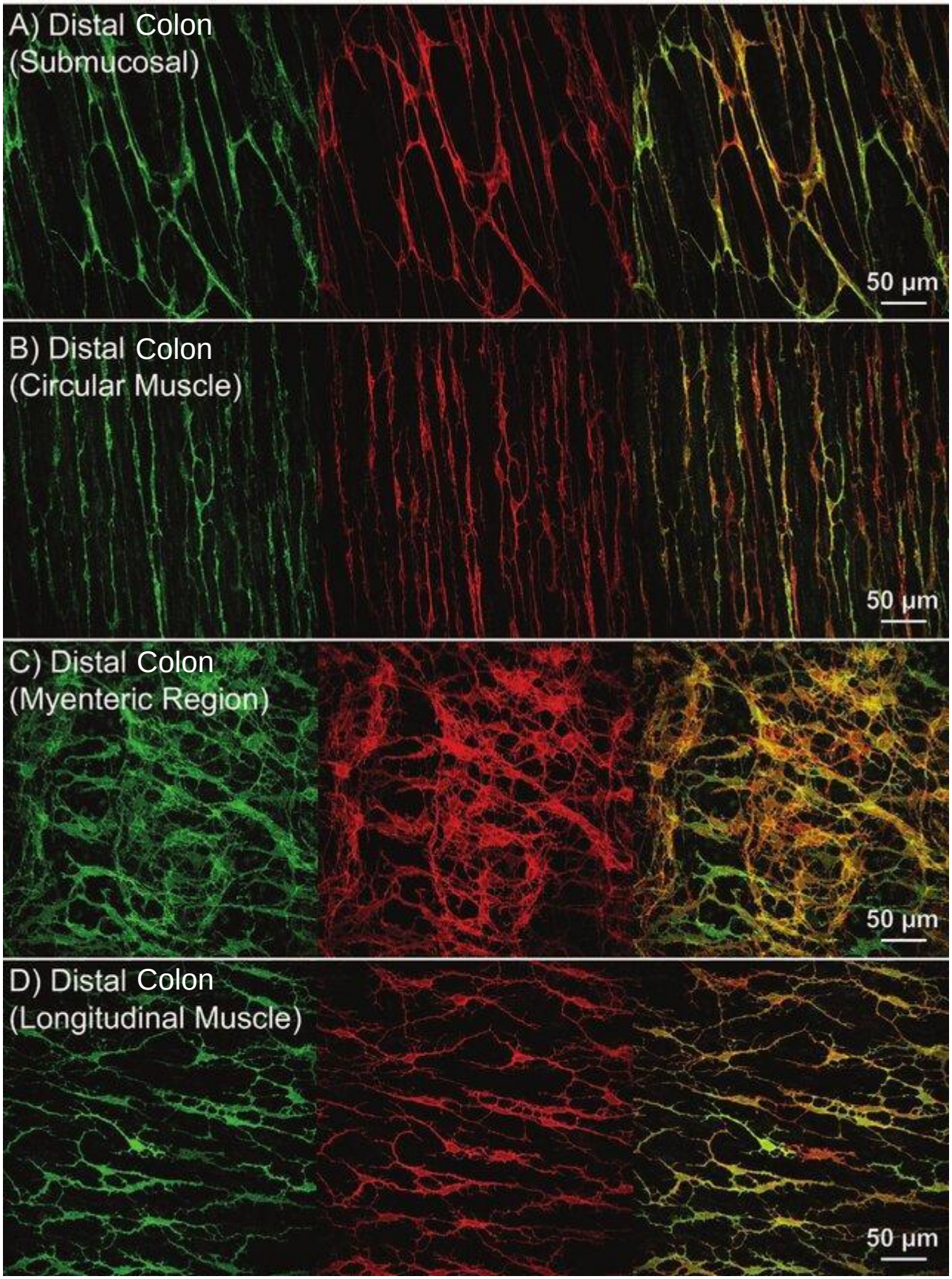

Figure 13. Ano1 antisera label ICC in adult murine distal colon. Representative enface projection images of confocal stacks collected at 400 magnification from a whole mount incubated with rabbit anti-Ano1 antiserum (Abcam, green in merged images at right) and ACK2, a rat anti-Kit antibody (red). Merged images are on the right. A: submucosal ICC. B: ICC-IM from circular muscle layer. C: myenteric region ICC. D: ICC-IM in longitudinal muscle. [from[100]].

The capacity of ICCs to generate slow waves was proved in 1998 by Jonathan Lee and Lars Thomsen in Huizinga's lab[101] and by Koh S.D., Sanders K.M., Ward S.M[101]. Both groups recorded rhythmic inward currents in isolated ICC. These currents are primarily generated by more than one type of chloride channels. These channels are activated by the rhythmic release and reuptake of calcium from the sarcoplasmic reticulum (SR), as these waves are blocked when IP3 receptor in the Ca2+ store or Ca2+ influx in the SR are blocked. Thanks to calcium imaging it was demonstrated that all ICCs in a network oscillate as a *unicum* at the same metric as the depolarization occurrence. The rhythmicity seems to be guided by a spontaneous opening of a high-conductance chloride channel and generation of pulsing changes in membrane potential, such channel has a high open probability at the resting membrane potential. Substance P induces a bursting activity of such channel in isolated cells and in situ. Substance P promotes IP3-sensitive calcium release from the sarcoplasmic reticulum in ICC and promotes inward currents via NK1 receptors [103].

In vivo the myenteric excitatory motor neurons and primary afferent sensory neurons release substance P inducing the same effect. M3 muscarinic receptors activate chloride channels in ICCs increasing spontaneous inward currents [104]. The Ano1 protein is found in all ICC and the Ano1 calcium-sensitive chloride channel is crucial for ICC pace making activity. The channel was discovered thanks to the homology of ICCs electrical properties with Ano1 channel in HEK293 cells[105,106]. Hwang and collaborators demonstrated that deletion of Ano1 in mice results in persistence of ICC-MP but in loss of slow waves in SMCs of the small intestine [107] because Ca^{2+} transients are present but are no more coordinated in the ICC network. In the colon, other channels were reported to contribute to rhythmic depolarization of ICCs in mice [100] and rats [107]. Not much is reported about the role of different ion channels in the different ICC subtypes function. To set the membrane potential and to repolarize the cell, K and K channels are deciding. KV7.5 is the prevailing voltage-sensitive K+ channel in mouse colon ICC, as changes in membrane potential and repolarization are blocked by XE991 a KV7.5 blocker, molecule that causes also an inward maxi channel activity. Adding carbachol to stimulate the muscarinic acetylcholine receptor the activity of K+ channel is inhibited. Double immunohistochemical staining of colons for Kit and KV7.5 in situ revealed an interesting difference between ICC-IM and ICC-MP networks as the ICC-IM were positive for KV7.5, but not the ICC-MP, moreover, there was a dense cholinergic innervation of ICC-IM [108].

In mice colon, Yoneda and collaborators[100,109] showed that the ICC-SMP generate strong rhythmic slow waves due to Ca2+ release from the SR as well as voltage-gated Ca2+ channels. In rats, Jimenez' group discovered the same configuration [107] stating that the circular muscle of rat colonic strips with the submucosal layer kept intact, showed spontaneous cyclic mechanical activity composed of two types of phasic contractions, Fig. 14 shows schemes of the contractions. Fig. 14A shows the trend of Low-frequency and high-amplitude contractions with superimposed high-frequency and small-amplitude contractions. In contrast, Fig. 14B shows that the longitudinal muscle in all the full-thickness preparations only has low-frequency and high-amplitude contractions. Fig. 14C reports the recording from circular muscle strips devoid of submucosa that present exclusively the low-frequency and high-amplitude cyclic contractions. Finally, Fig. 14D shows contractions recorded from the circular muscle with submucosa and without the longitudinal muscle layer where only the high-frequency and low-amplitude contractions are displayed.

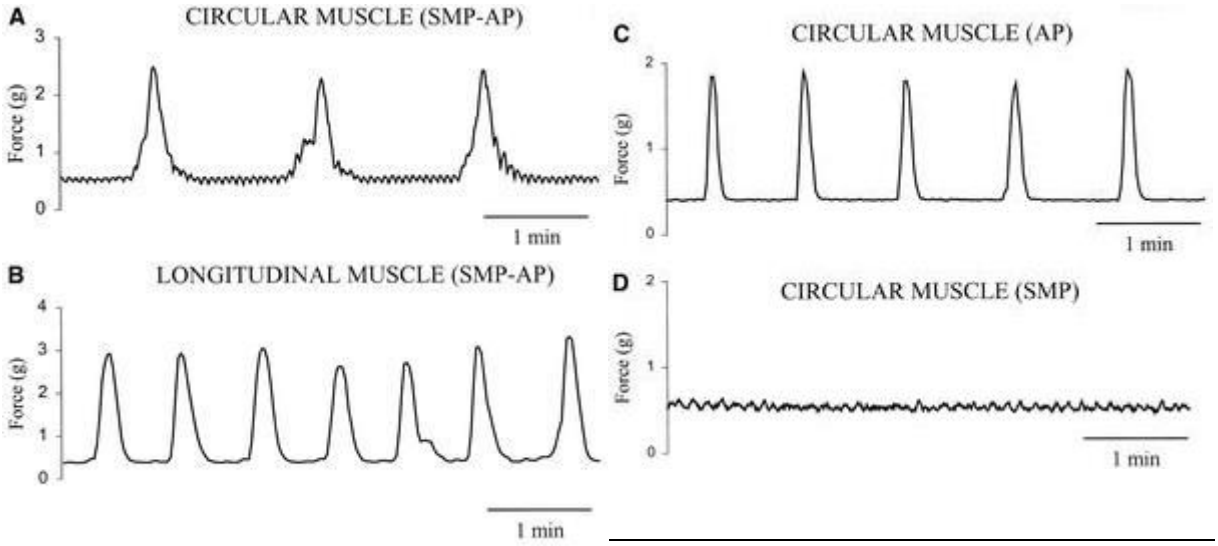

Figure 14. Organ bath recordings of rat colonic preparation, showing the spontaneous cyclic mechanical activity displayed by the circular (A) and longitudinal muscles (B) with the submucosa kept intact and therefore with both the submuscular plexus (SMP) and Auerbach's plexus (AP) intact. C: mechanical recording showing the spontaneous contractile activity of the circular muscle in a colonic preparation devoid of submucosa, but with AP intact. D: mechanical recording showing the spontaneous contractile activity of the circular muscle in a colonic preparation devoid of AP, but with the SMP intact. [Adapted from[106]]

The observed cyclic mechanical activity present in the colon could not be only caused by the pacemaker activity of ICC-SMP.–The lower frequency rhythmic depolarization was originated by the ICC-MP as it was

stimulus-dependent and very sensitive to calcium channel blockers in both mouse and rat tissues. Also, ENS or distension are driving stimuli of these contractions *in vivo*. In fact, NO released by nitrergic neurons acts on ICC via guanylate cyclases inducing ICC mediation of nitrergic inhibition, but is it not clear how ICC modulate nitrergic innervation before the signal is given to SMCs [110]. What is known is that, in absence of ICCs, a parallel innervation pathway acts directly on SMCs, indicating that ICCs are not fundamental for NO action on SMCs. Talking about distention stimulus, it was reported that ICCs are also stretch sensors and stretch induces cell depolarization. Stretch stimulus can also be transmitted to enteric and extrinsic sensory nerves. In stool retention during constipation an excessive wall stretch may suppress stem cell factor production resulting in ICC loss or ICC impairment [111].

4 GAP JUNCTIONS

Cells form junctions to protect tissue integrity, to guarantee intracellular communication and paracellular transportation[112]. Gap junctions (GJ), first described in 1967 in liver cells[113], are plasma membrane channels which lead to transport between cells of molecular metabolites smaller than 1.5 kilodalton like glutathione, ATP, cyclic adenosine monophosphate (cAMP), cyclic guanosine monophosphate (cGMP), inositol triphosphate (IP3) and ions like calcium. GJ are formed by connexins, proteins that were first isolated in 1974 by Goodenough [114] and that are named by their molecular weights, expressed in kilodaltons [115].

Connexins are membrane-spanning proteins with four transmembrane domains, a large extracellular loop, and intracellular C- and N-terminal domains. These proteins are synthesized by ribosomes attached to the endoplasmic reticulum (ER). Once synthesized, connexins are immediately translocated from the ER membrane to the Golgi apparatus. In the Golgi they undergo post-translational modifications such as phosphorylation and the assembly into connexons begins. Six similar connexin isoforms form homomeric connexons, while a combination of different connexins isoforms forms heteromeric connexons, respectively. The oligomerization into hexameric structures continues along the secretory pathway from the Golgi to the plasma membrane. Before reaching the plasma membrane, they may undergo further modifications and proper folding to ensure they form functional connexons [116]. From the ER/Golgi network, vesicles containing oligomerized hemiconnexons transport these structures along microtubules to the membrane [117] where the vesicles fuse with the membrane, inserting connexons into the cell membrane at the edges of existing gap junction plaques [118]. Once inserted into the plasma membrane connexons, from adjacent cells, can align and dock to form functional gap junctions. When connexons from two adjacent cells align, they form a continuous channel, allowing the passage of ions and small molecules between the cells [119].

Connexons are spaced about 9–10 nm centre to centre in a regular array in GJs and there may be from 1 to several thousand in one GJ. Connexins were first described using transmission electron microscopy and scanning electron microscopy. Small Gjs formed by less than 10 properly aligned connexons will be missed in TEM slides as ultrathin slides for TEM are 100nm thick, at least. Even with this limit, Garfield et al in 1977 and

1978[120,121] quantified that GJs may occupy >0.1% of SMC plasmalemma. GJs are found in all tissues apart from differentiated skeletal muscular fibers, erythrocytes and mature sperm cells.

Nowadays, 21 isoforms of connexin have been described in the connexin gene family and can be divided into five subgroups (α, β, γ, *δ*, or *ε*) with respect to their extent of sequence identity and length of the cytoplasmic loop. Using immunohistochemistry and specific antibodies, it is possible to visualize connexin distribution in all previous mentioned tissues; in the colon 8 connexin variants have been characterized Cx26, Cx31, Cx31.1, Cx32, Cx36, Cx40, Cx43 and Cx45[122].

Cx43 is a polypeptide of 382 amino acid (aa) with four conserved α-helical transmembrane domains, two extracellular loops, a cytoplasmic loop (CL, located in the intracellular space), and cytoplasmic amino (N)- and carboxyl-terminal (CT) domains. The N-terminus (NT) is 13 amino acids, while the CT is 150 amino acids. The CT may mediate pH gating in a "particle-receptor" interaction acting as a "ball" that attaches to the second half of the CL closing the connexon pore [123]. Cx43 is the most widely distributed connexin in rats and mice gut, stainable in both ICC and SMCs. Cx43 CT interacts directly with microtubules and indirectly with the actin-based cytoskeleton via adaptor proteins, with zonula occludens-1 (ZO-1) and Drebrin (developmentally regulated brain protein) being the best known (Fig. 15) [124].

Connexon physiological role is to connect different cell types biochemically and electrically; biochemical property is due to the fact that it allows molecules passage that act as second messengers while their electrical property is low resistance to current passage, so they allow fast electrical coupling between two cells. Without these two properties, it would be impossible to have slow phasic contraction in the gut; GJs permit the formation of a syncytium between the SMCs and ICCs.

The presence of connexons, even when they are very few, can be revealed through the spreading of dye or current from cell to cell. Connexons do not exist between LM and CM as there is no spreading of dye in one layer when injected in the other, but there is propagation of electrical pulse that happens via ICC-MP [125].

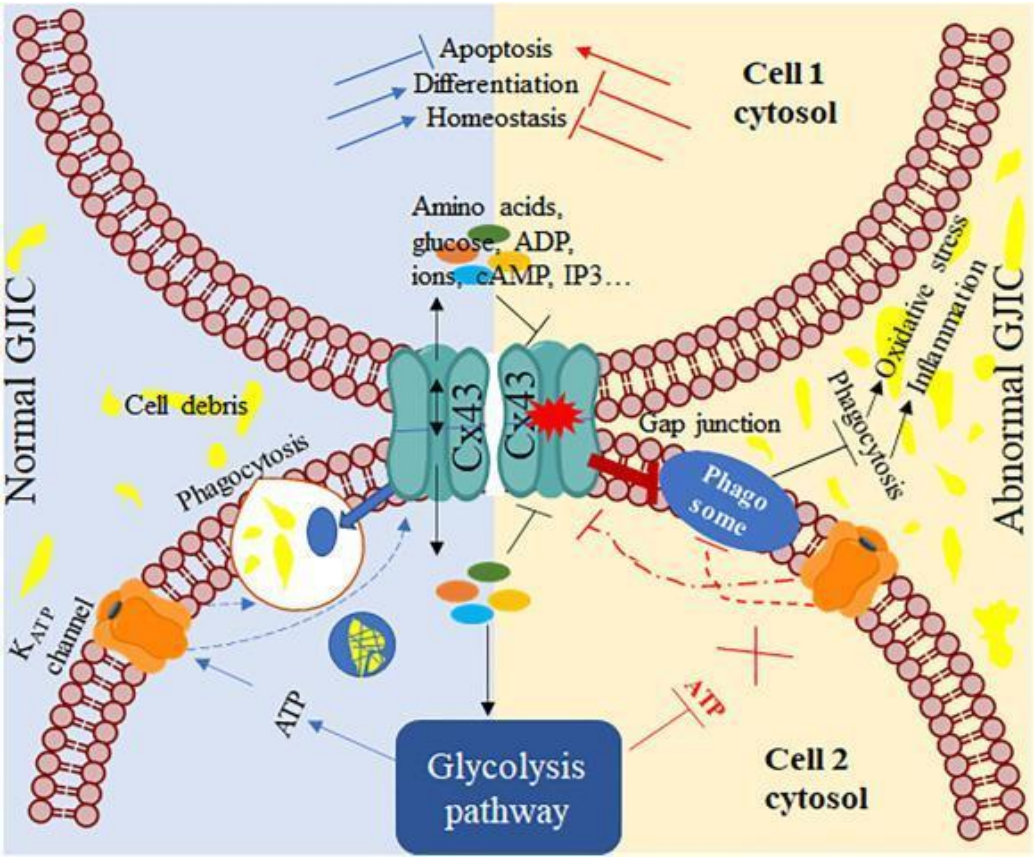

Figure 15. From[126] .Schematic representation of gap junction and cellular homeostasis with Cx43 role. The picture shows the role of intercellular communication between the cell's gap where Cx43 receives the molecules from another cell to process and produce ATP via glycolysis. ATP from glycolysis helps the K-ATP channel to regulate Cx43 and Cx43 mediates control and initiation of phagocytosis of the extracellular debris. Cell homeostasis helps in promoting cell development, cell differentiation and prevents apoptosis. Notes: Cx43: connexin 43; GJIC: gap junction intercellular communication; KATP: potassium adenosine triphosphate; ADP: adenosine diphosphate; cAMP: cyclic adenosine monophosphate; IP3: inositol triphosphate.

Doring and coll. (2007)[127] studied mice with Cx43 knockdown in intestinal smooth muscle cells and described: 1) smooth muscle hypertrophy and hyperplasia, 2) 13-fold increase of neutrophilic infiltration, 3) GI transit time slowed down by 29%, 4) hypercontractility, and 5) enhanced visceromotor response[127]. Other studies about the effect of Cx43 loss report changes in the cytoskeleton with consequent altered cell morphologies, adhesion, polarity, and migration [128,129]. This was also similar to what happens in gut chronic inflammation and seems to be related with what happens in irritable bowel syndrome where Cx43 modifications could contribute to visceral hypersensitivity and hyperalgesia [119,130].

5 GUT RELATED DISEASES

As outlined in the preceding chapters, the ENS, together with ICCs and SMCs, is capable of orchestrating a multitude of GI functions. Consequently, alterations attributed to one or more enteric components can result in a vast array of GI dysfunctions. Among these, the most clinically evident are those in which intestinal motility or sensory functions are affected. Alterations in the ENS may result from congenital abnormalities, such as Hirschsprung's disease, or from acquired alterations that are generally believed to be caused by neuronal degeneration, immune mediated inflammation, or infection. In certain cases, the ENS is the primary contributor to a disease process, whereas in others, it is a component of the enteric disturbance. The ENS plasticity is defined as the overall range of morphological and functional changes that can occur during physiological conditions as a morphological adaptation to environmental-induced changes [131]. It is also defined as the capacity of the ENS to undergo adaptive changes and/or reparative events during pathological conditions [132]. Moreover, in addition to alterations in enteric neurons, ICCs damage has been identified as a key component involved in GI diseases [133]. It is noteworthy that the ICC response to stress is likely to be aimed, at least in part, to prevent other cells damage and to help the restoring normal ENS homeostasis.

More recently, ENS has been proposed as a potential contributor to other major GI diseases, including cancers and their response to chemotherapy; also, an increasing attention has been given to the relationship between ENS and microbiome in recovery after chemotherapy.

Nevertheless, thus far, only a limited number of studies have addressed these issues. Consequently, they will be the two principal topics at the core of my thesis and will be further elaborated upon in the following paragraph of the introduction.

6 RESEARCH STUDY 1:

6.1 CHEMOTHERAPY: DEFINITION AND SIDE EFFECTS

The term chemotherapy refers to any treatment consisting of substances of chemical origin. In common usage, however, this word is used to refer to drugs for the treatment of cancer. Biological drugs or immunotherapeutic drugs are not part of chemotherapy.

Chemotherapy works by killing cells during their reproduction process (replication/differentiation). This is the reason why it is also called cytotoxic or antiblastic therapy [134]. This therapy has changed the treatment of cancer diseases and nowadays the combination of multiple chemotherapy using drugs with different mechanisms of action in the curative or palliative intervention has improved the patient's survival [135].

By targeting actively multiplying cells, however, chemotherapy also affects the body's healthy cells characterized by a high rate of proliferation, generating the important undesirable effects that occur not only during the use of chemotherapeutic agents but also after the end of the treatment. The longer life expectancy of patients has increased the incidence of those side effect worsening the quality of life (QoL)[136].

The side effects that can appear during the treatment are a consequence of early toxicity on high proliferating tissues (early side effects), or post-treatment (late side effects) and can persist for extended periods, ranging from 6 months to years[137]. Notably, the late side effects often affect tissue with a very low proliferation index or even cells that do not divide once differentiated such as neurons, cardiac cells, skeletal muscle and cells in the organ of Corti causing neuronal damage, fibrosis, atrophy and vascular damage. In long term cancer survivors, this late toxicity is a major health problem but is still unfathomable [138].

Platin derivatives are one of the principal chemotherapy classes clinically used and whose mechanisms of action consist in interfering with DNA replication, blocking the cell cycle and inducing apoptosis in replicating cells. Cancer cells, which replicate and cause nonspecific cytotoxicity in healthy cells, are not the only factors causing the previously mentioned side effect [135].

Platin derivatives were discovered by Rosenberg in 1973[139–141] while he was studying bacterial culture observed that platin derivative compounds blocked cell proliferation. Owing to this cell blocking property, today half of all chemotherapeutic protocols for cancer treatment contain platinum derivatives [142] like cisplatin, carboplatin and oxaliplatin (Fig. 16) [143].

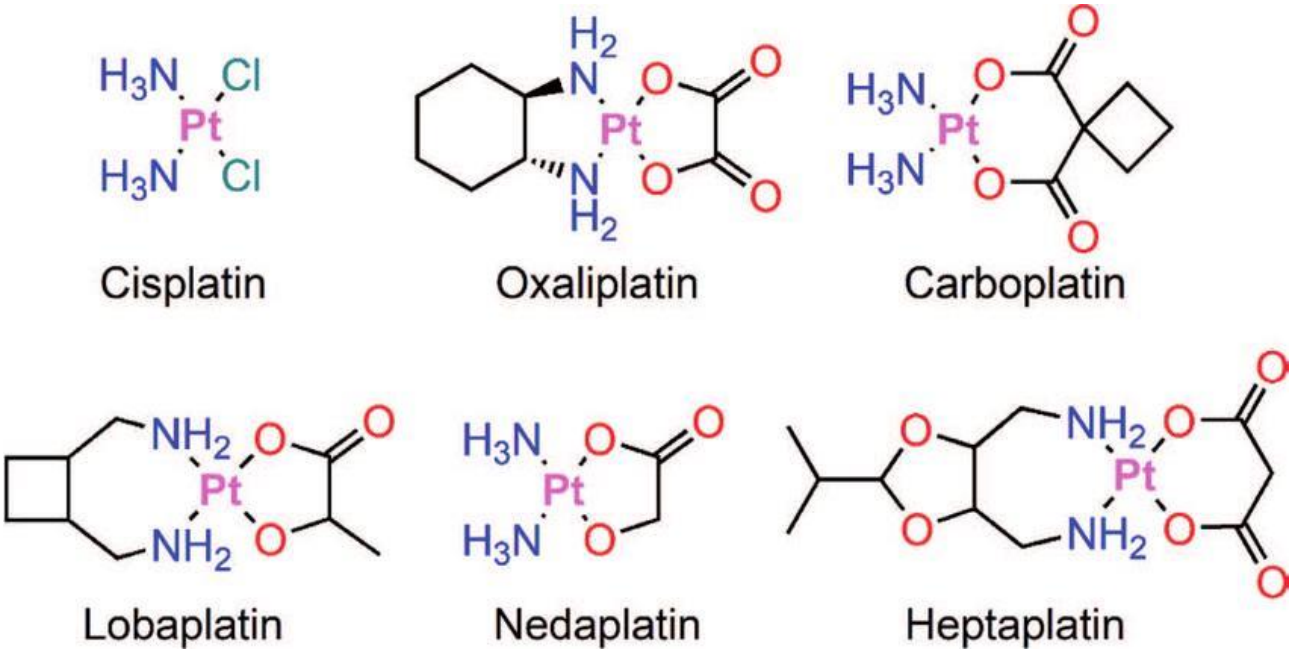

Figure 16. Chemical structures of Platin derivatives [143]

Cisplatin (cis-dichlorodiamineplatinum II; Fig. 17) (Cspl), in particular, was the first platinum-containing coordination complex applied for treatment of cancer as it was approved in 1978 for the treatment of testicular cancer [144].

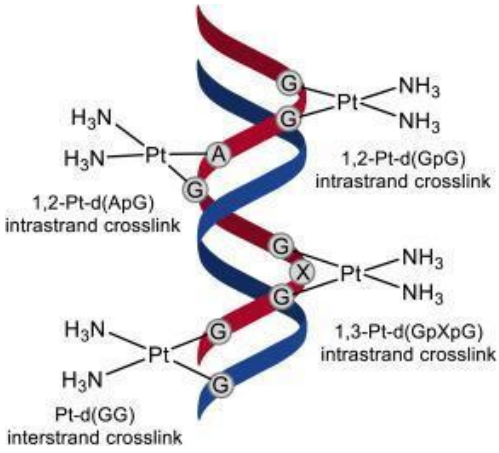

Figure 17. The species of cisplatin formed DNA crosslinks with cisplatin leaving two amino groups coordinated on the platinum atom. 1,2-Pt-d(GpG) intrastrand crosslink represents about 60%–65% of all cisplatin-formed adducts. 1,2-Pt-d(ApG) and 1,3-Pt-d(GpXpG) intrastrand crosslinks are formed with less frequency. The Pt-d(GG) interstrand crosslinks (ICLs) are formed with the lowest frequency. Image from[145]

Nowadays, Cspl is used in combination with other drugs for the treatment of solid neoplasms due to its synergistic effect.

Even if Cspl has been used for more than 30 years, its exact mechanism of action is not completely settled yet. The fundamental step so far accepted to induce cell death is stated to be DNA platination with the formation of intra-stranded and inter-stranded crosslinks, but recently it has been assessed that probably only 1-10% of intracellular cisplatin might eventually enter the nucleus and react with DNA. So other mechanisms of action are involved in Cspl toxicity, such as acidification of the cytoplasm, estrogen receptor (ER) stress, disruption of RNA transcription, inhibition of key oncogenic proteins, and decrease in metabolic plasticity of cancer cells and changes in their mechanobiology [146].

The chemical structure of Cspl shows a square planar structure constituted by a complex made by a metal platinum Pt linked to 2 chloride (Cl^-)and 2 ammonia (NH_3) ligands; this complex is water soluble and can assume a -*cis* or a *trans* conformation, but only the *cis* is showed pharmacologically active [147].

The 2 Cl^- allow reactivity with H_20 and other nucleophilic molecules but it hinges on the medium Cl^- concentration: the cytoplasmic Cl^- is lower (~4mM) than the serum Cl^- in the bloodstream(~100mM) so Cspl will remain neutral while it circulates in the bloodstream. Cspl passes the cell membrane thanks to passive diffusion but research has demonstrated that facilitated or active transport contribute to cisplatin uptake with intracellular accumulation. For example, OCTs but also CTR1 or MDR1 receptors weigh in Cspl uptake but also promote Cspl resistance (see below) [148]. After entering the cell, the low Cl^- concentration facilitates the hydration forming two main complexes monoaqua $[Pt(NH_3)2Cl(H_2O)]^+$ and diaqua $[Pt(NH_3)2(H_2O)_2]^{2+}$ [149]. These two complexes can bind nucleophile species in the cytoplasm and in the nucleus. The two most

important biological targets for cisplatin are DNA and RNA: the most favourable position for Cspl ligation with DNA is the N7 site of deoxy guanosine residue where Cspl forms one covalent bond named monofunctional Pt-DNA adduct, then a second reaction occurs between Cspl and an adenine base forming another cross link. With low affinity, a reaction with deoxyadenine can also occur. Crosslinks (also called platinum adducts) can be instrand, when both bases are on the same strand, or interstrand, when the bases are in different strands. Crosslinking formation induces DNA unwinding, DNA bending, replication inhibition, and transcription inhibition, which can further cause DNA strand breaks [145], all these modification can trigger diverse signalling pathways like AKT, c-ABL, p53, MAPK/JNK/ERK[150]. When the DNA repair mechanisms fail, cell death occurs due to necrosis or apoptosis [150,151].

The ataxia telangiectasia mutated (ATM) and ATM Rad3-related (ATR) kinases and other cellular proteins recognize these adducts and they are activated. ATM recognizes double strand breaks, auto-phoshorylates (p-ATM) and dissociates from inactivated homodimers to active monomers. p-ATM phosphorylates various substrates like the histone variant H2AX and checkpoint kinase 2 (Chk2) involved in cell cycle checkpoints. H2AX phosphorylation in histone 139, typical sign of cisplatin damage, activates the DNA damage response (DDR); while Chk2 becomes activated and phosphorylates downstream substrates including cell division cycle 25 homolog A (Cdc25A) and Cdc25C. Cdc25C becomes inactivated blocking the cell cycle. ATM also triggers p53 and meshes with ATR.

ATR detects stalled replication forks induced by 1,2-Pt-d(GpG) intrastrand crosslinks and phosphorites p53 and other proteins that cause cell cycle arrest and DNA repair. Another DNA repair mechanism involved in the aegis from cisplatin adducts is the nucleotide excision repair (NER) [151].

The adducts formed by oxaliplatin are sensed mainly by mechanisms that differ from those implicated in cisplatin adducts recognition; this variation allows changes in cytotoxicity and tumour range between these two platin derivatives [152].

Inside the cell, cisplatin ligates also intracellular molecules as cysteine-rich proteins like metallothionein, methionine or glutathione (GSH) and sequestrate them; for example the decrease of GSH in the cytoplasm causes oxidative stress but also cisplatin resistance as the cisplatin-GSH complex is excreted out of the cells by a member of the ABC family ATPases called multidrug resistance protein-2 (MRP2)[153]. Cspl, indeed, is a

metal compound with a high oxide-reductive potential so in high concentration or a long exposure time in the cytoplasm, many reactive oxygen species (ROS) will be created. Mitochondria are also damaged by Cspl in the electron transport chain. The chain disruption causes release of ROS in the cytoplasm, increasing oxidative stress and inducing apoptosis. Cytoplasmatic Ca^{2+} homeostasis is also modified by variations of mitochondrial respiration [147] this plays an important role in calcium homeostasis and therefore in the functions of the cell.

Despite the plethora of molecular actions that have been identified, the specific ones that are primarily responsible for the diverse set of toxicities remain unclear. However, some reports have indicated that, for instance, the oxidative stress induced by cisplatin is one of the mechanisms responsible for the severe nephrotoxicity and hepatotoxicity [154]. Although it has been postulated that cisplatin-induced DNA damage primarily affects proliferating cells, it has been proposed that the formation of DNA adducts is the primary contributor to dorsal root ganglion (DRG) neuron damage [152,155]. Indeed, despite the postmitotic nature of DRG neurons, in vivo studies have demonstrated that chronic cisplatin administration results in an accumulation of DNA adducts, leading to increased neuronal death. Furthermore, high DNA adduct levels have been shown to inhibit global transcription activities, which are essential for neuronal functions, given that neurons have a high metabolic rate. It can be therefore surmised that DNA damage can impede transcription processes, which may result in neuronal atrophy and disruption of neuronal connections. Furthermore, recent evidence has proposed that cisplatin-induced mitochondrial dysfunctions may serve as a secondary mechanism that contributes to and exacerbates neuronal damage.

Cspl enters the cell plausibly via organic cation transporters (OCTs). For example, OCT2 mediates the uptake of platin derivatives in the intestine, liver, kidneys, cochlea and dorsal root ganglia, allowing drug accumulation and unwanted toxic effect in these districts [156]. In the absence of cisplatin, these transporters serve to the absorption of substances and, in the gut, they contribute to the uptake of several dietary substrates [167].

Research by Santosa et al. [157] focused on the role of serotonin in cisplatin-induced nausea. They found that cisplatin triggers the release of serotonin in the gastrointestinal tract, which activates 5-HT3 receptors on

both the ENS and central nervous system, causing emesis and related symptoms. The relationship between ENS and cisplatin will be analysed in the next chapter.

The **interaction between Cspl and ENS** can result in both direct neuronal damage and changes in the neurochemical signalling pathways that regulate gastrointestinal function. Various authors including our laboratory group reported that platin derivatives cause important changes of the ENS implying both neuronal and glial populations as well as inflammation and secretion modifications [158–168]. Neuronal loss due to cisplatin is at the basis of motility alteration during cisplatin treatment that causes delayed gastric emptying and altered peristalsis [169]. Cisplatin also induces the activation of other pro-inflammatory cytokines, such as TNF-α and IL-6, that further exacerbate damage to the ENS. Inflammation affects the integrity of the epithelial barrier allowing an increase in gut permeability and bacterial translocation, which may further contribute to inflammation and neuronal damage, all leading to dysregulation of neurotransmission [169].

The epithelial barrier is made by the enterocyte and separates the gut luminal microbiota from the blood.

The gut barrier is composed also by the mucins and their secreted mucus. Mucus is a physical barrier for pathogens and commensal microbes and protects epithelium from mechanical damage as it allows dross and stool progression. The mucus contains antimicrobial peptides, proteins and secretory IgA (sIgA) which are produced by the immune system when it interacts with the resident microbes. sIgA promote anti-inflammatory responses at mucosal surfaces and have direct effects on immune exclusion of pathogens and pathogenicity factors. The enteric glial cells also contribute to the gut barrier homeostasis, as they modulate mucus secretion, epithelial barrier functionality and integrity.

The functions role and helpers of the microbiota will be described in the next chapter.

6.2 MICROBIOTA - MICROBIOME

The microbiota refers to the collection of microorganisms—such as bacteria, viruses, fungi, and archaea—that reside in a specific environment, particularly in and on the human body, animals, plants, soil, and other ecosystems. The term "microbiome" encompasses the genetic material of these microorganisms, as they collectively play a vital role in processes such as metabolism, immune system modulation, and disease prevention. Characteristics of the microbiota are the large diversity, the stability and resilience, the symbiotic

interaction with the host, the protection against pathogens. The gut microbiota plays a pivotal role in immune function against the colonization of pathogenic bacteria through a range of mechanisms, including the block of bacterial growth, the consumption of available nutrients, and the production of bacteriocins. It prevents pathogenic colonization through a number of competitive processes, including nutrient metabolism, pH modification, antimicrobial peptide secretion, and effects on cell signalling pathways. Furthermore, the microbiota helps to maintain the integrity of the intestinal epithelium. Additionally, recent studies have identified a critical role for commensal bacteria and their products in regulating the development, homeostasis, and function of innate and adaptive immune cells [170,171]. In the large intestine, which is characterized by slow flow rates and neutral to mildly acidic pH, obligate anaerobic bacteria are the dominant microorganisms, as they live in an environment with less than 1% of oxygen due to low concentration of oxygen in the lumen and in the mucus produced by goblet cells [13]. Resident bacteria break down ingested fibres to fermentation products that can: be absorbed by the enterocytes, form a niche protection against enteric pathogens, help colonic wound healing, regulate proliferation, differentiation, gene expression and maintain a functional immune system.

The fermentation products are short chain fatty acids (SCFA) and vitamins (like K, B, biotin folate). When dietary intake of vitamins is low in an individual, the colon plays a significant role in minimizing vitamin disparity. Acetate, propionate, and butyrate account for approximately 95% of colonic SCFA contents, and SCFA are also the preferred energy source for the colonic epithelium; their action will be described in chapter 3.7.

As stated above, bacteria are the most dominant group, and the main phyla in the mouse microbial community are *Firmicutes, Bacteroidetes, Proteobacteria,* and *Actinobacteria*. To identify and/or quantify the components of the gut microbiota, it is possible to extract and analyse nucleic acids (RNA and DNA) directly from stools and, define their taxonomy (phyla, classes, orders, families, genera and species). In particular, the amplification of the 16S ribosomal RNA gene (rRNA) and its sequencing, allows to highlight the diversity and the abundance of the microbiome [172]. There is a high interindividual variability, due to the diverse microbial composition between subjects [173] but the gut microbiota functions are highly preserved between individuals [172]. Approximately 90% of bacterial species belong to the phyla *Firmicutes* (genera as *Clostridium,*

Lactobacillus, Bacillus, Enterococcus and *Ruminococcus*) and *Bacteroidetes* (genera as *Bacteroides* and *Prevotella*), with the other important phyla being *Actinobacteria* (mainly *Bifidobacterium genus*), *Proteobacteria* (genera as *Escherichia* and *Helicobacter*), and *Verrucomicrobia* (*Akkermansia genus*) [174]. The relative abundance of these phyla varies based on factors such as diet and environment [175]. *Firmicutes* and *Bacteroidetes* phyla are the most investigate either for their abundance or because they have been associated with metabolic health and obesity in mice [176].

Bacteroidetes is a phylum of bacteria that includes several important genera such as *Bacteroides*, *Prevotella*, and *Parabacteroides*. These bacteria are often involved in polysaccharide degradation, of plant origin in particular, helping the host extract calories and nutrients from food that would otherwise not be accessible, thus contributing to energy metabolism. They are also involved in gut health and immune system modulation [177]. Complex polysaccharides (e.g., fibers and resistant starches) are indigestible by the host but Bacteroidetes utilize a range of glycoside hydrolases to degrade these complex carbohydrates into simpler sugars. Simple sugars can then be fermented by the bacteria into short-chain fatty acids (SCFAs), such as acetate, propionate, and butyrate. These SCFAs provide an energy source for both the bacteria and the host, especially for the enterocytes, and also have anti-inflammatory properties [178,179]. Bacteroidetes are also able to induce regulatory T cells that help the maintenance of immune tolerance and prevent excessive inflammation, which is crucial to avoid autoimmune conditions [180].

Firmicutes is another large phylum, with key genera including *Lactobacillus*, *Clostridium*, *Faecalibacterium*, and *Enterococcus*. These bacteria can ferment a broader range of carbohydrates, including complex sugars, and they are also involved in protein fermentation; Firmicutes have a higher capacity to extract energy from complex food sources and the fermentation of dietary fibers (like non-digestible carbohydrates) produces SCFAs and also lactic acid. Lactic acid is produced in particular by *Lactobacillus* species*;* this molecule lowers the gut pH and creates an environment that inhibits the growth of pathogenic microorganisms, while promoting the growth of beneficial bacteria [181]. Mu and coll. [182] demonstrated that in mice affected by lupus-nephritis there is a decrease in *Lactobacillus spp* in the gut microbiota. The administration of a mixture of *Lactobacilli*, exerted an anti-inflammatory effect by repairing the damaged gut barrier, suppressing proinflammatory factors in the lymphatic circulation, while improving renal function and prolongating mice

survival to lupus nephritis. Other species, such as *Faecalibacterium prausnitzii*, are known for their anti-inflammatory properties, too. Sokol and coll.[183] found that Crohn disease (CD) patients with a reduction in this Firmicutes member have a higher risk of post-operative recurrence of ileal CD. *In vitro* the supernatant of *F. prausnitzii* bacterial cultures abolished IL-1β-induced NF-κB activity in Caco-2 cells transfected with a reported gene for NF-kB activity. *In vitro* peripheral blood mononuclear cells stimulation with F. *prausnitzii* led to significantly lower IL-12 and IFN-γ production levels and higher secretion of IL-10. *F. prausnitzii* produces butyrate using acetate or glucose, but only when acetate levels are low. Butyrate nourishes enterocytes and enhances the expression of tight junction proteins[183]. A further description of butyrate function can be found in chapter 6.4.

The microbiota is also able to synthesize neurotransmitters, for example *Lactobacillus plantarum* produces *Acetylcholine* (Ach) [184]. Thus, change in the microbiota composition could also affect physiological neurotransmission, i.e. the Ach that can increase the frequency of gut contraction *in vivo*.

Dysbiosis is an imbalance in the gut microbiota with reductions in beneficial microbes and increases in potentially pathogenic ones. Dysbiosis can enhance inflammation and has been associated with autoimmune diseases like colitis [185]. A high-fat diet can promote an increase in *Firmicutes* relative to *Bacteroidetes*, and in animal models, a **higher Firmicutes-to-Bacteroidetes (F/B) ratio** has been observed in obese individuals compared to lean individuals. High-fat diets induce a vicious circle in which Firmicutes are more efficient in energy extraction from food so their increase, may causes even more weight gain [176].

Tan and coll. [186] demonstrated that an altered microbiota composition and metabolism with differential glutamate production leads to increased appetite in mice and leads to obesity, arguably due to the interaction between microbiome and intestinal enteroendocrine cells in the gut. Conversely, a decrease in F/B ratio diminishes the capability of the microbiota to extract energy from food and can lead to mucositis, diarrhoea and to weight loss [187]. Guo et al. (2022) determined that the main phyla of wild-type mouse gut microbiota were *Firmicutes* and *Bacteroidetes*, and the main genera were *Lactobacillus, Blautia, Bacteroides, Ruminococcaceae, and Clostridioides*[188]. The gut microbiota in C57BL/6J mouse strains is more stable and complex than that in BALB/c mouse strains, so C57BL/6J mice can be a good model to evaluate drug effects on microbiome composition [188].

Cisplatin's effects on the microbiome are significant and multifaceted: first, cisplatin penetrates all replicating cells including microbes. Cisplatin penetration causes death of eukaryotic and prokaryotic. This change alters the "commensal microbiome barrier" and the epithelial barrier, leading to microbial infiltration of the mucosa. Theinterplay between cisplatin and resident gut cells (either eucaryotic or prokaryotic) has important implications for chemotherapy side effects, treatment efficacy, and potential therapeutic interventions to improve patient outcomes. In 2014, Montassier et al [189] observed a considerable decrease in the diversity of the gut microbiota during a 5-day high-dose chemotherapy study in humans. The population of *Firmicutes* sp. and *Actinobacteria* sp. were found to be reduced drastically, whereas those of *Bacteroidetes* sp. and *Proteobacteria* sp. were increased. More recently, a study by Alsholi et al. [190] indicated that **Firmicutes** and **Bacteroidetes**, were affected by cisplatin treatment, and that restoring the microbiome could ameliorate some of the GI side effects. It also stated that the gut microbiome plays a crucial role in modulating the body's immune responses during chemotherapy, and its alteration due to cisplatin could affect the treatment outcomes [191].A study by Yu-Ping Hsiao et al.[192] found that cisplatin chemotherapy in mice led to significant changes in the gut microbiota, characterized by a reduction in beneficial bacteria like *Lactobacillus* and an increase in harmful bacteria like *Clostridia.* Cisplatin administrations results in a reduction of microbial diversity, which is often associated with negative health outcomes. The increased gut permeability caused by cisplatin allows bacterial products, such as lipopolysaccharides, to enter the bloodstream, triggering an immune response and further exacerbating the microbiota imbalance. These studies [191,192] suggest that microbiome-based therapies, such as the addition of probiotics or prebiotics to the diet or faecal microbiota transplants (FMT), could be helpful to restore the microbial balance and reduce the negative effects of cisplatin on the gut microbiota. Nowadays there are also some preclinical studies, like those by Chambers et al.[193], highlighting that modulating the microbiome can enhance the therapeutic response to cisplatin and reduce its toxicity also in humans.

In the present work we will focus on the use of prebiotics as a font of specific dietary fibres that can increase the abundance of beneficial microbes such as *Bifidobacteria* and *Lactobacilli*. Dietary influences also the production of metabolites such as short-chain fatty acids (SCFAs), which affect gut health and immune system function [194].

6.3 PREBIOTICS

Prebiotics are defined as selectively fermented ingredients that result in specific changes in the composition and/or activity of the gastrointestinal microbiota, with beneficial effect on the host. Fermentation is a process by which a microorganism transforms food into other products, usually through the production of lactic acid, ethanol and other metabolic end products, like short chain fatty acids (SCFAs) or tryptophan metabolites or secondary bile acids.

Prebiotics compounds were first introduced in 1995 by Glenn Gibson and Marcel Roberfroid[195] and recently reviewed by the World Gastroenterology Organisation in the Global Guidelines for Probiotics and prebiotics [196].

Prebiotics pass the stomach without major hydrolysis and are resistant to digestive enzymes. Those substances reach the colon where they are expected to protect the gut environment, serving as substrates to promote the growth and activity of trillions of beneficial microbes while limiting the growth of the pathogen ones. The metabolites produced by the microbes may then improve gut health and sustain both microbes and host survival, protecting the immune barrier from damage caused by pathogens. Typically used prebiotics are oligosaccharides like oligofructose (fructooligosaccharides, FOS), inulin, galactooligosaccharides (GOSs), lactulose and breast milk oligosaccharides (human milk oligosaccharides or HMOs), no starch polysaccharides and recently also resistant starch, conjugated linoleic acid, and polyphenols. Prebiotics have been shown to have beneficial effects on oligofructose fermentation by resident bacteria, to increase fecal weight, bifidobacteria numerosity, calcium absorption, shortening gastrointestinal transit time, lowering blood lipid levels [197].

Inulin effect on microbiota composition was tested by Li and collaborators [198] in mouse models where it produced an increase in the population of *Bacteroides* spp. and *Akkermansia muciniphila*.

Guo and coll. reported that [188] in C57BL6 /J mice fed with high-fiber diet (HFD) for 4 weeks and observed that inulin promoted the expansion of short chain fatty acids (SCFA)-producing Ruminococcaceae and Lachnospiraceae bacteria, which increased the faecal SCFA concentrations. Inulin also increased the levels of Bacteroides and Bifidobacteria. Hamilton and coll. [199] reported that inulin can also help post-injury enteric

recovery, via SCFA metabolites that prevent ENS disfunction in injured mice and this is Interleukin-10 signalling dependent.

Summarizing the existing literature, we can assess that prebiotics dietary supplementation may support resident microbiota and have a direct effect on the immune system. Thus, using molecules such as inulin, to support the microbiota during chemotherapy can be beneficial, although individual responses may vary. Increasing the amount of nutrients to a depleted population of Bifidobacteria and Firmicutes may help to maintain a balanced and diversified microbiota in the colon, which is crucial for gut health. Chemotherapy often causes gastrointestinal side effects like diarrhoea and constipation. A balanced gut microbiota, supported by prebiotics, can help alleviate these symptoms by promoting regular bowel movements and reducing inflammation in the colon. Prebiotics may help strengthen the gut barrier, preventing harmful substances from leaking into the bloodstream. This can be important during chemotherapy when the gastrointestinal lining may become more vulnerable due to the treatment. A healthy gut microbiota plays a role in supporting the immune system and the supplementation of prebiotics can help maintain a strong immune response. It's important to note that while prebiotics may have these potential benefits, individual responses may vary, and not all chemotherapy patients will experience the same effects. Furthermore, the choice of prebiotics and their dosage should be discussed with a healthcare provider to ensure they are appropriate for each specific situation as there is not a consensus of the dosage in humans so far. Additionally, it's crucial to consider the overall dietary and nutritional needs of cancer patients during chemotherapy, as a well-balanced diet and proper hydration are fundamental for managing side effects and promoting recovery.

6.4 Short-Chain Fatty Acids (SCFA)

Short chain fatty acids (SCFA) are carboxylic organic acids with an aliphatic tail and are produced by Bacteroidetes and Firmicutes. They include **formic, acetic, propionic, butyric, isobutyric, valeric, and isovaleric** acids. Fig. 18 shows the structure of these acids. Acetic, propionic and butyric acids are the three main aliphatic SCFA and represent 95% of the gut and faecal SCFA, with a molecular ratio 60:20:20 that is relatively constant in the colon as well as in the faeces. Acetic and propionic acid are effectively absorbed

from the colonic lumen, and they represent 10% of the animal daily energy intake, while butyric acid is one of the principal energy sources for colonocytes. SCFA are mainly produced in the caecum and in the proximal colon [200].

Carbon number	Nomenclature		Anion		Chemical structure
	Common	IUPAC	Common	IUPAC	
1	Formic acid	Methanoic acid	Formate	Methanoate	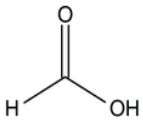
2	Acetic acid	Ethanoic acid	Acetate	Ethanoate	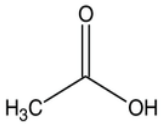
3	Propionic acid	Propanoic acid	Propionate	Propanoate	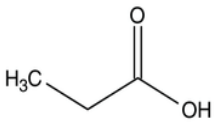
4	Butyric acid	Butanoic acid	Butyrate	Butanoate	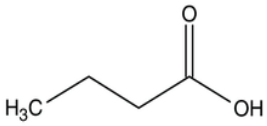
4	Isobutyric acid	2-Methylpropanoic acid	Isobutyrate	2-Methlypropanoate	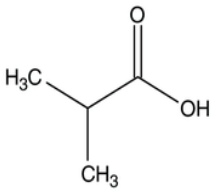
5	Valeric acid	Pentanoic acid	Valerate	Pentanoate	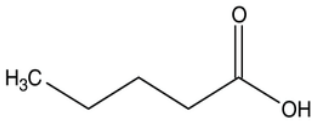
5	Isovaleric acid	3-Methylbutanoic acid	Isovalerate	3-Methylbutanoate	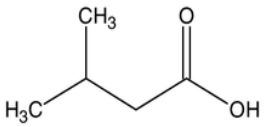

Figure 18. A list of Short Chain Fatty acids [201].

These acids are major candidates for mediating crosstalk between microbiota and ENS but also between microbiota and brain (through the microbiota-gut-brain axis) [202]. Fig. 19 summarizes the effects of acetate, propionate and butyrate. SCFAs constitute specific products of bacteria like *Bifidobacterium* sp. and *Lactobacillus* sp. The growth and proliferation of intestinal epithelium are sustained by these three compounds. *In vitro* in *lamina propria* culture cells obtained from intestinal biopsies of CD patients, butyrate administration (2mM and 10mM) significantly decreased tumour necrosis factor (TNF) and proinflammatory

cytokines compared to untreated cell cultures. Butyrate i*n vitro*, also helps regulating the immune system, suppressing excessive response to lipopolysaccharide and promoting a balanced immune response. While *in vivo*: butyrate (150mM) administration to mice infected with *Clostridium difficile*, protected mice gut from the infection as it improved gut health as observed with histology. It seems that butyrate is a good anti-inflammatory agent by improving immunomodulation. Apart from this, butyrate has many other positive effects on the body, including reduction of oxidative stress and electrophilic products detoxifying [203].

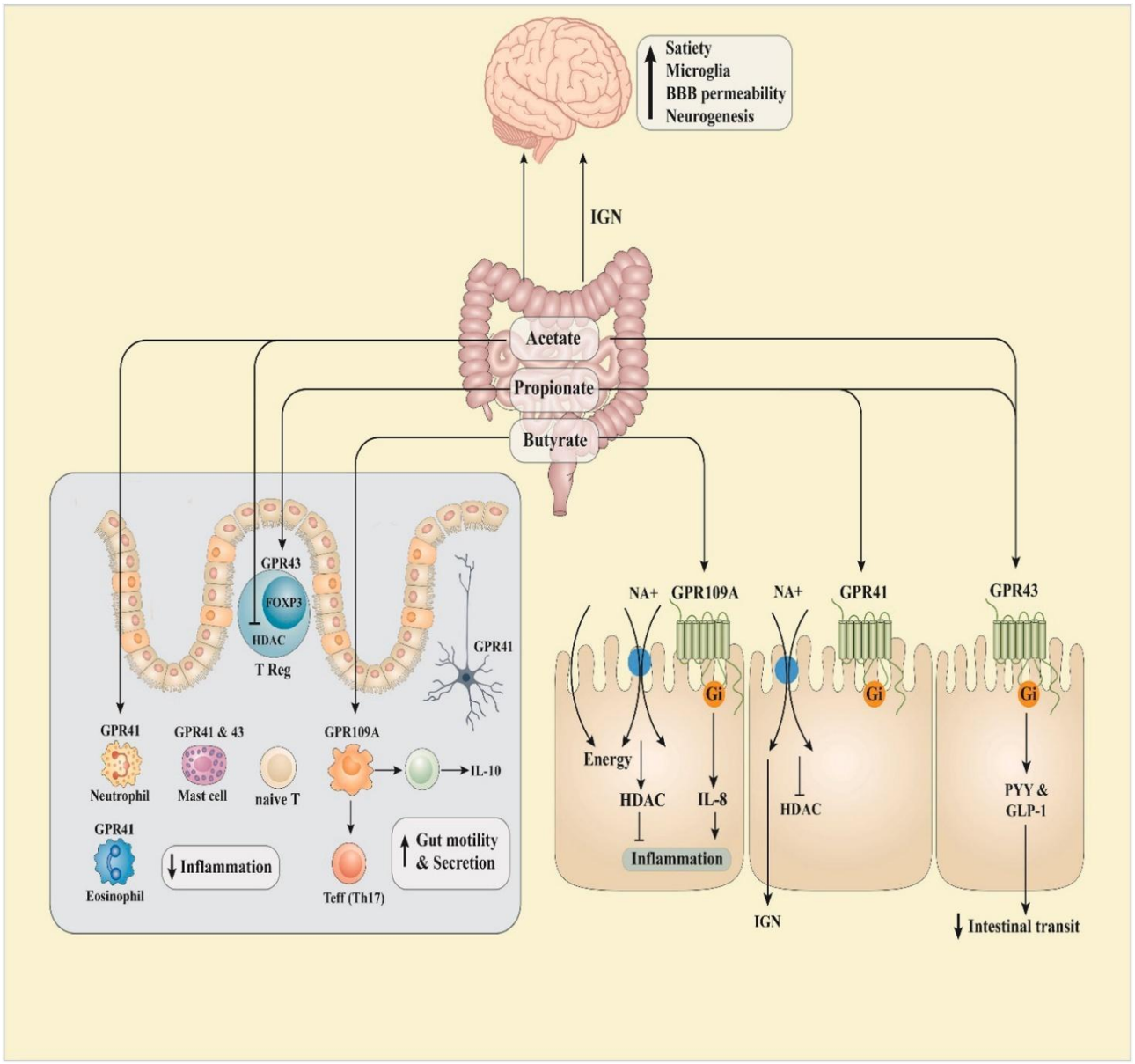

Figure 19. The various activity of microbiota-derived short-chain fatty acids (SCFAs). SCFAs enter the cells of the distal gut through simple diffusion or Na+-coupled SLC5A8-mediated transport and act as a histone deacetylases (HDAC) inhibitor or an energy source. Luminal propionate or acetate induces the production of Glucagon Like Peptide-1 (GLP-1) and peptide YY (PYY) in a GPR41- and GPR43-dependent fashion, which affects satiety and intestinal transit. Luminal butyrate inhibits inflammatory effects through HDAC inhibition and GPR109A activation. Besides, propionate is converted into glucose by intestinal gluconeogenesis (IGN), leading to satiety and reduced hepatic glucose production. SCFAs also act on the Enteric nervous system (ENS) and stimulate motility and secretory activity. Immune cells in the

intestinal lamina propria can also be affected by SCFAs, which reduces inflammation. SCFAs can also affect other tissues, such as the brain, through circulation and induce beneficial metabolic effects[203].

In the epithelium, many enteroendocrine cells (EECs) express several G-protein-coupled receptors (GPCRs) through which SCFAs may act, including the fatty acid receptor 2 (FFAR2 or GPR43) and 3 (FFAR3 or GPR41). FFAR3 is also expressed by a subset of enteric neurons [204]. Whether SCFA signal to neurons via mediators released from EECs or by diffusing through the epithelium directly acting on underlying enteric neurons, or both, remains unclear. Nonetheless, commensal bacteria acting via SCFA have been shown to increase the density of ECCs and upregulate Tph1 expression (Tph1 encodes the synthesizing enzyme for 5-HT), which, in turn, impacts ENS activity by modulating serotonergic signalling [205,206].

The use of SCFAs in combination with cisplatin could increase chemotherapy efficacy. As reported in the previous paragraph, SCFAs are also ligands of two orphan GPCRs, GPR41 and GPR43, which inhibit histone deacetylases (HDACs), modulate cell proliferation, and induce apoptosis.

GPR43 is highly expressed in the colon while its expression decreases in colorectal adenocarcinomas [207]. Kaboyashi and coll. [208] demonstrated *in vitro* that propionate and cisplatin synergistically and significantly induce apoptosis of HepG2 human hepatocellular carcinoma (HepG2) cells by increasing expression of autocrine TNF-α via reduction of HDACs through GPR41 signalling. Also, SCFA have immune-modulatory properties and the ability to alter cellular metabolism, which might reduce resistance and augment cisplatin's cytotoxic effects. SCFA improve immune cell infiltration and activation in tumours, thereby enhancing cisplatin's efficacy, and potentially overcome the immunosuppressive tumour microenvironment. SCFA epigenetic modulation capabilities, such as HDAC inhibition, might sensitize cancer cells to cisplatin.

7 RESEARCH STUDY 2:

7.1 IRRITABLE BOWEL SYNDROME (IBS)

Irritable bowel Syndrome (IBS) is a non-life threatening characterized by symptoms like bloating, constipation or diarrhoea resulting from non-infectious inflammation of the colon.

Depending on predominant stool pattern, IBS can be classified into four subtypes: IBS with constipation (IBS-C), IBS with diarrhoea (IBS-D), IBS with mixed bowel habit (IBS-M), or IBS unclassified (IBS-U; where stool pattern cannot categorize the person accurately into one of the other three subtypes). The symptom-based diagnostic criteria, such as the Rome criteria, were developed by consensus among experts in the field, the last one published as the Rome IV criteria, in 2016. In 2020, a meta-analysis [209] reported a global prevalence ranging from 3.8% to 9.2%, depending on the diagnostic criteria applied. In 2023, the Italian consensus on IBS reports a prevalence rate ranged between 1.3% and 7.6%, with a pooled prevalence of 4.1% using Rome IV criteria [210].

The diagnosis of IBS is made with psychological comorbidities assessment and the exclusion of other pathologies and alarm symptoms, together with the digital rectal examination, full blood count, C-reactive protein, serology for coeliac disease, breath test for lactose intolerance, and faecal calprotectin assessment. Endoscopy (gastroscopy or colonoscopy) should also be employed to exclude the presence of inflamed/ulcerated tissue [210,211].

Patients with IBS report episodes of abdominal pain or discomfort, hypersensitivity, abnormal motor responses, diarrhoea, but many patients also experience fluctuation with asymptomatic periods and remission or exacerbation. IBS patients show brain-gut axis dysfunction, low-grade inflammation, mucosal barrier alterations and dysbiosis [212]. The syndrome impacts significantly patients' quality of life but does not present alarm features as bleeding or mucositis as in inflammatory bowel disease (IBD). IBS can evolve to IBD if there is an hyperactivation of the immune system attacking the GI tract, causing exacerbation of gut inflammation and ulceration [213].

IBS is thought to be caused by stress, intestinal motility disfunction, and dysbiosis; faecal microbiome seems to be impaired (dysbiosis) in both IBS and IBD which indicates an organic component [214,215]

The exact cause of IBS is still unknown, but 80% of patients show psychological disorders like anxiety or depression. An increase of gut symptomatology can worsening of the psychological or psychiatric condition; vice versa the increase in severity of the psychiatric condition can exacerbate IBS symptoms[212,216].

IBS exacerbation can also happen in periods of psychological stress. Stress will be defined in the next chapter. 3.5). The first line of treatment for IBS is diet: with traditional dietary advice suggested as first line approach [210], while second line approach is a diet with a low percentage of fermentable oligosaccharides, disaccharides, monosaccharides, and polyols (low FODMAP diet). FODMAP are in fact carbohydrates that in some individuals are not well absorbed by the small intestine leading to bloating or abdominal pain, so their decrease should reduce these symptoms. Supplementation of soluble but not insoluble fibre can be used to treat IBS symptoms as well as probiotics as a combination of *Lactobacillus, Bifidobacterium*, and *Escherichia*, can be useful to improve abdominal pain. In patients with IBS without constipation, molecules as rifaximin and antispasmodics can be administrated for global symptom improvement. Antispasmodics are a group of substances that include direct smooth muscle relaxants (e.g. papaverine, mebeverine), anticholinergic agents (e.g., butylscopolamine, hyoscine, cimetropium bromide, pirenzepine) and calcium channel blockers (e.g., alverine citrate, otilonium bromide, pinaverium bromide, peppermint oil). For some of these molecules the pharmacological action is not fully known and the mechanisms are often mixed. In the chapter 3.5 the action of the calcium channel blockers, otilonium bromide, will be discussed.

To diminish abdominal pain in adult patients, tricyclic antidepressant (TCAs) can be administrated, these molecules can also induce global relief, but also selective serotonin reuptake inhibitors (SSRIs) can be administrated. IBS-C patients can take a minimally adsorbed osmotically acting laxative like polyethylene glycol (PEG) to treat constipation; the dose must be titrated on stool consistency; another possible therapy for these patients is based on secretagogues (like linaclotide, the only one approved by the European Medical Administration so far), but a consequence can be diarrhea. In IBS-C patients that have failed other therapies also 5-HT4 agonists can be given. In IBS-D patients with proven bile acid malabsorption, bile acid sequestrants can be administrated. In IBS-D who have failed conventional therapy 5-HT3 antagonists is used to treat global

symptoms; while opioid agonists can be given to manage diarrhea and mixed opioid agonists/antagonists to treat global IBS-D patient symptoms.

7.2 OTILONIUM BROMIDE

Otilonium bromide (OB) is a quaternary ammonium derivative (Fig. 20) weakly absorbable from the GI tract [217] and almost completely excreted in the faeces in about 7 days. Menarini discovered this drug. It seems that after oral administration it accumulates and acts in the large intestine [218]. OB has a trivalent action: it relieves abdominal pain and spasms and reduces pain transmission to the CNS. The first two actions are due to its capability to blocks L-type calcium-channels, and to bind also muscarinic M1, M2, M4 and M5 receptors, the third is carried out by its antagonist action on tachykinin NK-2 receptors, decreasing peripheral sensory afferent transmission to the CNS. For these reasons OB is a worldwide used and effective drug to control the signs and symptoms of IBS. OB also interferes with neurotransmission and affects the bacterium population of the microbiota [219–225]. In adults the dosage is 40-80mg taken 2-3 times before meals. In 2018 Evangelista and coll. [221] made a systematic review about otilonium bromide actions but, so far, the cellular mechanisms responsible for the efficacy of OB in controlling IBS symptoms is not completely understood. The use of animal models treated with this drug could help in comprehending the pathogenesis of IBS.

OB pharmacokinetics has been investigated administering [^{14}C]-OB to rats and dogs and healthy volunteers. In the plasma, the level of radioactivity was very low, with no accumulation in red blood cells. Less than 1% radioactivity was excreted in urine 96h after administration while up to 97.8% of radioactivity was excreted in faces in 7 days [217].

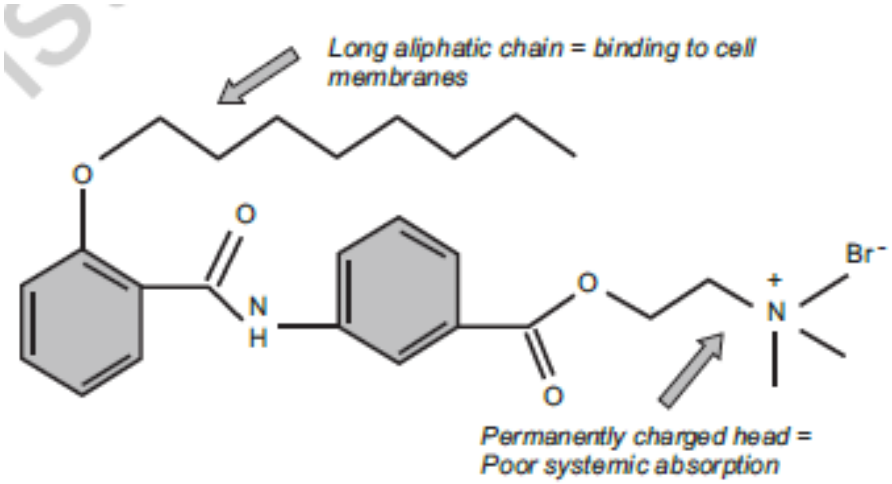

Figure 20. Otilonium Bromide structure. From [221].

Using light microscope autoradiography in rats it was demonstrated *ex vivo* that the affinity of [14C]-OB for stomach and small intestine was 50 times lower respect to colon and rectum, so when administrated *in vivo* with intracolonic injection, the [14C]-OB localized in the muscular layer, decreasing in the mucosa already 15 minutes after injection. Amenta and D'Amico [217] confirmed colonic muscular layer preferential uptake also doing a similar procedure in colonoscopy. Evangelista et al (2018) [226] confirmed the same preferential localization of OB in rats, after oral administration of 2mg/kg [14C]-OB, reporting that [14C]-OB levels in the plasma were 1000 times lower than in the colon. Catalioto and coll. [227], reported that OB absorption is facilitated by bile salts, that the drug is transported paracellularly and that p-glycoprotein stimulates OB efflux, adjuvating the removal of the drug in excess. What makes OB a safer drug respect to other Ca2+ channel blockers is that it is bereft of atropine-like side effect at both central and peripheral level and it allows gastric emptying [221].

OB exerts smooth muscle relaxation through various mechanisms, in fact, OB blocks Ca2+ influx and efflux, acting on Voltage-Gated Calcium channels (of L-type) and also blocks tachykinins (NK2) and muscarinic (M2) receptors on SMCs, both *in vitro* and *in vivo* [221].

The spasmolytic action induced by OB looks to be due to OB inhibitory action on T-type VGCs channels, as so, OB inhibits membrane depolarization and muscle contraction ascribable to cholinergic and methacholine excitatory junction potential, in facts OB reduces methacholine-induced membrane depolarization and the

subsequent SMC contraction [221]. Thanks to OB action on VGCs channels, OB also inhibit NK1 receptor activation downstream, while it blocks NK2 receptor upstream to L type VGCs [221].

Studying motility interference of OB in gastrointestinal preparations, it was observed that OB inhibits the muscle contraction induced either electrically or chemically (adding Acetylcholine, $BaCl_2$, carbachol, histamine, serotonin and tackykinis). It was also reported that OB inhibits epithelial M3 muscarinic receptors with a potential antisecretory activity, important to decrease diarrhoea in IBS-D patients [221].

OB reduces visceral sensitivity but its beneficial effects need repeated and prolonged treatment. Prolonged treatment causes similar effects as single once. OB in facts blocks of L-type VCGs channels and induces NK1 receptor internalization in SMCs, making NK1 receptor unfunctional. NK1 disfunction decreases SP expression; on the opposite, long OB administration has no effect on NK2 receptor expression. The effect of OB on ENS was also evaluated, noticing that in myenteric neurons of rat colon it gives rise to internalization of L-type Ca2+ channel, decrease in nNOS expression and increase in NK1 receptor immunoreactivity. Chronic OB expression modifies excitatory and inhibitory junction potentials in electric field stimulation experiments. Those observation permit to assess that OB could act on neuron-to-neuron communication at the presynaptic level, interfering with the changes of colonic myenteric and submucous neurons induced by psychosocial stress. Finally, OB is also able to interfere with cortical releasing factor (CRF), which is the primary psychosocial stress mediator secreted by the hypothalamus. CRF binds to CFR receptors (CFR1 and CFR2) and when CFR is injected it induces visceral sensitivity and increased colonic transit; in chronic stress rats CFR receptors are increased; OB, given chronically, prevents the increase of CFR1 receptor but not CFR2 receptor [221].

7.3 PSYCHOSOCIAL STRESS

In the previous chapter, we assessed that among the possible etiopathogenetic factors for IBS, psychosocial stress might have a main role. In this chapter we define what stress is. Stress is a state of mental strain caused by mentally or physically threating situations. The response to acute stress is essential for survival with the activation of the “fight-or-flight” mechanisms. However, as confirmed by many

epidemiological studies, recurrent psychological stress exacerbates IBS symptoms as intestinal inflammation is exacerbated by the constant activation of pathways associated with the “fight-or-flight” mechanisms [228].

In psychosocial stress response, five systems are involved: the sympathoadrenal system, the hypothalamic-pituitary-adrenal axis (HPA Axis), the renin-angiotensin-sldosterone system (RAAS), the arginine vasopressin (AVP) and the immune system.

The instantaneous or acute (seconds to minutes) "fight or flight"-type stressful situation is due to the activation of the sympathoadrenal system [229,230], which encompasses the sympathetic nervous system and the adrenal medulla [231]. Originating in the spinal cord, the sympathetic nervous system innervates (via norepinephrine neurotransmitter) various target tissues and organs to generate physiological adaptations to stress [232]. The adaptations include increased cardiac output, leading to enhanced blood flow and oxygen supply to skeletal muscles and vital organs [233]. Simultaneously, there is vasoconstriction to reduce blood supply to non-essential organ (skin, digestive system, kidneys, reproductive system, and extremities)[234] that can tolerate a temporary hypoperfusion without compromising vital functions or immediate survival. Also, bronchial dilatation occurs to improve oxygen intake, and mydriasis enhances visual acuity [235]. The endocrine extension of the sympathetic nervous system, the adrenal medulla, releases epinephrine (80%) and a smaller amount (20%) of norepinephrine[236] into the systemic circulation. While both catecholamine hormones have similar vasoconstrictive effects, the former has broader systemic impact e.g., enhanced cardiorespiratory performance, glycogenolysis, and lipolysis [235]. Negative feedback mechanisms within the sympathoadrenal system are aimed at preventing overstimulation. For example, the paraventricular nucleus (PVN) of hypothalamus receives a feedback from the locus coeruleus to modulate the sympathetic response [236]. These axis releases neurochemical factors in a highly controlled fashion to fine-tune the overall stress response. The HPA Axis is made of three components connected via reciprocal interactions, namely, 1) the PVN secreting corticotropin-releasing factor (CRF) into the hypothalamic-pituitary portal system during stress exposure; 2) the anterior lobe of the pituitary gland reacting to CRF by releasing adrenocorticotropic hormone (ACTH) into the bloodstream. The ACTH is sensed by 3) the middle fasciculate zone of the adrenal cortex, which releases glucocorticoid cortisol[236]. Cortisol facilitates stress response by mobilizing energy reserves (via gluconeogenesis and diminished insulin’s secretion and signalling), increasing blood pressure,

and suppressing the immune system [236]. Rising plasma cortisol concentrations exert negative feedback on the hypothalamus and pituitary gland via the medial prefrontal cortex and hippocampus, inhibiting the release of CRF and ACTH, respectively [236]. The integration of the sympathoadrenal system and HPA axis involves intricate feedback mechanisms synchronizing several brain nuclei [236]. The amygdala and related limbic regions [236] such as prefrontal cortex and hippocampus serve as a key interface between the perceptual and cognitive appraisal of a stressor with the ensuing physiological responses by providing emotional and contextual information to the PVN, which, in turn, regulates sympathetic activity and coordinates the release of HPA axis' hormones [236]. When the PVN detects a stressful or threatening stimulus, it initiates the sympathoadrenal response to stress by triggering norepinephrine release from the locus coeruleus responsible for augmented body's sympathetic activity [236], arousal as well as attention prioritization across stressful challenges. The locus coeruleus neurons' activity is tightly regulated by the convergence of several inputs, particularly the CRF [236]. Cortisol modulates the release of epinephrine and norepinephrine whereas catecholamines can stimulate the HPA axis to release more cortisol[236]. Prolonged- or chronic (minutes-hours) stress is characterized in more complex interactions [236]. By and large, three classes of interaction (co)exist between sympathoadrenal system and HPA axis, including addition, competition, and synergism. During acute stress, sympathoadrenal systems' activity may predominate against the backdrop of a relatively limited HPA axis' activation [236]. Conversely, over time, the HPA axis becomes prominent and the interactions between the two systems gradually shift from competitive to synergistic [236]. Cortisol plays a role in both stress response modes by interacting with two types of receptors: type 1 (mineralocorticoid receptors - MR) and type 2 (glucocorticoid receptors - GR). These receptors are found in the limbic neural circuitry [236]. MR regulate the baseline sensitivity or threshold of the fast stress system, thereby preventing disruption of homeostasis [236]. On the other hand, GR facilitates the recovery process by dampening stress responses in stress circuits and mobilizing energy resources [236]. During acute stress sympathoadrenal systems' activity may predominate against the backdrop of a relatively limited HPA axis' activation [236]. Conversely, over time, the HPA axis becomes prominent and the interactions between the two systems gradually shift from competitive to synergistic [236]. Cortisol plays a role in both stress response modes by interacting with two types of receptors: type 1 (mineralocorticoid receptors - MR) and type 2 (glucocorticoid receptors - GR).

These receptors are found in the limbic neural circuitry [236]. MR regulate the baseline sensitivity or threshold of the fast stress system, thereby preventing disruption of homeostasis [236]. On the other hand, GR facilitates the recovery process by dampening stress responses in stress circuits and mobilizing energy resources [236]. When there is an exhaustion of the homeostatic abilities to shield the body's myriad systems from cumulative wear and tear [236], the allostatic load emerges, due to a prolonged sympathoadrenal stimulation with the disruption of negative feedback mechanisms [236]. Clinical manifestations of this condition are hypertension, disrupted sleep patterns, compromised immune function, abnormalities in gastrointestinal motility, and disturbances in glucoregulatory function [236].

Acute stress favours humoral immunity by down-regulation of T helper 1 cells and up-regulation of T helper 2 cells-mediated cytokine activity [236]. Stress-induced activation of the sympathoadrenal system predominately amplifies proinflammatory pathways engaging interleukin (IL) 6 and 8 [236] as the body prepares to possible infections due to injuries during stressful periods. Proinflammatory ILs released during immune responses stimulate hypothalamus to increase AVP and the HPA axis' activity [236], leading to cortisol surge that dampens proinflammatory cytokines like IL-6, TNF-α and IL-1β [236]. Prolonged stress may dysregulate immune function including an overproduction of proinflammatory ILs and an underproduction of anti-inflammatory ILs manifested in susceptibility to infections, and the development of inflammatory and autoimmune conditions [236].

Psychosocial stress has been shown to induce dysbiosis in mouse models of IBD altering the landscape of myeloid cells in the colon, with an accumulation of inflammatory monocytes that elevate the levels of TNF leading to TNF-mediated colitis exacerbation. Furthermore, chronic stress can involve also the gut-brain axis by inducing chronical elevation of glucocorticoids that mediate the impact of stress perception by the brain [226,228,237,238].

CRF is one of the first mediators of psychosocial stress in mammals. When CRF is injected in humans or in experimental animals, it induces mast cells degranulation in the colon[239], a similar action is induced by stress. The granules released by mast cells contain preformed or newly generated mediators such as nerve growth factor (NGF) [240], tryptase [241], prostaglandin E2 [242], histamine [241] that can all activate or sensitize sensory afferents [239] giving visceral hypersensitivity and pain.

Intestinal epithelial barrier (IEB) damage is at the basis of visceral hypersensitivity episodes in both humans and rodents. Stress can disrupt the IEB with a subsequent nociceptor's sensitization due to increase of antigens in the lamina propria. CRF system activation is involved in alterations of epithelial permeability following stress and the damage to the IEB can be also independent from mast cells activation [239].

What is known is that pain signals derive from intrinsic primary afferent neurons and are transmitted by extrinsic primary afferent neurons. Afferent neurons, at their endings, present receptors and ion channels that are anti- and pronociceptive, what determines their conformation is the balance between activating and blocking signals of pain. As previously stated, the neurotransmitters that are entangled in visceral pain are neurokinins, CFR and 5-HT, but also transient receptor potential (TRP) ion channels that sense thermal or chemical stimuli and induce acute or persistent pain thanks to the activation of sensory neurons. Chloride channels and guanylate cyclase (GC) has gained attention for the development of IBS drugs [226].

CFR receptors are located in the effector neurons of the amygdala, the cingulate cortex, the hypothalamus and the locus ceruleus complex. Millon, Fukudo, Tachè and collaborators[247–249] have demonstrated that the brain CRFr/CRF1 signaling pathway activation seems to mediate the stress-related alterations of colonic motor and visceral functions, while an opposite action seems to be obtained after CRF2 receptor activation. Acute psychological stress can be reproduced by central injection of CRF.CRF1-2/CRF signals are also involved in the GI response to stress; enteric neurons and mucosal cells express CRFr in the GI and male Wistar rats with delayed stress-induced hyperalgesia present an upregulation of these receptors but there are not functional molecules to act on CRFr approved for IBS treatment so far[226].

Serotonin (or 5-Hydroxytriptamine (5-HT)) signalling is altered in the central nervous system of IBS patients, in particular in the post-prandial time, 5-HT is high in IBS-D patients and low IBS-C patients[250].

Enterochromaffin cells produce serotonin regulating sensory, motor and secretory functions of the digestive system. Taguschi R. and collaborators[251] have demonstrated in WRS-subjected rats that is possible to reduce defecation and visceral pain administrating to rats 5-HT3r antagonist alosetron and the CRF1r antagonist E2508. anti-serotoninergic drugs present several side effects (diarrheal, cardiovascular side effect, ischemic colitis) and are only effective in a limited group of IBS patients. New 5-HT4 agonists seems to be effective only in idiopathic constipation so for now, no valuable drugs against serotonin action are available.

In conclusion, stress induces visceral hypersensitivity due to an alteration of visceral sensation with an enhanced perception of physiological or experimental visceral stimuli along with hypervigilance to visceral pain. Hyperalgesia is defined as an abnormally increased sensitivity to pain that is present in IBD patients at the visceral level. Notwithstanding, there are several factors to be considered, as stress can occur in very different situations. Moreover, the biological diversity of living beings must be considered. For instance, human samples are difficult to obtain, and there is a high variability in the response to factors inducing psychosocial stress in humans so animal models of stress have been developed to decrease interindividual variability and mimic the symptomatology of the disease[226]. Among them, chronically applied water avoidance stress (WAS), i.e. repeated (r)WAS, is considered one of the most effective when used in the right model[217,224,243].

7.4 Experimental models of stress: Water Avoidance Stress

In the attempt to reproduce stress related IBS induction, psychosocial stressors like neonatal maternal separation (MS), WAS and wrap restraint stress (WRS) can be used in animal models creating an unfavourable social environment. MS is a good model to replicate childhood traumas that can put the basis to develop IBS later in life but is considered a strong stress[244]. In adult animals an acute stress model is represented by WRS[219,221].

Nevertheless, to best reproduce chronic stress and subsequent induced IBS in adults, a repetitive stressful environment must be applied; the test that best replicates chronic psychosocial stress in adulthood is represented by water avoidance stress (WAS). Notably, WAS has also been demonstrated to be a milder and more '*physiological*' chronic stress respect to MS.

Water stress avoidance consists in positioning the rat in a dark glass platform surrounded by water for an hour daily for 10 consecutive days. This model is called rWAS. Bradesi and coll[245]. reported that in male Wistar rats, a strain with high responsiveness, chronic application of WAS for 10 days provoked colonic hyperalgesia, increased colonic motility and caused local inflammation. Moreover, the colonic signs persisted for the following 20 days. Peculiarities of WAS test are that there is no appearance of tolerance even after repeated applications and after stress removal, hyperalgesia and hypermotility are maintained. These

peculiarities make WAS test reliable to evaluate drug capability to attenuate or prevent the mien and the progression of stress induced colonic alterations, and also to assess if the drug capability last for long term after the end of the stressful stimuli[217,220,238,243].

Rats from the Wistar rat strain are a good model in which rWAS can be applied. When Wistar rats undergo rWAS endure two different types of stress, isolation and immobility. After ten days of repeated exposure to this stressful test, rats develop chronic enteric hyperalgesia, increased production of fecal pellets, a mild mucosa inflammation[222,243,246] with the presence of polymorphonuclear cells aggregations, increased mast cells number and Interleukin (IL)-1 and Interferon (INF)-γ cytokine expression[245]. In 2021 Traini et al.[222] demonstrated that 10-days rWAS caused animal immobility when the elevated plus maze (EPM) behavioral test was applied. Furthermore, mechanical experiment in colonic tissue sample of rWAS animals showed a block of the giant contractions in the circular muscle layer while immunostainings of inducible Nitric Oxide Synthase (iNOS), showed an increased in the enzyme expression in the myenteric neurons. Much less is known about the potential role of the cholinergic system in the genesis of IBS. The few studies available are limited to the role of this neuronal pathway in the development of mucosal inflammation [243,245].

The cholinergic neurotransmission as not yet been studied so the present work will focus on the effect of stress in cholinergic neurotransmission.

AIMS

8 GENERALITY

The ENS, in a complex circuit that alone, together with the ICC, or in concert with extrinsic parasympathetic and sympathetic innervation, controls not only bowel movements/motility but local blood flow, immune responses and transmucosal movement of fluids. Therefore, assaults to the ENS endanger gut health and normal physiology, prompting to severe GI comorbidities[252]. Nevertheless, although the ENS has been reported to play a major role in the aetiology of several gut diseases[253], it is not clear what roles it plays in chemotherapy-induced neuropathies or in stress-induced IBS.

The present doctoral thesis addresses, in part, these two particular topics, which have been developed along two different research studies. As we will try to demonstrate, these studies, although aimed at investigating different pathological conditions, share several elements: i) both are studies on laboratory rodents subjected to chronic exposure to pathological stimuli; ii) both investigate the colon using similar techniques and aimed at common objectives; iii) both involve pharmacological treatments to prevent or reduce the effects of pathogens.

8.1 RESEARCH STUDY 1 - AIMS

As previously reported, it is well known that chemotherapy causes deep and disabling gastrointestinal symptomatology and that many of the attempts made so far to mitigate cisplatin toxicity have resulted in reduced efficacy of chemotherapy, or have been followed by otherwise disabling side effects[169]. Thus, the possibility to control drug toxicity while maintaining antitumor efficacy is a challenge for researchers and clinicians. Over the past decade, it has emerged that protecting the microbiota could both reduce the toxicity of chemotherapy and improve its efficacy[254].

The aim of this study was to evaluate if a mix of prebiotics, added to the normal chowing diet, could counteract or at least reduce the effects of chronic cisplatin treatment in the mouse colon (3mg/Kg) injected intraperitoneally for four weeks. To reach this aim, morphological and functional experiments were carried out.

Specifically, we directed our focus on:

The intestinal behaviour *in vivo* as it is known that cisplatin treatment causes changes in its functionality;

the colonic mucosa, evaluated *in vitro* as common location of chemotherapy-induced mucositis and in strict anatomical and functional relationship with the microbiota. We examined histological and histochemical parameters such as mucosal area, mucus secretion quantity and quality as well as the presence of tissue inflammation. Mucositis is considered the main acute toxic effect of cisplatin.

The neurotransmission, investigating the entire myenteric neuronal population and the cholinergic and nitrergic pathways where the cisplatin can cause neuropathy.

The interstitial cells of Cajal. Since these cells are the main mediators of neurotransmission, we aimed to verify whether they could also be a target of cisplatin-induced toxicity.

The motility of the proximal colon, that was assessed *ex vivo* in colonic strips to identify the origin of the changes in contractility due to cisplatin treatment.

8.2 RESEARCH STUDY 2 - AIMS

Irritable Bowel syndrome (IBS) is a highly widespread gastrointestinal disorder whose symptomatology mainly affects the large intestine[255]. Among the risk factors, psychosocial stress is the most acknowledged [238]. The repeated water avoidance stress (rWAS) is considered an animal model of psychosocial stress capable inducing disorder that mimic IBS[226]. Otilonium bromide (OB), orally administered, concentrates in the large bowel and controls most of the IBS symptoms in humans[221].

The aim of this second study was to gain insight into the role of the ENS in stress-induced IBS in a rat model (rWAS) and to assess whether OB could interfere with the ENS damage. These objectives were achieved by combining functional and morphological studies in animals subjected to a chronic exposure to a psychosocial stress characterized by isolation and immobility (rWAS). OB was administrated daily starting from the day before rWAS exposure.

At the end of the rWAS exposition, we measured:

- variations in stool production *in vivo* as signs of stress induced changes in colonic motility;
- colonic mechanical and electrical responses *ex vivo* in strip preparations and the effect of TTX and atropine to correlate these data with those obtained in vivo;
- mucosal area and mucous secretion using histological and histochemical procedures to evaluate the presence of local damages;
- the colonic myenteric neurons, focusing the attention on cholinergic neurotransmission using immunohistochemistry because of the well-known antimuscarinic activity of OB.

MATERIALS AND METHODS

9.1 RESEARCH STUDY 1 – MATERIALS AND METHODS

Animals and Treatments

The present research was designed in compliance with the guidelines of the European Communities Council Directive 2010/63/UE and was authorized by the Italian Minister of Health (code: 217/2020). C57BL/6JolaHsd male mice (18–22 g; n = 25) were purchased from ENVIGO (S.Pietro al Natisone - UD, Italy). The animals were housed on a 12-hour light/dark cycle (8am lights on and lights of at 8pm) under standardized conditions of temperature and humidity with free access to food and water. They were allowed to acclimatize to the animal facility for one week. Then they were randomly divided as follow:

Control group: untreated mice, n=8, Ctrl;

Cisplatin group: mice treated with cisplatin (details below), n=8, Cspl;

Prebiotics group: mice fed with enriched diet with prebiotics (details below), n=4, Prebio;

Prebiotics-cisplatin group: mice fed with enriched diet with prebiotics and treated with cisplatin, n=5, Cspl-Prebio;

Each group was housed in a separate cage. Each cage housed 4 animals, apart from the Cspl-Prebio cage that housed 5 animals, so we had 6 cages in total. The animals' general condition was assessed daily. Specifically, body weight was measured upon arrival and every 2-4 days during the treatment. Food and water intake was evaluated daily, measuring the water consumed in ml and the food ingested in g, weighting the food pellet left over in the grid.

Cisplatin injectable solution (kindly provided by Dr. M. Cecchi, AOU Careggi, Florence, Italy) was intraperitoneally (i.p.) administered twice a week (on Tuesday and Friday) at a dosage of 3 mg/kg. To prevent cisplatin-induced nephrotoxicity, 0.5 ml of saline solution was injected subcutaneously just before each cisplatin injection[256] apart from the controls, received the same number of injections. The treatments last 4 weeks. Three days after the last cisplatin injection, the animals were sacrificed by cervical dislocation.

Prebiotics were multi-extracts of fibres and plant complexes, mainly composed of inulin/FOS (fructo-oligosaccharides) that were kindly provided by the Aboca Company (Plantaflor®, Aboca Sansepolcro (AR), Italy). The dose of prebiotics was 50mg inulin/FOS/g diet, corresponding to a 5% increase in inulin/FOS in the standard diet; this choice aligns with the existing literature [257,258]. The mix of prebiotics was directly added to the daily diet and maintained for the 4 weeks of treatment. Cisplatin treatment induces nausea and animals chow non-food substances to diminish gut symptoms, this phenomena in called PICA. PICA is measurable giving a non-food like kaolin. To measure PICA kaolin was added to all cages [259] and prepared as a mixture of silicates (97%), arabic gum (2%) and water (1%), mixed in a clean pot, kneaded into pellets, and left to air dry. We positioned two pellets per cage in the grid and weighed the pellets daily, the last two weeks on treatment the pellets were positioned inside the cage to facilitate animal consumption.

Tissue Sampling

Full thickness samples of proximal (starting 0.5 cm far from the ileo-caeca junction) and distal colon were collected from each animal, fixed in 4% paraformaldehyde in 0.1 M phosphate buffered saline (PBS, pH 7.4) overnight (ON) at 4°C, dehydrated in graded ethanol series, cleared in xylene and embedded in paraffin. Histological transverse sections, 5 µm thick, were cut using a rotary microtome (HistoCore MULTICUT, Leica, Buccinasco, MI, Italy) and collected on normal or positively charged slides, as appropriate.

Histology and histochemistry

The full-thickness sections were deparaffinized in xylene and re-hydrated in descending ethanol series up to distilled water. The sections were stained with hematoxylin-eosin (H&E) to evaluate the tissue architecture, quantitative morphometric analysis of mucosal area, and cell infiltrate.

To perform Toluidine Blue (TB) staining, the sections were soaked for 10 min in pre-filtered 0.1% TB in 30% ethanol; washed in distilled water, dehydrated in ascending ethanol and mounted in synthetic resin. TB was used to evaluate the quality of mucous secretion.

All sections were stained in a single session to minimize artefactual staining differences.

Digital images were acquired with a video camera-equipped microscope (Eclipse 200; Nikon Instruments, Tokyo, Japan) with ×20 objective.

To evaluate colonic inflammation, we applied a score analysis adapted from Vera et al. [162]. The score analysis was performed on two sections per animal by two blinded observers (CB, MGV) the criteria are described in the quantitation and analysis chapter.

Immunohistochemistry

The paraffin-embedded sections, once deparaffinized and rehydrated as usual, were treated for antigen retrieval for 20 min at 90-92°C in Tris buffer (10 mM) with EDTA (1 mM, pH 9.0), followed by cooling to room temperature (RT). The sections were then washed in PBS and blocked for 20 min with 5% normal donkey serum (NDS, Jackson Laboratories, Inc.) in PBS. The primary antibodies (Table 2) were diluted in 5% NDS and incubated ON at 4°C. The next day, the sections were incubated for 2 h at RT in the dark with appropriate fluorochrome-conjugated secondary antibodies (Table 2) diluted 1:333 in 5% NDS. Tissue sections were thoroughly washed in 0.1 M PBS and mounted in an aqueous medium (FluoreGuard Mounting Medium, ScyTek Laboratories inc. Utah, USA).

To identify the potential localization of Connexin (Cx)43 on ICC, sequential sections, 4µm thick, were collected on slides (4 sections/slide, 2 slides/specimen) in two separate areas, one area containing the first and the third section, the other area containing the second and the fourth section. Each area was bordered with a pap pen, and the two sections of one area were incubated with Cx43 antibody as described above the two sections of the neighbor area were incubated with c-Kit antibody ON at 4°C.The two immunoreactions were revealed by using the appropriate secondary antibodies diluted 1:333 in 5% NDS, incubated for 2 h, at RT. To exclude the presence of non-specific immunofluorescence labelling, negative controls were always performed by omitting the primary antibody. Double labelling experiments were done with ChAT and NeuN antibodies, as described below. After the first incubation, the sections were re-incubated with the second primary antibody and with the appropriate secondary antibody, following the same procedures.

Table 2 summarizes information on primary and secondary antibody sources and used concentrations. Immune reaction was observed and the image of the entire transverse section was acquired with 20x or 60x objectives by Olympus BX63 fluorescence microscope (Olympus, Italy) or by a Leica Stellaris 5 confocal microscope (Leica Microsystems, Mannheim, Germany) equipped with lasers that emit at 488 or 594 wavelengths to excite green and red fluorescent labels, respectively.

Table 2. Primary and secondary antibodies

Primary antibody	**Host**	**Dilution**	**Coniugated**	**Producer**
Anti-NeuN	Mouse	1:100	No	MAB377, Millipore Corporation, CA, USA
Anti-ChAT	Goat	1: 200	No	AB144P; EMD Millipore Corporation, CA, USA
Anti-CD117, c-kit	Rabbit	1: 200	No	A4502; Dako Agilent, CA, USA
Anti Cx43	Rabbit	1:100	No	3512; Cell Signaling Technologies, MA, USA
Anti-Beta3tubulin	Mouse	1:100	No	sc-80005; Santa Cruz Biotechnology, Inc, TX, USA
Anti-nNOS	Rabbit	1:2000	No	Millipore Corporation, CA, USA
bisBenzimide H 33342 trihydrochloride (Hoechst 33342)	no	1:1000	No	B2261; Sigma-Aldrich, Merck KGaA, Darmstadt, Germany
Secondary antibody	**Host**	**IHC**		**Producer**
Anti-goat	Donkey	1:333	AlexaFluor ® 488	A11055; RRID AB_2534102, Thermo Fisher Scientific.
Anti-mouse	Donkey	1:333	Alexa Fluor® 594	715-585-151; Jackson Laboratories, West Grove, PA, USA
Anti-rabbit	Goat	1:333	AlexaFluor ® 488	111-547-003; Jackson Laboratories, West Grove, PA, USA

Functional studies: spontaneous mechanical activity.

As reported in Squecco's paper [335], full-thickness circular muscle strips were dissected from colon segments, mounted in double-jacketed 5 mL organ baths containing Krebs Henseleit solution of the following composition (in mmol/L): 118NaCl, 4.7KCl, 1.2MgSO4, 1.2KH2PO4, 25NaHCO3, 2.5CaCl2 and 10glucose, pH7.4 and bubbled with 95%O2 -5%CO2. Temperature was maintained within a range of 37±0.5°C. One end of each strip was tied to a platinum rod while the other was connected to a force displacement transducer (FT03; Grass Instrument, Quincy, MA) by a silk thread for continuous recording of isometric tension. The transducer was coupled to a polygraph (7K; Grass Instrument) (Fig. 21).

Strips equilibrated for 1 hour under an initial load of 0.2g. During this period, the preparations underwent repeated and prolonged washes with Krebs-Henseleit solution to prevent accumulation of metabolites in the organ baths. Smooth muscle contraction was obtained by addition of methacholine to the bath medium. The interval between two subsequent applications of methacholine was no less than 30 min, during which repeated and prolonged washes of the preparations with Krebs-Henseleit solution were performed.

Drugs: the nerve blocker tetrodotoxin (TTX, 1 ×10-6 M) and the muscarinic receptors agonist methacholine (2 x 10-6 M) were used. The concentrations were those previously used in murine gastrointestinal preparations and proved to be effective[260]. All drugs were obtained from Sigma (St. Louis, MO, USA). Methacholine solution was freshly prepared while a TTX stock solution was kept stored at -20 °C.

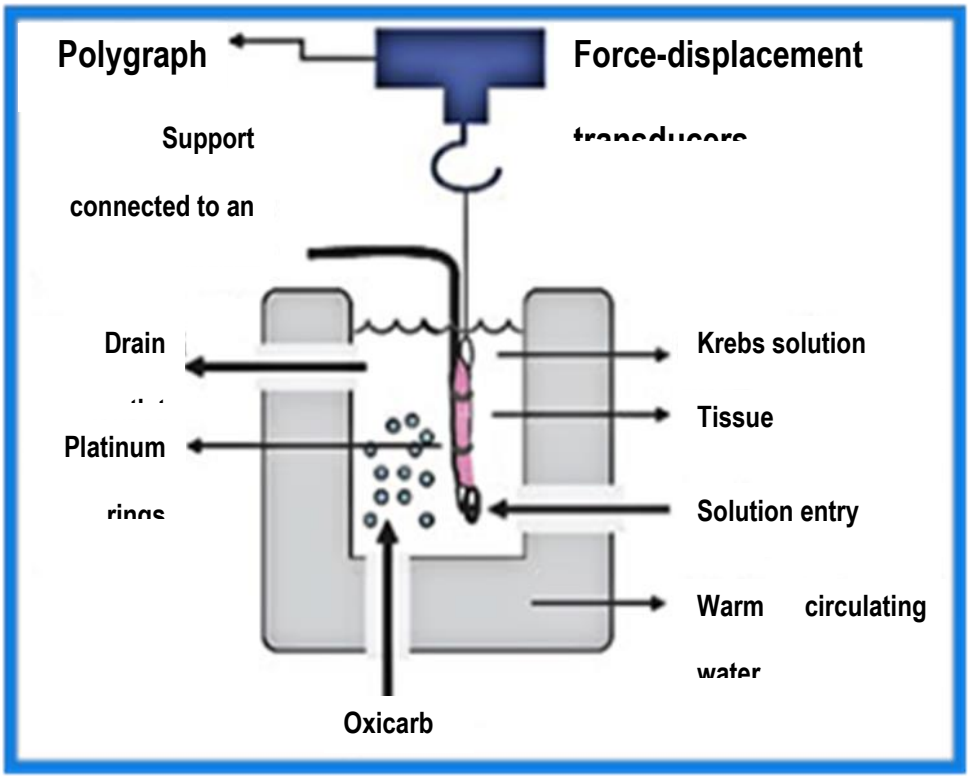

Figure 21. Scheme of force displacement transducer (FT03; Grass Instrument, Quincy, MA) with full-thickness circular muscle strips dissected from colon segments. The strips are tied to a platinum ring on one side and on the other to a silk thread attached to the transducer, allowing continuous recording of isometric tension. The strips are mounted in double-jacketed 5 mL organ baths containing Krebs Henseleit solution of the following composition (in mmol/L): 118NaCl, 4.7KCl, 1.2MgSO4, 1.2KH2PO4, 25NaHCO3, 2.5CaCl2 and 10glucose, pH7.4 and bubbled with (Oxicarb) 95%O2 -5%CO2. Temperature is maintained within a range of 37±0.5°C. The transducer is coupled to a polygraph (7K; Grass Instrument). Scheme kindly given by Dr. Eglantina Idrizaj.

Short-chain fatty acids (SCFA) quantification in faecal samples:

Chemical reagents were: Acetic acid (99.9% purity), propionic acid (99.8% purity), iso- butyric acid (99.7% purity), butyric acid (99.6% purity), isovaleric acid (99.8% purity), valeric acid (99.8% purity), hexanoic acid (99.6% purity) and 2-methylvaleric (99.9% purity) were obtained from Sigma–Aldrich (St. Louis, Missouri, USA) and sulfuric acid (95–97% purity) was obtained from Merck (Darmstadt, Germany); all these chemicals were used to build the standard corves. Water was of Chromanorm quality and provided by VWR International (West Chester, Pennsylvania, USA).

Standard solutions. Seven individual stock solutions (1–4.5 mg/ml) were prepared by dissolving each SCFA standard in High Performance Liquid Chromatography (HPLC) grade water. A pool containing deuterated acetic, propionic, isobutyric, butyric, isovaleric, valeric and hexanoic acids at a concentration of 0.720, 0.405, 0.080, 0.350, 0.070, 0.240 and 0.160 mg/ml, respectively, was prepared by diluting a specific volume of each of the stock solutions with HPLC grade water in a 20 mL volumetric flask. A 0.2 mg/ml solution of 2-methylvaleric acid was prepared in water to be used as internal standard (IS). All standard solutions were stored in glass vials for maximum 6 months at +4 °C. A 0.9 M H2SO4 solution was prepared by diluting H2SO4 in water.

Fecal sample collection and preparation. Fecal pellets were collected before the beginning and at the end of the treatment. Each animal was placed in a single cage with absorbing paper at the bottom and a grid where the animal could walk. Animals had free access to food and water for all the treatment and remained in the cage for 4h. At the end of this period, the mouse was brought back to its cage with its similars. Faecal samples were collected from the absorbing paper with an autoclaved spatula in single autoclaved safe lock Eppendorf. Samples were weighted and stored at -80°C until the day before the analysis. PBS solution was prepared the two days before usage, then autoclaved to ensure that there was no microbial contamination and stored at -20°C until the day of usage. The daily PBS and each stool sample was collected from the -80°C or -20°C and left to defrost at +4°C in a cotton envelop to avoid that fast defrosting could damage the short chain fatty acids. Once samples and PBS were defrosted, a 1:1 PBS volume was added to the stool samples depending on their weight, i.e. 100mg stool + 100ul PBS and samples were vortexed and then sonicated until faeces were completely dissolved. Than the Eppendorf with feces and PBS was centrifuged at 15000rpm for 10

minutes at +4°C and the supernatant was recovered in a new clean autoclaved Eppendorf. Supernatant samples were stored at -20°C until the beginning of the day of analysis with GC-MS. Concentrations of SCFAs were determined in 100 µL supernatant, that were transferred in a vial containing 320 mg NaCl. We used 5 µL of a mixture of deuterated acids containing 50 ng D3-propionic, 50 ng D7-butyric acid, and 500 ng D4-acetic acid as internal standard. A calibration curve was prepared, adding the mixture of internal standards (5 µL) to scalar amounts of the acids. Perchloric acid 10% was added (10 uL) immediately before SPME sampling. The vial was thermostated at 65 °C for 5 min and the fiber was exposed in the head space for 10 min, then desorbed into the injector port of the GC-MS instrument. The vial was vortexed and placed in a heater at 65°C than the fiber was introduced and left to absorb the volatilized SCFA and the standards. The fiber was removed, 5 minutes after the fiber injection, and inserted in th SPME-GC–MS camera and the analysis was started.

Solid-phase microextraction-gas chromatography-mass spectrometry (SPME-GC–MS) parameters. The Solid Phase Microextraction- Gas Spectrometry-Mass Spectrometry (SPME-GC-MS) determinations were performed using an Agilent Technologies (ex Hewlett Packard) GCMS instrument composed by a 5890 series II GC and a 5973 MSD. The SPME fibre was a Carboxen/Divinylbenzene 75 µm. The capillary column was a Phenomenex ZB-WAX 60 m × 0.25 mm, 0.5 µm film thickness. The injector and transfer line temperatures were 260 °C and 265 °C, respectively. The analytes were desorbed in the GC injector port at 260 °C for 20 min. The GC oven temperature program was as follows: initial temperature 42 °C for 3 min, then to 115 °C at 25 °C/min, to 210 °C at 8 °C/min, and to 260 °C at 22 °C/min. The retention times for individual SCFAs were determined by injecting each standard into the column. The peaks were identified by comparing their mass spectrum and retention times with those of the corresponding standards. The SCFA were detected using full scan mode in a mass range between 40 and 150 Da in a single segment window. In each chromatographic run, different ions were monitored for each SCFA analyzed, which allowed to perform detection. MS data were acquired in scan mode from m/z 30 to m/z 350 at a scan rate of 2.3 scan/sec. The Agilent MS ChemStation software was used for data acquisition and processing. The SCFA concentration in fecal sample was expressed in micromoles per gram (µmol/g) of faeces. The MS conditions were: transfer line: 230 °C; ion source: 220 °C; collision energy: 35 eV; positive ionization mode.

Quantitation and statistical analysis

The quantitation of TB staining, c-Kit and Cx43 labelling was done by two observers (CB, CT), blind to each other, in the entire transverse section (2 sections/animal; 4 animals/group) of proximal colon and of distal colon. The blind procedure consisted of randomly assigning the specimens a progressive number, from 1 to 16 (4 animals/4 groups), so that the researcher did not know which group each specimen belonged to. At the end of the quantitation, the values obtained from two sections/animal were attributed to the corresponding specimens.

The images were acquired using 10x, 20x or 63X objective and the entire section was reconstructed to correctly overlapping the shared tracts with Image J.

For the ascending colon, mucin content was quantified on full sections (2 section/animal) measuring on the photographs the PAS-positive areas or the metachromatic TB-positive areas, exclusively selected using colorimetric threshold values with Image J. In particular, each experimenter established the threshold based on the hue, saturation and brightness that defined PAS-positivity (hue 203-255; sat 106-255; bri 132-255) or metachromatic TB-positivity (hue 160-255; sat 50-255; bri 112-255). Each observer used the same threshold as they both concluded that these parameters allowed to distinguish goblet cells with their mucin content from the rest of the cell populations. In the descending colon, metachromatic TB-positive goblet cells and PAS-positive goblet cells were counted on full sections (2 section/animal), one for each experimenter.

Data quantitation was done using Image J software (NIH, Bethesda, ML, USA) and the results were expressed goblet cell number/section for the PAS and TB staining for the descending colon and as pixel/section for the proximal colon as well as for the immunolabelling of the descending colon. Specifically, for the mucosal area, for the PAS labelling and for TB labelling a ROI (region of interest) line corresponding to the mucosa was drew; then the area of interest was identified setting up the threshold; lastly the corresponding pixels were calculated using the analyse function of Image J.

For c-Kit- and Cx43-labelled structures, the entire section was commuted to 8 bit grey scale, then the quantification followed the steps described above. The mucosal integrity and inflammation degree were evaluated by two observers independently, by a semi-quantitative scoring system adapted from[162] and using the following four criteria: loss of crypt architecture (graded 0–3, normal, mild, moderate, severe); extent of

inflammatory cells infiltrate in the lamina propria (graded 0–3, normal, mild, moderate, severe); goblet cell depletion (graded 0–3, normal, mild, moderate, severe), loss of muscularis mucosa continuity (graded 0–1, presence–absence).Thus, for each section, a numerical score of 0–10 was assigned. The count of labelled neurons was done by the same observers in the myenteric ganglia along the entire transverse section (2 sections/animal; 4 animals/group). The results were expressed as total number/section of NeuN or ChAT positive neurons and as percentage of ChAT labelled neurons per NeuN labelled neurons per section. Only neurons with a NeuN labelled nucleus surrounded by ChAT-labelling were included in the count, as double labelled neurons.

Amplitude of the spontaneous contractile activity was expressed as absolute values (grams) and measured when the maximal amplitude was reached. Contractions to methacholine were measured 30 s after a stable plateau phase was reached.

All the results were reported as value ± S.E.M. Statistical analysis was performed by Student's t-test or ANOVA as appropriate. When ANOVA indicated significant differences, we performed multiple comparisons between groups by Newman-Keuls post hoc test or Bonferroni's post hoc test. $p<0.05$ was considered significant. The number of the specimens is designated by *n* in the results.

9.2 Research Study 2 – Materials and Methods

Animals and Treatments

The present research was designed in compliance with the guidelines of the European Communities Council Directive 2010/63/UE and was authorized by the Italian Minister of Health (code: 916/2016).

Male Wistar rats (n = 30) weighing 150–200 g were purchased from Charles River Laboratories Italia srl (Lecco, Italy). The animals were housed 2–3 per cage at CeSAL (Department of NEUROFARBA, University of Florence, Florence, Italy) with a 12/12 h light/dark cycle (8am lights on and lights of at 8pm) at 22°C room temperature (RT), and with free access to food and water.

Efforts were conducted to maintain animal's health, safety, and welfare to minimize suffering and to reduce the number of animals used in the experiments. On the day of arrival, the rats were transferred into the room adjacent to the testing room and stayed there for the entire period of the experiment. The rats were randomly divided into five experimental groups:

- Controls (Ctrl; n = 4);
- Subjected to repeated water avoidance stress (rWAS; n = 7) for 10 consecutive days;
- Experience of the stress environment without being subjected to it (Sham; n = 5);
- Subjected to rWAS for 10 consecutive days and, meanwhile, orally treated with Otilonium Bromide (OB) (rWAS+OB; n = 7);
- Oral OB treatment for 10 days onlu (OB; n = 7).

Each rat was weighed every 2 days to assess their weight gain.

Repeated Water Avoidance Stress (rWAS) Protocol

The rWAS was applied as reported in Traini et al. [222]. Briefly, a Plexiglas tank (45 cm length, 25 cm width, and 25 cm height) with a polygonal platform (10 cm length, 8 cm width, and 8 cm height) was fixed to the center of the tank floor and filled with fresh water (25°C) up to 1 cm above the top of the platform. The water was dyed using a non-toxic dark colour and it was changed before each session to remove the smell of the previous rat and to collect the faecal pellets. The animals were placed on the platform for 1 hour/d for 10 consecutive days between 9:00 AM and 02:00 pm, during the rest period of the circadian cicle. Sham rats

were placed on the platform in the waterless tank for 1 hour daily for 10 consecutive days. The locomotor activity of the rats was recorded by a video-tracking/computer-digitizing system (HVS Image, Hampton, UK) and the time spent by the animal on the platform (zone 2) or swimming in the water (zone 1) was quantified and used to evaluate the effective application of immobility stress.

Colonic function

To evaluate colonic function the number and weight of fecal pellets was recorded at the end of each experimental session. The fecal pellets produced by each rat were collected from the tank, counted, stored in separated bins (one for each animal) and exposed to the same conditions of temperature and humidity for 24 hours to allow dehydration. Then, the pellets were weighed. Increments in number and weight of faecal pellets were scored for colonic hyperactivity.

OB Preparation and Administration

OB (10 mg/kg/day) was added to the drinking water the day before the start of the rWAS, and its concentration was adjusted every 2 days based on water intake and body weight gain. Intake of the drug with water was checked by measuring residual water in the trough every 2 days.

Tissue Sampling

The day following the last rWAS application, the rats were anesthetized and killed by guillotine. The abdomen was opened, and the colon was rapidly removed. The distal colon was divided in two segments: one for the functional experiments, and the other for the morphological and biomolecular studies.

Functional studies

As in previously described in chapter 9.1, two full-thickness circular muscle strips (0.4 ± 0.1 cm) were dissected from each colon segment and mounted in 5 mL organ baths containing Krebs–Henseleit solution composed of (in mM) 118 NaCl, 4.7 KCl, 1.2 $MgSO_4$, 1.2 KH_2PO_4, 25 $NaHCO_3$, 2.5 $CaCl_2$, and 10 glucose, pH 7.4, and bubbled with 95% O_2 5% CO_2. Temperature was maintained within a range of 37±0.5°C. One end of each strip was tied to a platinum rod, while the other was connected to a force displacement transducer (FT03; Grass Instrument, Quincy, MA, USA) by a silk thread for continuous recording of isometric tension. The transducer was coupled to a polygraph (7K; Grass Instrument, Quincy, MA, USA). Strips equilibrate for 1 h

under an initial load of 1 g. During this period, the preparations underwent repeated and prolonged washes with Krebs–Henseleit solution to prevent accumulation of metabolites in the organ baths.

Electrical field stimulation (EFS) was applied via two platinum wire rings (2 mm in diameter, 5 mm in apart) through which the preparation was threaded. Electrical pulses (rectangular waves, 80 V, 4 Hz, 0.5 ms for 15 s) were provided by a Grass model S8 stimulator.

Direct smooth muscle contractions were obtained by adding methacholine to the bath medium. The interval between two subsequent applications of methacholine was no less than 30 min, during which repeated and prolonged washes of the preparations with Krebs–Henseleit solution were performed.

The following drugs were used: the nerve blocker tetrodotoxin (TTX, $1x10^{-6}$ M), the muscarinic receptor agonist methacholine ($2x10^{-6}$ M), and the muscarinic receptor antagonist atropine ($1x10^{-6}$ M). Drug concentrations were those previously used in rodent gastrointestinal preparations and proved to be effective[260]. All drugs were obtained from Sigma (St. Louis, MO, USA). Solutions were freshly prepared, except for TTX, for which a stock solution was kept at -20°C.

Morphological Studies

The full-thickness segments of distal colon were fixed in 4% paraformaldehyde in 0.1 M PBS, (pH 7.4) ONat 4°C, dehydrated in graded ethanol series, cleared in xylene, and embedded in paraffin with the cut section transversal to the longitudinal axis. Sections of 5 µm-thick segments were cut using a rotary microtome (MR2, Boeckeler Instruments Inc., Tucson, AZ, USA) and collected on positively charged slides. All the paraffin-embedded sections were deparaffinized and rehydrated as usual for routine histology, histochemistry, and immunohistochemistry. Some sections were stained with H&E to evaluate the tissue integrity, and others were submerged for 10 min in Toluidine Blue 0.1% in 30% ethanol, after filtering with the same procedure reported in chapter 6.1.6. At the end of each staining procedure, the slides were dehydrated, clarified, and mounted in synthetic resin. For immunohistochemical experiments, the deparaffinized sections were treated for 20 min at 90–92°C in tris buffer (10 mM) with EDTA ($1x10^{-3}$ M, pH 9.0), followed by cooling to RT for antigen retrieval. Then, they were washed in PBS and blocked for 20 min at RT with 1.5% bovine serum albumin (BSA, Applichem, Darmstad, Germany) in PBS. The number of total myenteric neurons and the number of cholinergic positive myenteric were estimated using the rabbit polyclonal PGP9.5 (1:200; Millipore

Corporation, Temecula, CA, USA) pan-neuronal antibody and the goat polyclonal choline acetyl transferase (ChAT) (1:100; Millipore Corporation, Temecula, CA, USA) antibody, respectively. As both antibodies were polyclonal, sequential sections were collected on slides (4 sections/slide, 2 slides/animal) in two separate areas, one area containing the first and third sections, the other area containing the second and fourth sections. Each area was bordered with a pap pen, and the two sections of one area were incubated with the pan-neuronal marker PGP9.5 and the two sections with the ChAT antibody. This procedure made it possible to recognize the same ganglia and count the same neurons. The primary antibodies that were diluted in 1.5% of BSA in PBS were applied ON at 4°C. The day after, the sections were washed in PBS and incubated for 2 h at RT in the dark with appropriate fluorochrome-conjugated (Invitrogen, San Diego, CA, USA) secondary antibodies diluted in PBS. The sections were washed in PBS, incubated for 10 min with Hoechst 33342, a nuclei marker (20 µg/mL; Sigma), dissolved in PBS, washed in distilled water, and mounted in an aqueous medium (Immuno-Mount, Thermo Scientific, Rockford, IL, USA). Negative controls were simultaneously performed, omitting the primary antibody to exclude the presence of non-specific immunofluorescence staining. The reaction was observed under the Olympus BX63 fluorescence microscope (Olympus, Segrate, Italy), the signal was obtained using 488- and 370 nm excitation wavelengths for the green and blue, fluorescent labels, respectively, and the photos were taken via the associated imaging system (CellSens Dimension Imaging Software, Olympus, Italy).

Quantitative and Statistical Analysis

The animal weight and the parameters related to faecal pellet (number and weight) were quantified and expressed as means ± S.E.M. The number of animals used is indicated as n in the legends. Amplitude of contractile responses is expressed as absolute values (grams). Responses to EFS referred to the maximal peak obtained during the stimulation period, whereas contractions to methacholine were measured 30 s after a stable plateau phase was reached. Results are given as means ± S.E.M. The number of muscle preparations is reported in the results.

Digital images of PAS- and TB-stained structures were acquired with a video camera equipped microscope (Eclipse 200; Nikon Instruments, Tokyo, Japan) with x10 objective, and the reconstruction of the entire section (4 sections/slide, 2 slides/animal) was performed using appropriate software. Quantitation were

performed with ImageJ software (NIH, Bethesda, ML, USA) using the color threshold toll and the results were expressed as pixel2/section.

The count of the number of PGP9.5 and ChAT positive myenteric neurons in the entire transverse section (4 sections/slide; 2 slides/animal) was performed by two observers who were blind to each other, along the entire section, using a 20x objective. Only the neurons containing the nucleus were included. The results were expressed as the total number of positive neurons and as percentage of ChAT out of the PGP9.5 positive neurons per section ± S.E.M. The number of animals used is reported as n in the legends.

Statistical analysis was performed by means of paired or unpaired Student's t-test to compare two experimental groups or one-way ANOVA followed by Newman–Keuls post-test when more than two groups were compared. Values were considered significantly different with $p < 0.05$.

RESULTS

10.1 RESEARCH STUDY 1- RESULTS

Body weight, Food, Water and Kaolin intake

The mouse body weight before the beginning of treatment (day 0) displayed no significant difference among the groups (Ctrl 21.97±0.75; Prebio 22.67±0.38; Cspl 22.02±0.49; Cspl+Prebio 23.30±0.65; Fig. 22A). The time course (Fig. 22B) shows a constant and continuous increase in Ctrl and Prebio groups; at the end of the treatment (day 28) the mean weight of these two groups is 29.31±0.47g and 27.62±0.56g, respectively and these values are not significantly different (Fig. 22B,C). Conversely, Cspl and Cspl+Prebio groups manifest no significant weight augment during the four weeks and start to significantly differ from Ctrl and Prebio group already from day 14, and, at the end of the treatment, their weight is 21.56±0.80g and 22.46±0.54g, respectively (Fig. 22B,C). These values overlap those recorded at the beginning of the treatment and are significantly lower respect to Ctrl and Prebio groups (Fig. 22A,C). During the 4 weeks, the mean quantities of the daily food intake and drank water are not significantly different among the groups (Fig. 22D, E). In contrast, the Cspl group consumes significantly more kaolin than the Ctrl and Prebio groups (Fig. 22F) as an attempt to buffer drug induction of pica. Interestingly, the Cspl+Prebio group showed a value of kaolin intake intermediate between the Cspl and the other two groups. The statistical analysis, however, disclosed no significant differences respect to the other groups (Fig. 22F).

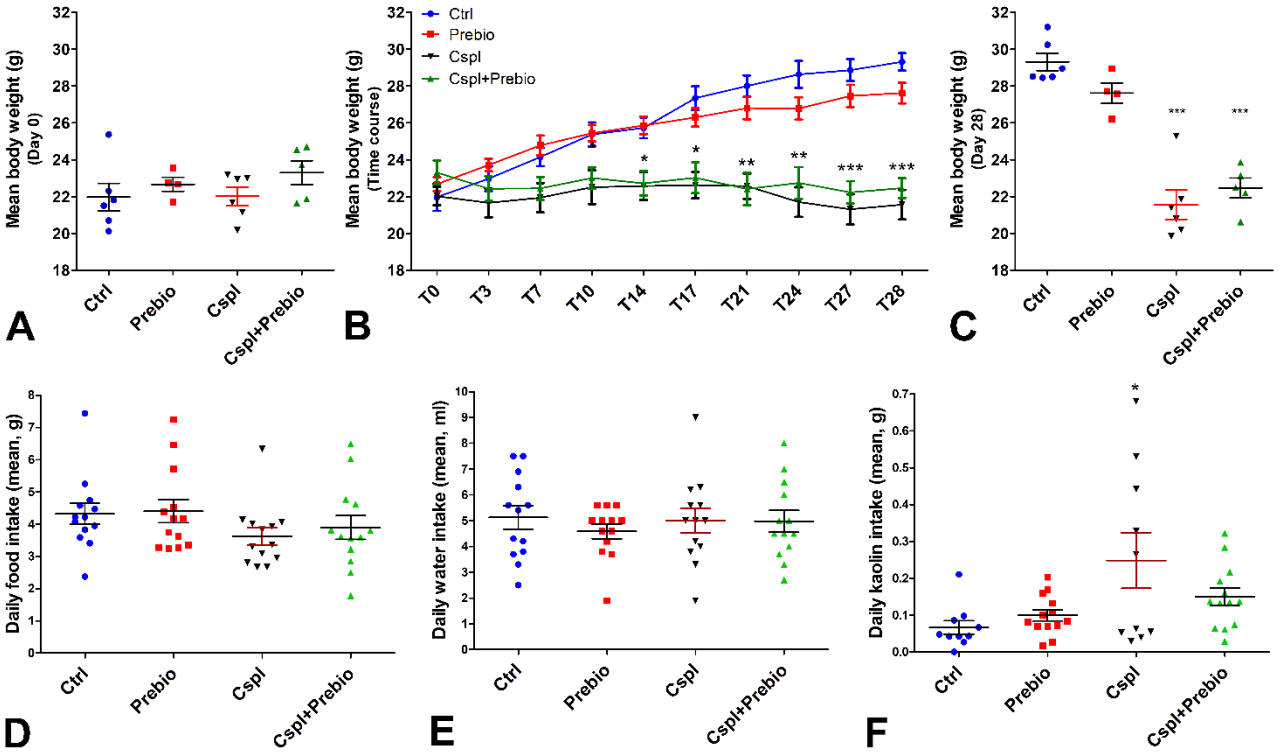

Figure 22. ***In vivo measurements. A****. The body weight was measured at day 0. The results were similar among all the groups.* ***B****. Time-course of the body weight gain during the 28 days of treatment. With time the Cspl and Cspl+Prebio treated mice did not show any weight gain contrary to the Ctrl and Prebio mouse groups.* ***C****. The body weight before the sacrifice was significantly lower than in Cspl and Cspl+Prebio mice. Daily food (**D**) and water (**E**) intake were similar in all groups during the treatment.* ***F****. The kaolin intake during the treatment was significantly higher for the Cspl mice compared to all the other groups. Data are expressed as Mean±SEM. B, C=*p<0.05; **p<0.005; ***p<0.001 vs Ctrl and Prebio mice.* ***F****=*p<0.05 vs all the other groups (mixed ANOVA, post hoc Newman-Keuls test for B, while one-way ANOVA post hoc Newman-Keuls for all the other groups)*

Stool production

To evaluate the colon functionality, we collect and measure the quantity of stool production/hour which is similar among the experimental groups before the beginning of the treatment (Fig. 23A), while at day 28, the stool production is significantly lower in the Cspl group when compared with all the other three groups (Fig. 23B), indicating colonic dysfunction.

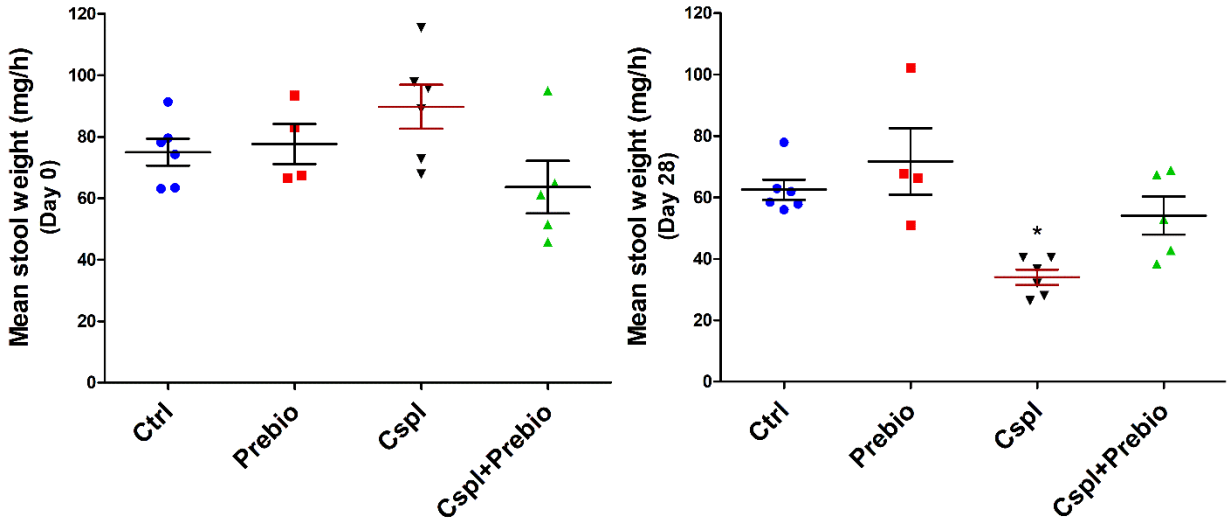

*Figure 23. **Stool production**. **A**. The fecal production the day before the beginning of the treatment was similar among the four groups of mice. **B**. At the end of the treatment (28th day) the Cspl group showed a significant decrease of fecal production vs all the other groups. Data are expressed as Mean±SEM. *p<0.05 vs all the other groups (One way ANOVA, post hoc Newman-Keuls test).*

Histology and Histochemistry

Haematoxylin & eosin (H&E)

Quantitation of mucosal area in the H&E stained ascending colon sections (Fig. 24A-H) showed a reduction in Cspl group that did not reach the significance (Fig. 24I). Quantification of mucosal damage using a semi-quantitative composite score revealed that cisplatin induced a significant increase in the score as compared to Ctrl group (Fig. 24Figure J).

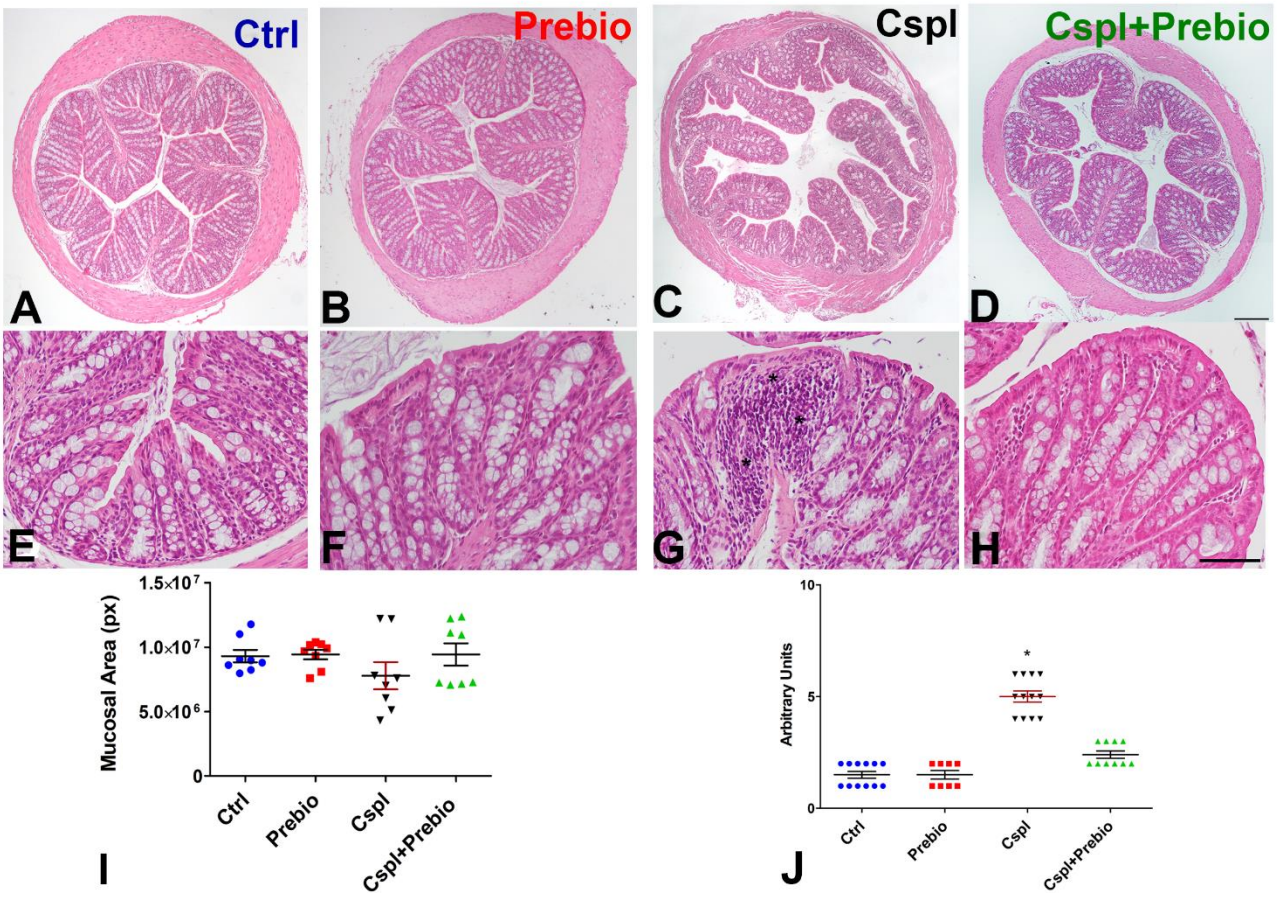

Figure 24. ***H&E staining of ascending colon****. Ctrl (**A, E**), Prebio (**B, F**), Cspl (**C, G**), Cspl+Prebio (**D, H**) mouse groups. Note the thinness of the colonic epithelium and the dilatation of the crypts in Cspl treated mice compare with the other groups of animals. Bar (A-H) = 200 µm. The rectangle indicates inflammatory cell infiltrates in the mucosa. Quantitation of the mucosae area (**I**) showed no difference among the groups of mice. Score analysis (**J**) was performed as described in Materials and Methods. Values are the Mean±SEM. *p<0.05 vs all the other groups (One Way ANOVA, post hoc Newman-Keuls's test.)*

Periodic Acid and Schiff reagent (PAS) and toluidine blue (TB) staining in ascending and descending colon.

Ascending colon:

PAS staining (Fig. 25A-F) was located in the goblet cells, in the glandular crypts and in the lumen of the transverse sections (Fig. 25A-D). Quantitation of the staining in the epithelium showed no significant changes among the groups (Fig. 25E). The evaluation of the luminal PAS+ area revealed a significant decrease in Cspl and Cspl+prebio groups (Fig. 25F).

TB staining (Fig. 26A-F). The staining had a similar distribution to the previous one (Fig. 26A-D). Quantitation of the TB+ area showed a significant decrease in Cspl group respect to the other groups in the epithelium (Fig. 26E). Notably, TB+ staining was significantly increased in the colonic lumen of Prebio group respect to the other groups (Fig. 26F).

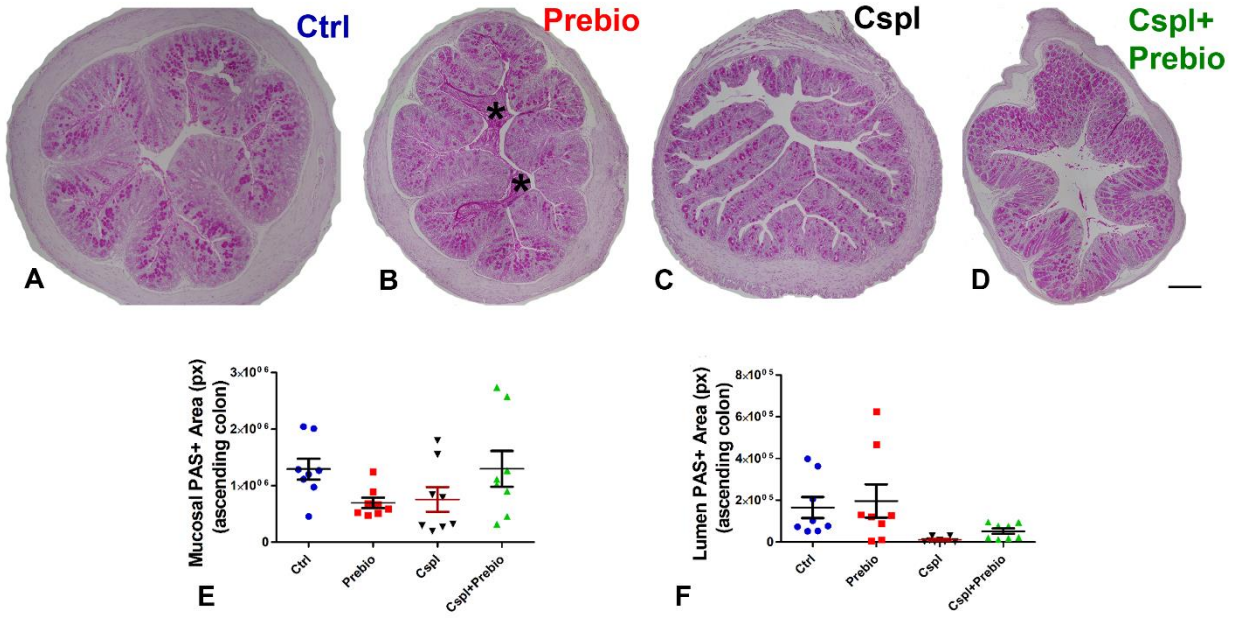

Figure 25. ***Periodic Acid and Schiff reagent (PAS) staining.*** *The PAS dye stained the goblet cells and the glandular cells in the crypts, in all groups. In Prebio group (B) the colonic lumen was filled of PAS+ mucous secretion (asterisks). Bar=200 µm. E-F Quantitation of PAS+ material showed no significant changes among the all groups of mice in the epithelium (E), while a significant decrease in Cspl and Cspl+prebio treated animals was observed in the lumen (F) compared to the other two groups. **p<0.02 vs all the other groups (One way ANOVA, post hoc Newman-Keuls test).*

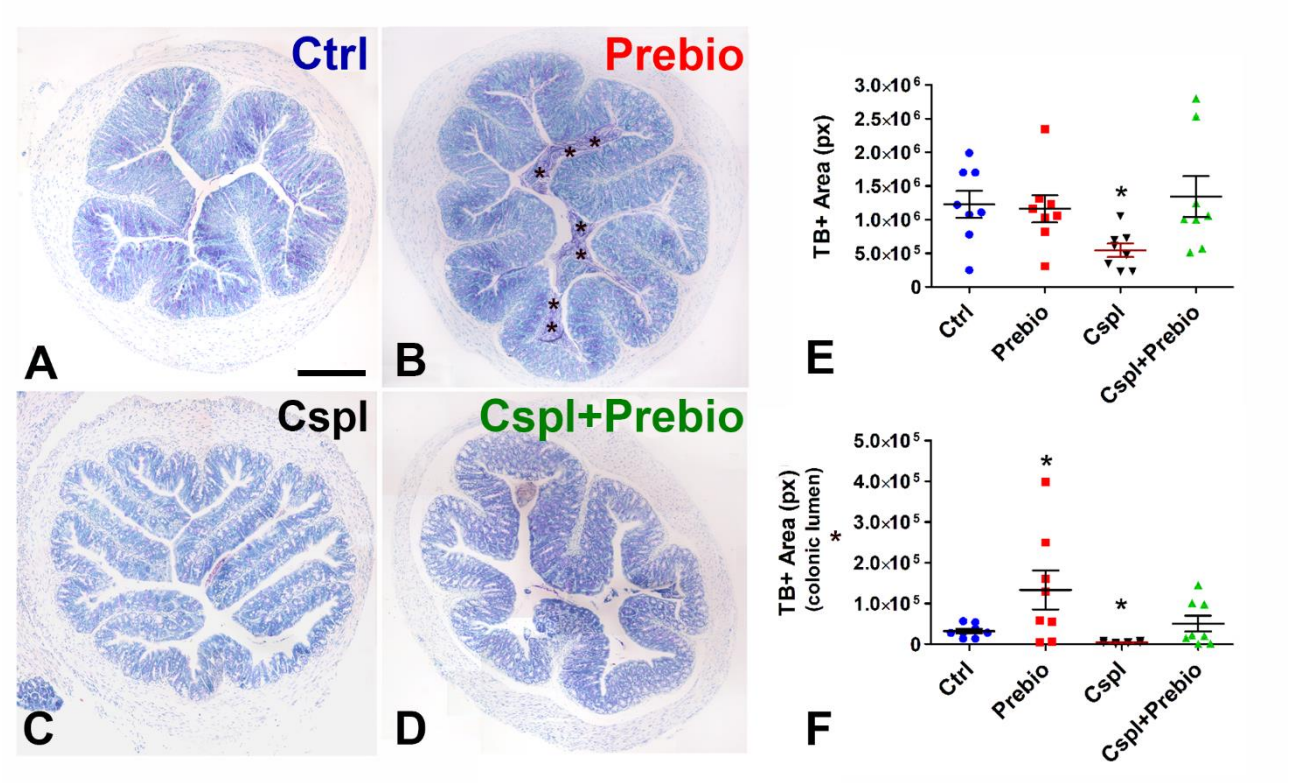

Figure 26. ***Toluidine blue (TB)staining****. A-D. The dye stained the goblet cells and the glandular cells in the crypts in all groups. In Prebio group (B) the colonic lumen was filled of TB+ mucous secretion (asterisks). Bar=200 µm. E-F Quantitation of TB+ material showed a significant decrease in the epithelium (E) and in the lumen (F) of Cspl group and a significant increase in the lumen of Prebio group compared with the other groups (F). *p<0.05 vs all the other groups (One way ANOVA, post hoc Newman-Keuls test).*

Descending Colon

PAS staining (Fig. 27A-E) was located in the goblet cells along the epithelium and in the glandular crypts of the transverse sections (Fig. 27A-D). A negligible quantity of secretion was sometimes seen in the lumen. Quantitation of the positive cell number showed a significant decrease in the Cspl and Cspl+Prebio group versus the Ctrl and Prebio groups (Fig. 27E).

TB staining (Fig. 27F-J). Count of the TB+ goblet cells in the epithelium showed a significant decrease in Cspl group respect to the other groups (Fig. 27J); the treatment with prebiotics significantly increased the number of TB+ goblet cells in the Cspl+Prebio group respect to the Cspl one but not compared with Ctrl and Prebio groups (Fig. 27J).

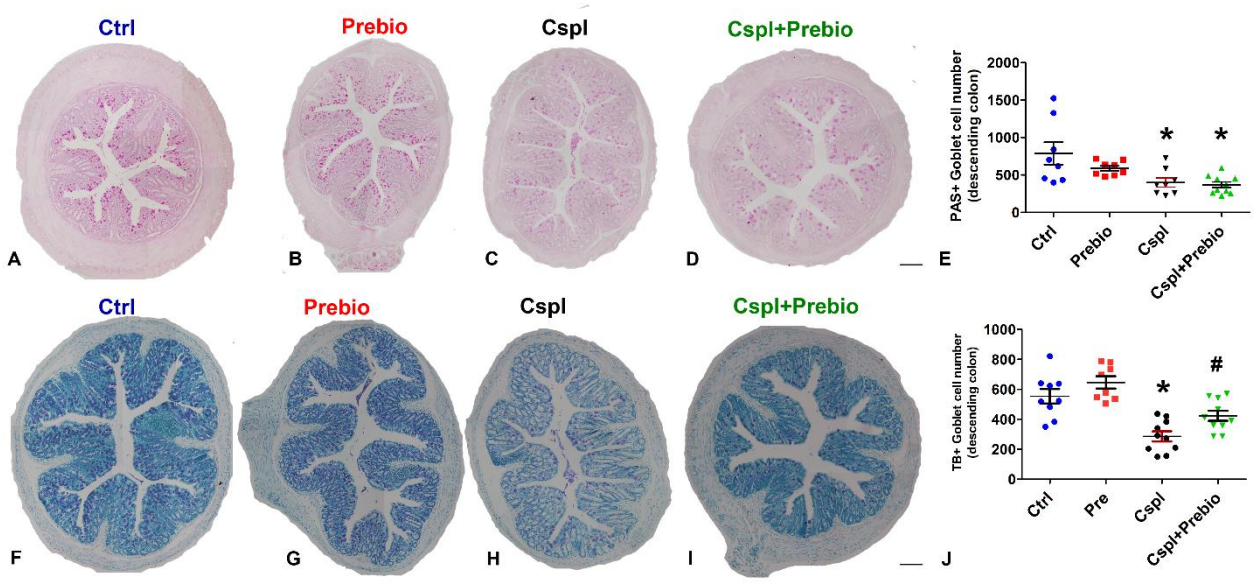

*Figure 27. **PAS (A-E) and TB (F-J) positive cells in descending colon**. Ctrl (**A,F**), Prebio (B,G), Cspl (**C,H**), Cspl+Prebio (**D,I**) groups. Bar (A-D, F-I) = 200µm. Quantitation of the PAS+ cells (**E**) showed a significant decrease in the Cspl group and Cspl+Prebio group respect to the Ctrl and Prebio groups. Quantitation of the TB+ cells (**J**) showed a significant decrease in the Cspl group compared to all the other groups. In Cspl+Prebio group the number of TB cells was significantly increase compared with Cspl but not respect to Ctrl and Prebio groups. *p<0.05 vs the other groups; # p<0.05 vs Cspl group (One way ANOVA, post hoc Newman-Keuls test).*

Immunohistochemistry

c-Kit- and Connexin (Cx)43-immunoreactivity (IR).

c-Kit-IR was detected in myenteric plexus ICC (MY-ICC), intramuscular ICC (IM-ICC) and, at lower intensity, in the ICC located at the submucosal border of the circular muscle layer (SM-ICC) (Fig. 28A). Cx43-IR was detected on the plasma membrane of elongated and branched cells corresponding to the ICC. All the types of ICC showed Cx43-IR and the labelling intensity was comparable among the three cell types (Fig. 28B). Quantitation of the c-Kit-IR in Ctrl and Cspl group gave similar results (data not shown). Quantitation of the Cx43-IR showed a significant decrease in the Cspl group respect with all the other groups (Fig. 28C).

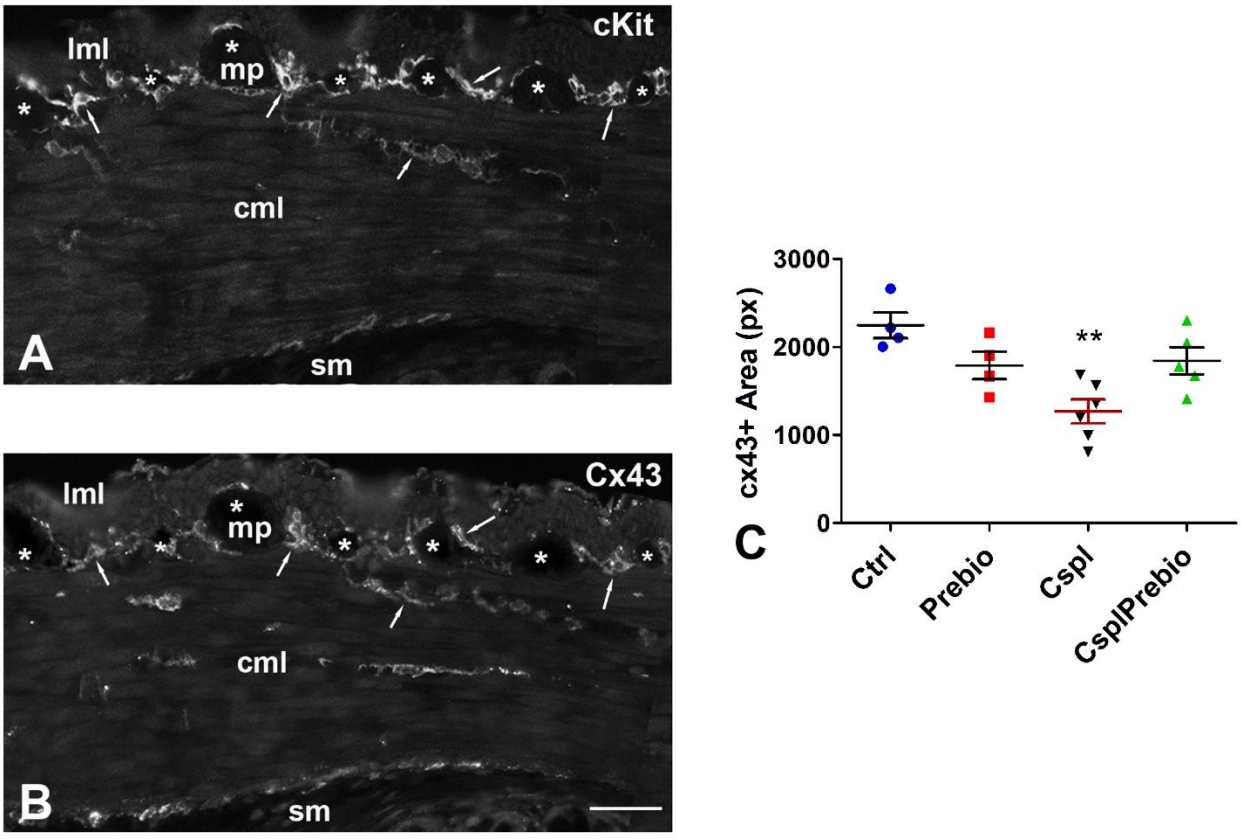

Figure 28. ***c-Kit- and Cx43-immunoreactivity (IR). A.*** *c-Kit-IR was detected in the ICC at the myenteric plexus (MY-ICC), in muscle layers (IM-ICC) and at the border with the submucosa (SM-ICC).* ***B.*** *Cx43-IR overlapped that of c-Kit.* ***A,B.*** *The arrows highlight some of the several sites of overlapping between the two markers. The asterisks indicate the myenteric ganglia. Bar=50µm.* ***C.*** *Quantitation of the Cx43 labelling showed a significant decrease in Cspl treated group. mp=myenteric plexus; lml= longitudinal muscle layer; cml=circular muscle layer; sm=submucosa. **p<0.001 vs all the other groups (One way ANOVA, post hoc Newman-Keuls test).*

Choline acetyl-transferase (ChAT)- and neuronal nuclei (NeuN)-IR.

The pan-neuronal marker NeuN-IR was exclusively located in the nuclei of the myenteric neurons while the ChAT-IR was observed in the cytoplasm of several myenteric neurons and in few intramuscular nerve fibres (Fig. 29A,B). The quantitation of NeuN- and ChAT-IR neurons displayed no significant differences among the groups (Fig. 29C-E).

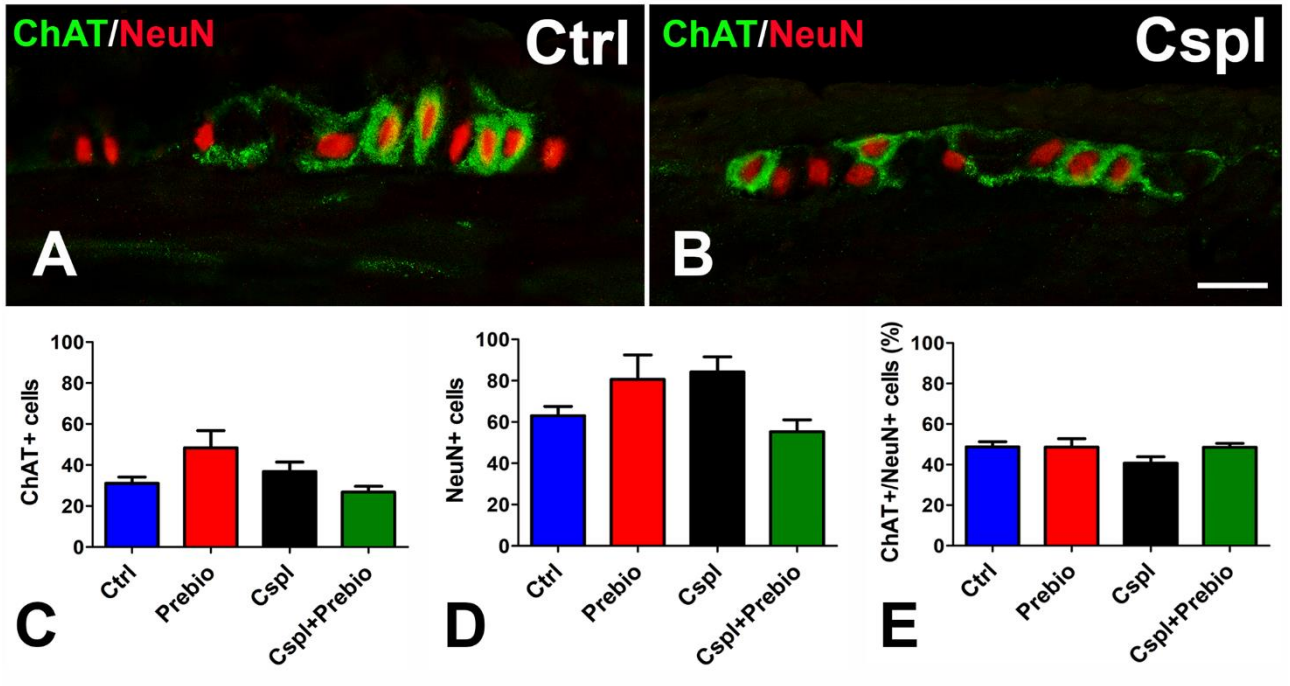

Figure 29. ***Choline Acetyl-Transferasi (ChAT)- and Neuronal Nuclei (NeuN)-IR. A-B.*** *NeuN-IR was detected in the nuclei of several myenteric neurons. Some of them showed the ChAT labelling in the cytoplasm and processes. Bar=50µm. Quantitation of the total number of NeuN- and ChAT-IR neurons (**C,D**) and of the percentage of the cholinergic ones respect to the total myenteric neurons (**E**) showed no differences among the four groups.*

nNOS (neuronal nitric oxide sintase)- and Beta 3 Tubulin (Beta3Tub)-IR.

The pan-neuronal marker β3 Tubulin-IR was exclusively located in the nuclei of the myenteric neurons while the nNOS-IR was observed in the cytoplasm of several myenteric neurons and in few intramuscular nerve fibres (Fig. 30A-D). The quantitation of β3 Tubulin - and nNOS-IR neurons displayed no significant differences among the groups (Fig. 30E-G).

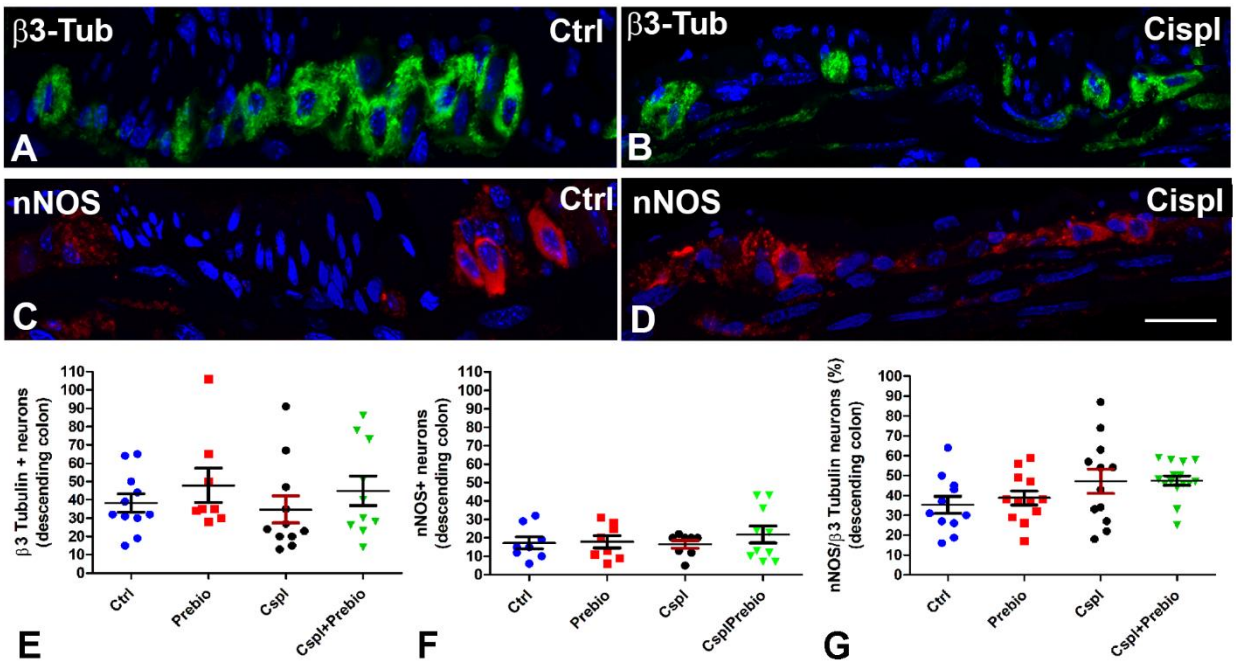

Figure 30. ***ß3-tubulin (ß3-tub) and neuronal nitric oxide synthase (nNOS)-immunoreactivity (IR). A.*** *ß3-tub (A-B) labeled the cytoplasm of several myenteric neurons and nerve fibers. nNOS-IR (C-D) was homogenously distributed in the cytoplasm of some myenteric neurons and in thin nerve fibers. Bar=50µm15*

Quantitation of the total number of ß3-tub - and nNOS-IR neurons (E,F) and of the percentage of the nitrergic ones respect to the total myenteric neurons (G) showed no significant differences among the four groups. (One way ANOVA, post hoc Newman-Keuls test)

Functional studies: Spontaneous mechanical activity

Colonic preparations from Ctrl (*n* = 8) mice exhibited spontaneous contractile activity, consisting of rhythmic changes in isometric tension (mean amplitude, 0.51 ± 0.03 g) (Fig. 31A,B). Addition of TTX (1×10^{-6} M) to the bath medium (*n* = 3) did not affect the motility pattern and the amplitude of the spontaneous contractions (mean amplitude, 0.54 ± 0.05 g), indicating their muscular nature. Strips from Prebio mice (*n* = 6) showed the same motility pattern as Ctrl animals (Fig. 31A,B) (mean amplitude, 0.50 ± 0.04 g). In preparations from Cspl mice (*n* = 8), the motility pattern did not differ from that observed in strips from the other groups (Fig. 31A,B), whereas the amplitude of the spontaneous contractions was significantly reduced (mean amplitude, 0.22 ± 0.2 g) (Fig. 31A,B).

In strips from Cspl+Prebio mice (*n* = 6), the motility pattern showed no differences with respect to that observed in preparations from all the other animal groups (Fig. 31A,B). However, the amplitude of the spontaneous contractions was statistically greater (mean amplitude, 0.35 ± 0.03 g) with respect to that observed in strips from Cspl mice (Fig. 31A,B) but still statistically reduced compared to that of Ctrl and Prebio mice (Fig. 31A,B). In order to prove that all the above-reported effects were muscular in origin, the direct smooth muscle responses to methacholine were evaluated. Addition of the muscarinic agonist methacholine to the bath medium caused a sustained contracture whose amplitude was greatly reduced in strips from Cspl (*n* = 5) and Prebio+Cspl (*n* = 5) in respect to Ctrl (*n* = 5) and Prebio (*n* = 5) animal groups (Fig. 31C).

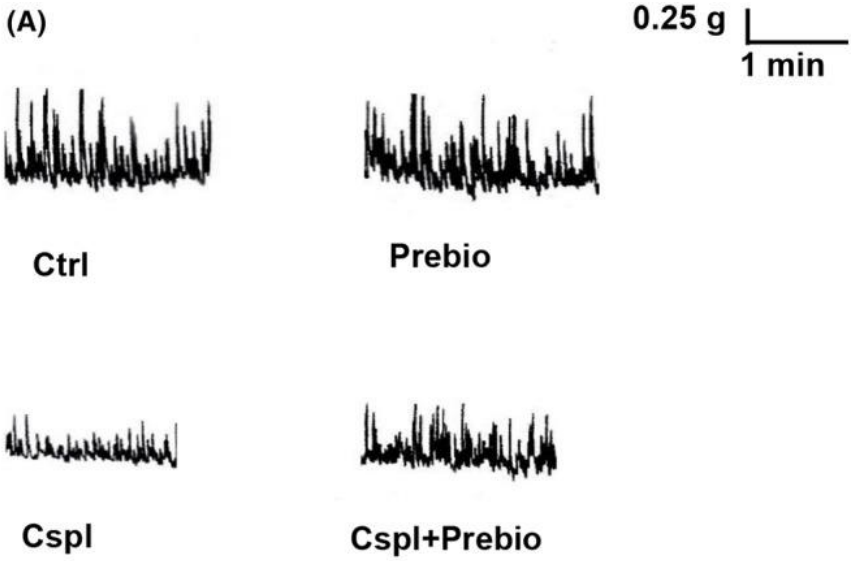
(A)
0.25 g
1 min
Ctrl
Prebio
Cspl
Cspl+Prebio

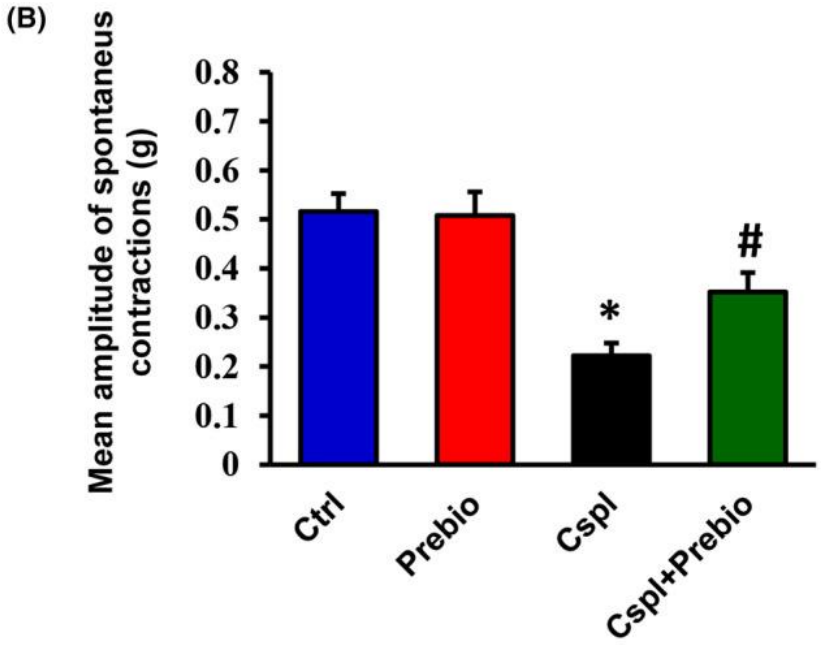
(B)
Mean amplitude of spontaneus contractions (g)
0.8
0.7
0.6
0.5
0.4
0.3
0.2
0.1
0
*
#
Ctrl
Prebio
Cspl
Cspl+Prebio

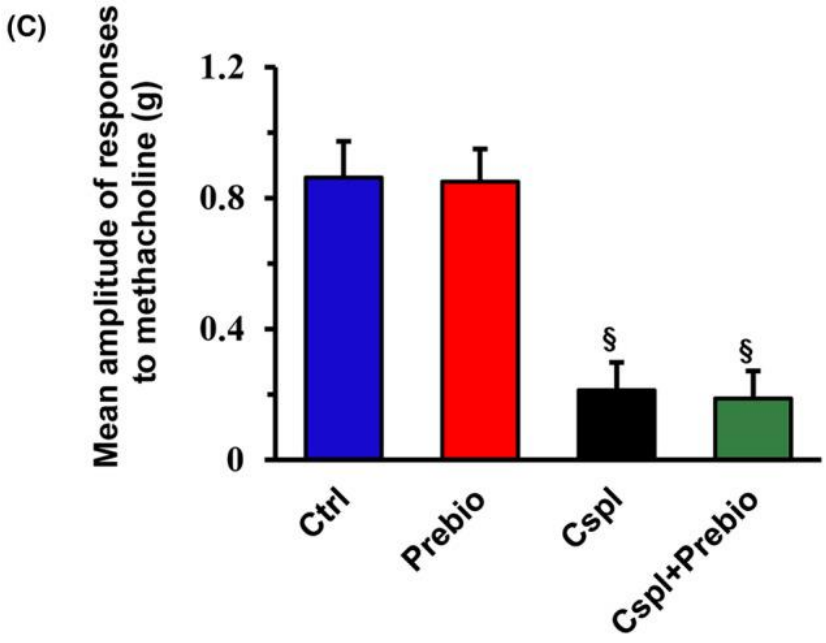
(C)
Mean amplitude of responses to methacholine (g)
1.2
0.8
0.4
0
§
§
Ctrl
Prebio
Cspl
Cspl+Prebio

*Figure 31. (A) Typical tracings showing the spontaneous mechanical activity recorded in preparations from the different animal groups. In strips from Prebio-treated animals (right-hand upper trace), the amplitude of the spontaneous contractions was not different with respect to that obtained in the Ctrl mice (left-hand upper trace). The amplitude of the spontaneous contractions was significantly reduced in preparations from Cspl-treated animals (left-hand lower trace). In strips from Cspl+Prebio-treated mice (right-hand lower trace), the amplitude of the spontaneous contractions was significantly increased with respect to Cspl mice. The motility pattern showed no differences among preparations from the four animal groups. (B) Bar chart showing the mean amplitude of the spontaneous contractions in preparations from the different animal groups. No statistical differences in the amplitude of the spontaneous contractions were present between preparations from Ctrl and Prebio mice. Note the great reduction in amplitude of the spontaneous contractions in strips from Cspl mice and its partial recovery in Cspl+Prebio-treated mice. (C) Bar chart showing the mean amplitude of the direct muscle contractions elicited by methacholine in preparations from the different animal groups. No statistical differences were revealed between preparations from Ctrl- and Prebio-treated mice. Note the great reduction in amplitude of the response to methacholine in strips from Cspl- and Cspl+Prebio-treated mice. All values are means ± SEM of 5–8 preparations. *$p < 0.05$ vs. all the other groups; #$p < 0.05$ vs. Cspl mice § $p < 0.05$ vs. Ctrl and Prebio-treated mice (One way ANOVA, post hoc Bonferroni's test).*

Short Chain Fatty Acids (SCFA)

The estimation of the Short Chain Fatty Acids content in the mouse faecal pellets demonstrated there is no difference between control animals and animals that received prebiotics so we decided to pull together the data of these two groups. Nevertheless, in Cspl treated mice no changes were observed among the four SCFA quantified. Similarly, the co-treatment with prebiotics had no significant effect on the SCFA concentration (Fig. 32).

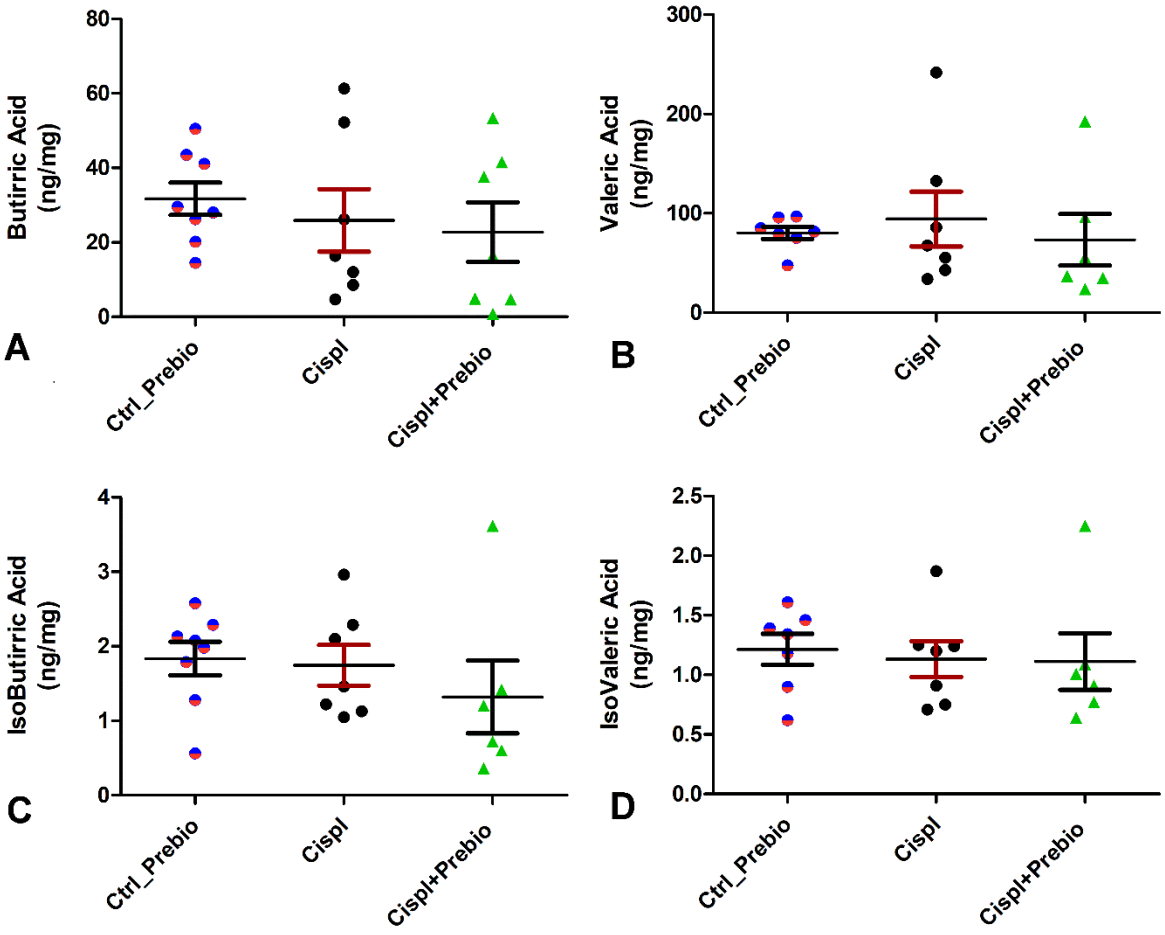

Figure 32. ***Short Chain Fatty Acids Chart.*** *Quantitation of the SCFA in the faeces shows no significant changes among all the groups.*

10.2 Research Study 2- Results

10.2.1 Body weight gain, water intake and fecal pellet production

All the animals were weighed before the beginning of the rWAS application, every two days during the stress period and at the end of the treatment. No significant differences were observed among the experimental groups at any time point (Fig. 33). The water intake, evaluated daily, was not different among Ctrl, Sham and rWAS groups (Ctrl=42,34±1,5ml; Sham=40,50±2,2ml; rWAS=43,38±2,1) while, as expected, the bitter taste of OB dissolved in the drinking water caused a significant decrease of water intake in OB and rWAS+OB groups (OB=31,42±1,2ml; rWAS+OB=30,59±1,6ml); ($p<0.005$). The mean number and mean weight of the faecal pellets were significantly higher in the rWAS and rWAS+OB groups compared to the Sham group (Fig. 34, grey columns). With time, the faecal pellets production decreased significantly in the Sham and rWAS+OB groups (Fig. 34, blue columns) suggesting the appearance of environment habituation for the former, and confirming the drug efficacy for the latter. Conversely, in the rWAS rats, the faecal production did not decrease with time (Fig. 34, blue columns). The faecal production in controls and OB rats during the ten experimental days did not differ from that obtained in the Sham (Fig. 34, grey columns).

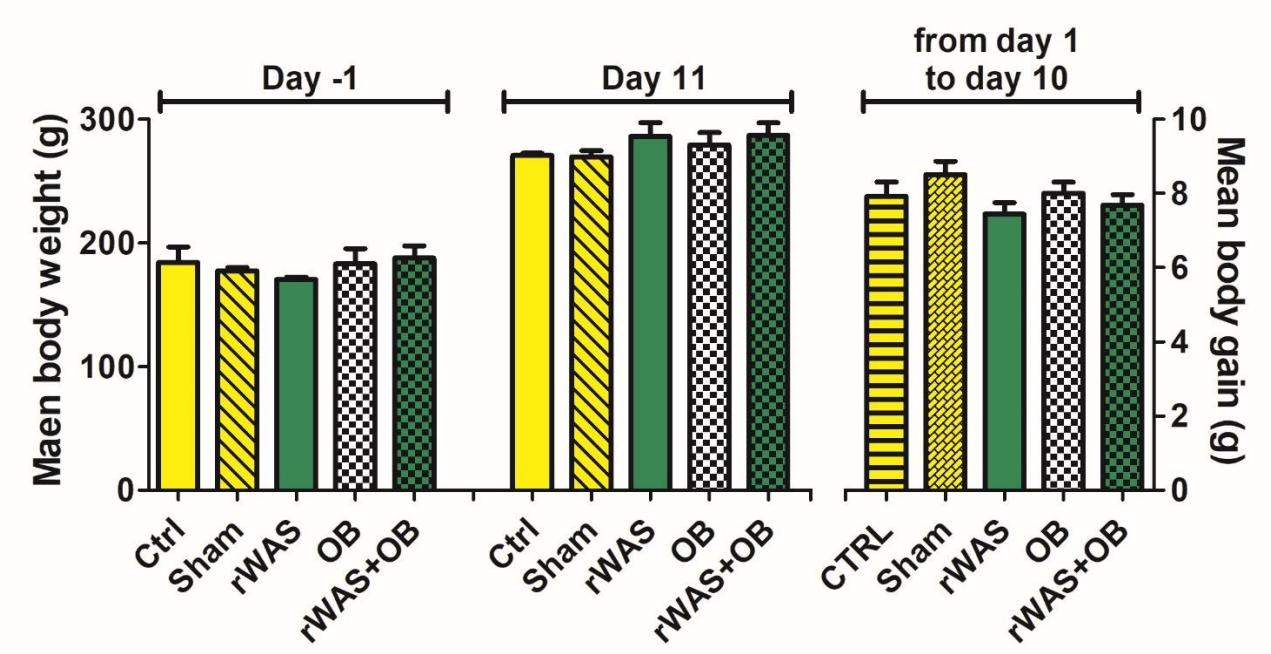

*Figure 33**. Weight gain time-course**. All animal groups had similar weight at day -1 (left columns) and at day 11 (central columns); the daily weight gain during the 10 days of stress application was comparable among the groups (right columns). One-way ANOVA followed by Newman-Keuls post hoc test, (n=7).*

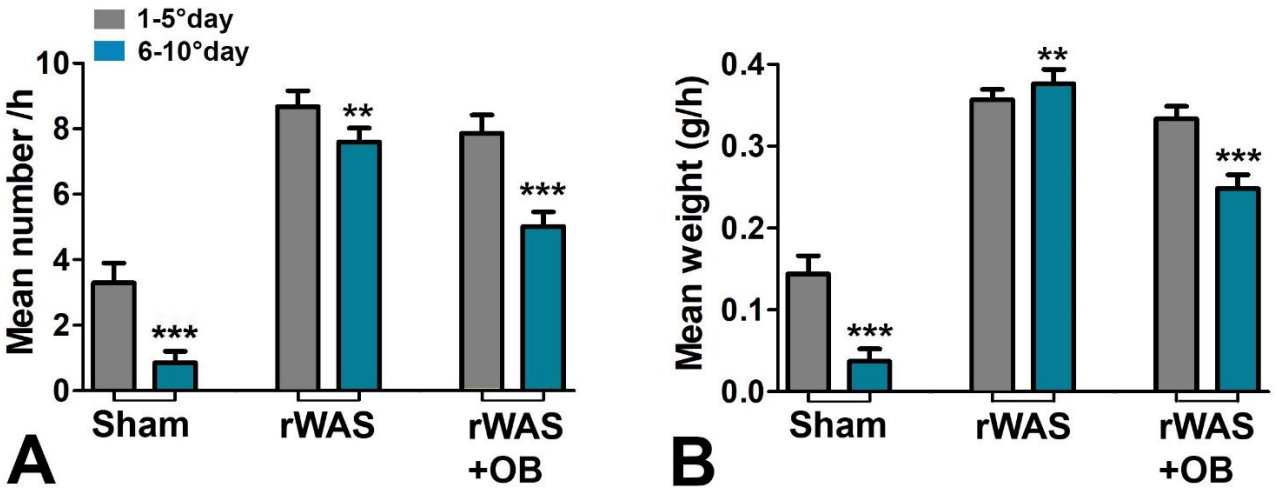

Figure 34. ***Faecal pellet production*** *is expressed as mean number (A) and mean weight (B) per hour. In the rWAS both parameters were significantly higher compared to the Sham all along the entire period of stress application (columns grey and blue). In the rWAS+OB, the faecal pellet production decrease significantly in the second half period of stress exposition (blue columns) of treatment compared to the rWAS and similarly to the Sham (blue columns vs grey columns). Paired two-tailed Student t test, Sham; rWAS+OB ***p<0.0001 compared to the first 5 days of each group. One-way ANOVA followed by Newman-Keuls post-test, **p <0.005 compared to all the other groups. (n=7).*

Histochemistry

Mucus Production and Mucus quality evaluated with PAS and TB staining respectively

The mucus production estimated with PAS staining (Fig. 35A-C), was similar among all the groups of animals. In OB group the secretion was the highest. Quantitation of the staining confirmed these observations but the result obtained in OB rats did not reach the statistical significance (Fig. 35G, right columns). The quality of the mucus (i.e. the acidity), estimated with TB staining (Fig. 35D-F), was significantly increased in rWAS rats compared to the other groups of animals (Fig. 35G, left columns).

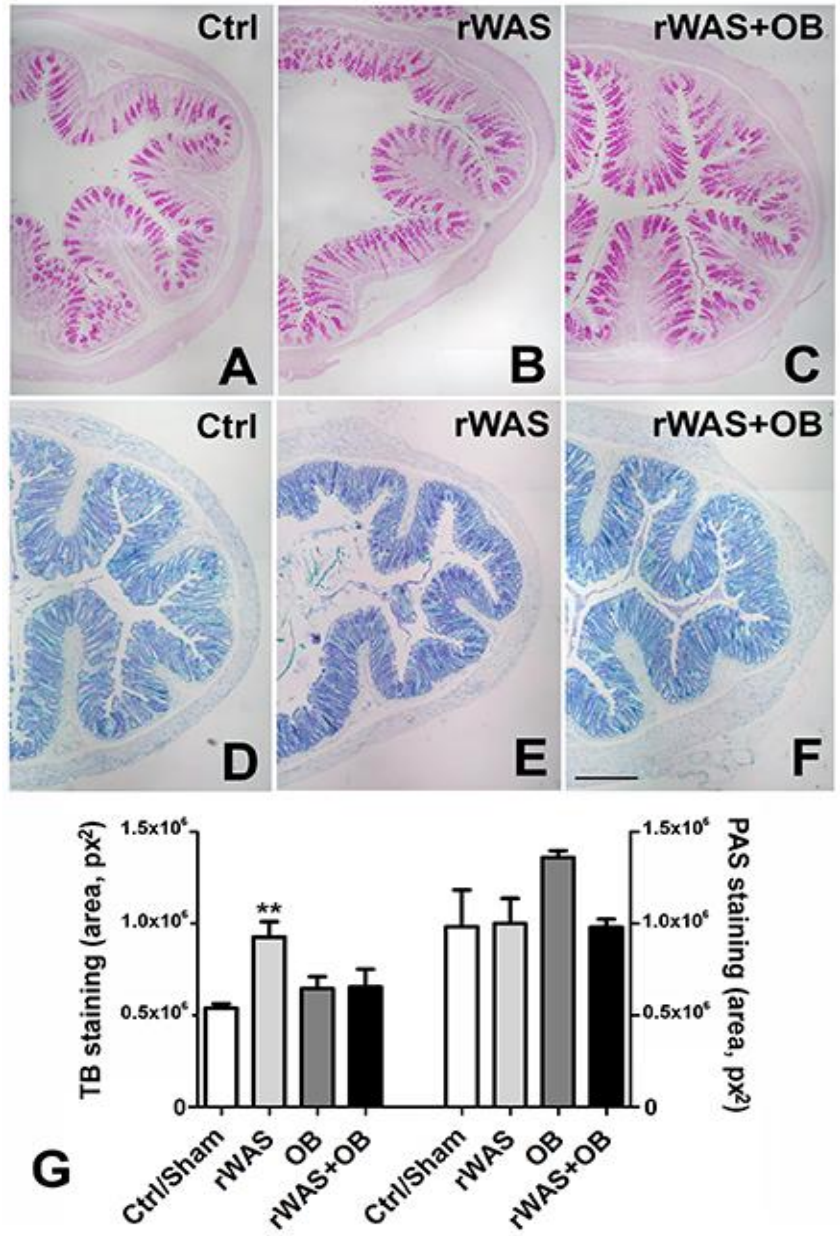

*Figure 35. **Mucus secretion.** Periodic Acid and Schiff's reagent (PAS) **(A-C)** and Toluidine Blue (TB) staining **(D-F).** The two staining were located in the glandular funds and in the goblet cells. Quantitation of PAS staining showed no difference in the total quantity of mucus production among the groups of rats (G, right columns). Conversely, the quantitation of the acidic component, measured as TB metachromasia, demonstrated a significant increase in the rWAS group compared with the other three (G, left columns). (**A-F** bar=50µm). One-way ANOVA followed by Newman-Keuls post-test, **p<0.005. (n=7), Bar=100□m.*

Functional studies

Contractile responses elicited by electrical field stimulation (EFS) in strips from the different animal groups.

In preparations from Ctrl rats, EFS (4 Hz) induced a rapidly arising contractile response (mean amplitude 0.97±0.19g) (Fig. 36 A,B,C) which was abolished by TTX or atropine, indicating its nervous and cholinergic nature, respectively (Fig. 36 A). In a minority (20%) of recordings no responses were elicited during EFS but at the end of the stimulation period an "after contraction" was observed. These responses did not enter the statistics. The amplitude of the contractile responses to EFS in preparations from Ctrl rats was not statistically different from that obtained in Sham ones (mean amplitude 0.95±0.16g). Thus, the statistical data were put and analyzed together (Fig. 36 C).

In preparations from rWAS rats, the amplitude of the contractile responses elicited by EFS (mean amplitude 1.6±0.20 g) was greatly enhanced with respect to that obtained from the Ctrl/Sham animals (Fig. 36 B, C). In strips from OB animals, the amplitude of the EFS-induced contractile responses (mean amplitude 0.52±0.13g) was reduced with respect to the Ctrl/Sham and even more with respect to rWAS groups (Fig. 36B,C). In preparations from rWAS+OB rats, the amplitude of the EFS-induced contractile response (mean amplitude 0.63± 0.12g) was reduced with respect to either Ctrl/Sham or rWAS group but was not statistically different from that obtained in OB animals (Fig. 36 B, C).

TTX or atropine abolished EFS contractile responses in all groups of animals.

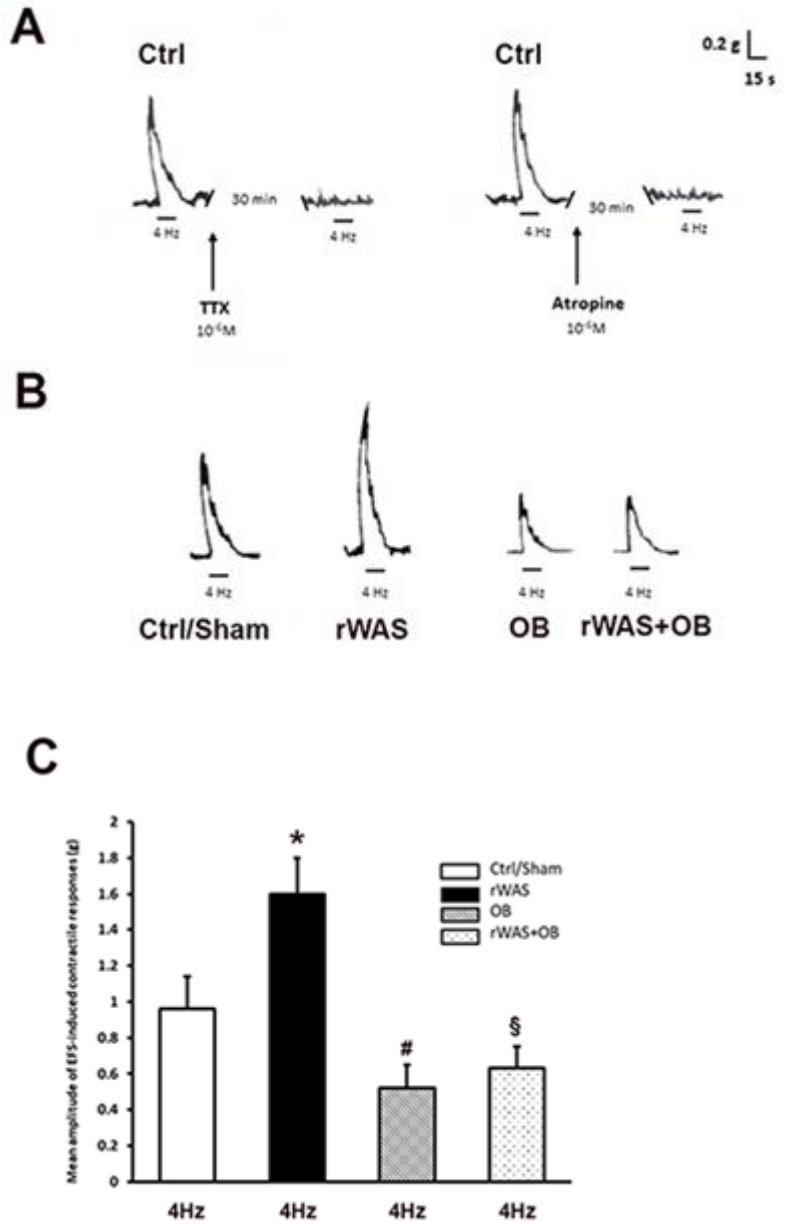

Figure 36. ***EFS in preparations from the different animal groups and effects of TTX and atropine.*** ***A:*** *Typical tracings showing the contractile response to EFS in preparations from Ctrl rats. The response elicited by EFS (4Hz) is abolished following the addition to the bath medium of either TTX (left hand panel) or atropine (right hand panel).* ***B:*** *Typical tracings showing the contractile response to EFS in preparations from: Ctrl, rWAS, OB and rWAS+OB rats. The amplitude of the neurally-induced contractile response to EFS is higher in preparations from rWAS in respect with that recorded from the Ctrl ones. In preparations from both OB and rWAS+OB rats, the amplitude of the contractile response to EFS appears greatly reduced in respect with that of the rWAS or even Ctrl ones.* ***C:*** *Bar chart showing the mean amplitude of the EFS-induced contractile responses in preparations from the different groups. No statistical differences were observed in the amplitude of the contractile responses to EFS between preparations from Ctrl and Sham rats, so all these data were put and analyzed together (Ctrl/Sham). The mean amplitude of the contractile responses to EFS in preparations from rWAS animals is increased in respect with the Ctrl/Sham ones. At variance, that of both OB and rWAS+OB rats is reduced, without statistical differences between these two groups, in respect with Ctrl/Sham and rWAS ones. All values*

*are means ± S.E.M. of 8-12 preparations. *p <0.05 vs Ctrl/Sham; #p <0.05 vs Ctrl/Sham or rWAS; §p <0.05 vs Ctrl/Sham or rWAS and p>0.05 vs OB (ANOVA and Newman-Keuls post-test).*

Direct smooth muscle contractions elicited by methacholine in strips from the different animal groups.

To investigate whether the reduction in amplitude of the EFS-induced contractile responses observed in OB and rWAS+OB preparations could be due to a direct effect of OB on the smooth muscle muscarinic receptors, the effects of methacholine were tested and compared to those obtained in the other animal groups. As previously observed [260], in preparations from both Ctrl and rWAS rats, addition of methacholine to the bath medium caused, after 10-15s of contact time, a sustained contracture which reached a plateau phase that persisted until washout (Fig. 37A). In the present experiments, the amplitude of the contractile responses to methacholine in preparations from Ctrl rats (*n*=6) was not statistically different from that obtained in Sham ones (mean amplitude 1.08±0.1g and 0.99 0.15 g, respectively). Thus, the statistical data were put and analysed together (Fig. 37B). No statistical differences were observed in the amplitude of the direct muscular response to methacholine between the Ctrl/Sham animal group and rWAS rats (mean amplitude 1.04±0.1g and 1 ±0.16g, respectively) (Fig. 37B). The amplitude of the direct muscular responses to methacholine obtained in preparations from either OB (mean amplitude 0.57±0.11g) or rWAS+OB (mean amplitude 0.64±0.08 g) rats was reduced in respect to that of both Ctrl/Sham and rWAS animal groups, thus indicating that the observed reduction in amplitude of the EFS-induced cholinergic contraction in OB and rWAS+OB was, at least in part, ascribable to a direct antimuscarinic effect of OB on the smooth muscle.

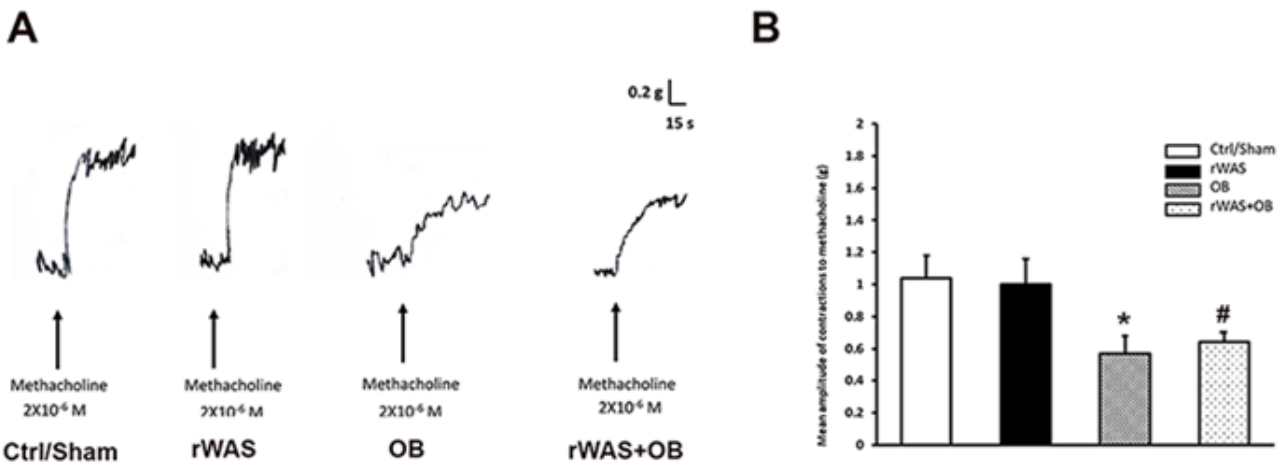

Figure 37. ***Direct muscular responses elicited by methacholine in strips from the different animal groups. A:*** *Typical tracing showing the muscular contraction elicited by the addition of methacholine to the bath medium in preparations*

from: Ctrl, rWAS, OB and rWAS+OB rats. Note the similar amplitude of the response in preparations from Ctrl and rWAS animals and its reduction in both OB and rWAS+OB rats. ***B:*** *Bar chart showing the mean amplitude of the direct contraction induced by methacholine in preparations from: Ctrl/Sham, rWAS, OB and rWAS+OB rats. The amplitude of the response to methacholine was not statistically different between Ctrl and Sham rats, so all the data were put and analysed together (Ctrl/Sham)**.*** *No statistical differences are present in the mean amplitude of the response to methacholine between preparations from Ctrl/Sham and rWAS rats. At variance, the mean amplitude of the direct response to methacholine appears reduced in preparations from both OB and rWAS+OB rats, without statistical differences between these two groups, in respect with the Ctrl/Sham and rWAS ones. All values are means ± S.E.M. of 6-8 preparations. *p <0.05 vs Ctrl/Sham or rWAS; #p <0.05 vs Ctrl/Sham or rWAS and p>0.05 vs OB (ANOVA and Newman-Keuls post-test).*

Immunohistochemistry

Protein Gene Product 9.5(PGR9.5) and Choline Acetyl Transferase (ChAT)-immunoreactivity (IR).

In all groups of animals, the pan-neuronal marker PGP9.5-IR was detected in the neurons of both enteric plexuses an in the nerve fibres of the muscle coat (Fig. 38A-D). The labelling was homogenously distributed in the cytoplasm. The quantitation of the myenteric neurons expressing PGP9.5 displayed no significant differences among the groups (Ctrl=80±5,2; Sham=79,47±4,9; rWAS= 78,81±3,1; OB=85,00±3,2; rWAS+OB=80,41±3,5). ChAT-IR was observed in the cytoplasm of several myenteric neurons and in few intramuscular nerve fibres (Fig. 38E-H); the labelling was homogenously distributed. The quantitation of the ChAT-IR neurons, expressed as total numbers as well as percentage of PGP9.5-IR neurons, showed a significant increase in the rWAS rats respect to all the other groups (Fig. 38I).

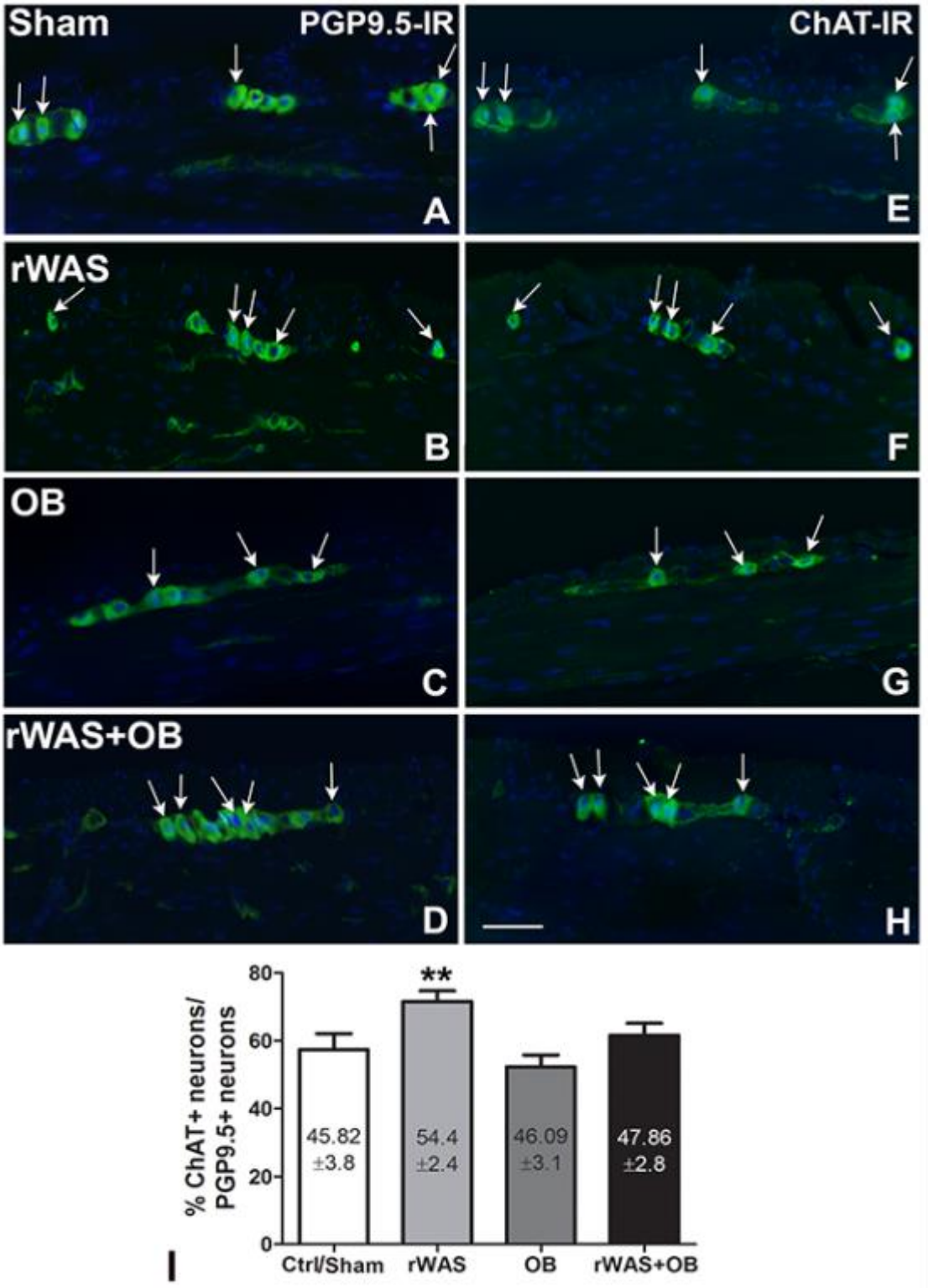

Figure 38. ***Protein Gene Product 9.5 (PGP9.5) and Choline Acetyl-Transferasi (ChAT)- immunoreactive (IR) myenteric neurons.*** *PGP9.5 (A-D) and ChAT (E-H) labelling (green) in the myenteric neurons of Sham (A,E), rWAS (B,F), OB (C,G) and rWAS+OB (D,H) rat distal colon. The Hoechst 33342 labelled the nuclei (blue). The arrows indicate the neurons that express both PGP9.5 and ChAT. Bar=50 µm. Quantitative analysis of the percentage (%) of ChAT-IR neurons respect to the total PGP9.5-IR neurons and of the total number of ChAT-IR neurons. (I). The columns express the %. The number of ChAT-IR neurons is reported inside the columns. Both parameters showed a significant increase in the rWAS compared*

*with all the other groups. Only the labelled neurons containing the nucleus were included in the statistical analysis. One-way ANOVA followed by Newman-Keuls post-test, ** P <0.005. (n=5).*

DISCUSSION & CONCLUSIONS

11.1 RESEARCH STUDY 1 - DISCUSSION

The findings obtained from this study indicate that cisplatin, administered in mice at a dosage comparable to that used in humans (3mg/kg), can induce several behavioural, morphological and functional gastrointestinal changes. The daily monitoring of the physiological parameters showed a gradual decline in overall condition, characterized by a lack of weight gain and an eating behaviour that involved a greater intake of kaolin. These observations could be indicative of pica. At the end of the treatment period, the mice displayed a notable reduction in stool production, accompanied by a decline in mucus secretion in both proximal and distal colon and signs of mucosal inflammation in the proximal colon.

Daily administration of prebiotics prevented alterations in stool production, mucus secretion and inflammation, and significantly reduced kaolin intake. However, the treatment had no effect on weight gain deficits. The functional studies indicated a notable decline in the amplitude of both spontaneous and methacholine-induced muscular contractions in colonic strips of mice treated with cisplatin. The immunohistochemical results displayed no neuronal loss in ascending and descending colon, whereas a reduction in Cx43 expression in the ICC of the proximal colon was detected. Prebiotics treatment partially prevented the alterations of spontaneous contractions and of Cx43 expression while had no effect on methacholine responses. SCFA assays showed no significant differences between groups.

In agreement with previous studies, chronic cisplatin impaired the animal's growth[167,168]. From the first week of treatment onwards, regardless of whether prebiotics were present in the diet, there was a noticeable halt in weight gain, which lasted until the end of the fourth week. It seems likely that the failure to gain weight is attributable to mucositis. This is the most common finding following cisplatin treatment, and the upper GI regions (stomach, ileum) are particularly susceptible to the drug toxicity. Stomach injury, in particular, would play a major role. Using a dose lower than the current one, we found a remarkable fundus distension, mucosal damage and neuropathy.

Functional studies showed a significant delay of gastric emptying responsible for nausea and pica[161,162]. Likewise, comparable or lower doses of cisplatin caused ileum injury that compromises food absorption[161,162,164,169]. Thus, because of the gastric and ileal damages, our animals did not growth although they assumed as much food as controls.

The reduction in mucin production in the proximal and distal colon of Cspl-treated mice may be due to the drug's antimitotic activity, which could potentially lead to reduced cell renewal and/or impairment of mucin synthesis by surviving glandular cells[160]. It seems likely that our finding depends on both conditions, as the decrease in TB+ area was accompanied by a decrease in PAS+ cells. In the colon, unlike the ileum, the mucus forms a continuous and thick layer on the epithelium, which serves two important functions. Firstly, it protects the epithelium, reinforcing the intestinal barrier. Secondly, it nourishes the microbiota. Thus a reduction of the mucus layer may favour mucosal damage, dysbiosis and appearance of mucositis. It is possible that the efficacy of prebiotics to prevent mucus loss may be due to their ability to interact with soluble molecules present in the mucus, which may help to avoid their degradation and loss and/or to select bacterial strains producers of molecules able to recruit myeloid cells, which in turn stimulate mucin synthesis[261–263].

The significant reduction of stool production found in the Cspl group at the end of the treatment agrees with the finding recorded in the functional study. The motility pattern of the colon is a highly complex phenomenon, with a variety of patterns having been described in different species and colonic segments[264,265]. In the present study, the strips of proximal colon exhibit a spontaneous contractile activity consisting of rhythmic changes in isometric tension. While no differences in motility patterns were observed among all mouse groups, there was a notable reduction in the amplitude of the spontaneous contractile activity in strips from the Cspl-treated mice. Notably, co-treatment with prebiotics partially counteracted this reduction and prevented the decrease in stool production. The amplitude of the muscular spontaneous contractions did not differ between strips from Ctrl and Ctrl+Prebio mice, thus indicating that prebiotics pretreatment 'per se' had no effect on the spontaneous contractile activity. It has been previously reported that impaired intestinal motility may occur following chronic treatment with cisplatin, potentially due to a neuropathy mainly consisting in a reduction of the myenteric neuronal population.[162,164,167,168] However, in

our specimens, from both proximal and distal colon, we did not observe any change in the total number of myenteric neurons.

In light of these findings, we decided to explore the possibility that other cell types, such as the ICC, might also be affected by Cspl damage. In the colon, these cells generate spontaneous contractions and mediate a complex synchronization of excitation and inhibition of the smooth muscle as in functional syncytium [26,266,267]. In the colon, the three ICC subpopulations, all c-Kit positive, through gap junctions, form a 3D network along the entire muscle wall and contact smooth muscle cells controlling their activity. Finally, ICCs receive innervation through synapse-like contacts[96]. Previous experiments demonstrated that the c-Kit expression in the ICC of the gastric antrum of Suncus Murinus was significantly reduced following the administration of a sublethal dose of cisplatin in a single injection[268]; while an increase of c-Kit mRNA levels was described in the ileum of mice subjected to chronic cisplatin treatment[165]. To the best of our knowledge, ICC have never been investigated in the colon of rodents treated with cisplatin. Based on these findings, by using immunohistochemistry, investigate ICC changes related to the altered amplitude of the motor pattern observed in Cspl mice. The results indicated that there was no change in c-Kit labelling among the groups, while a notable reduction in the expression of the gap-junction protein Cx43 was observed. Cx43 is one of the main proteins forming connexons, so this reduction could be a relevant finding. It is worth noting that while some studies have described Cx43 as the common connexin of both smooth muscle cells and ICC gap junctions, others have reported a selective Cx43 labelling of the ICC in human bowel[269–271]. In our samples of mouse proximal colon, Cx43 labelling was present at the level of the MP and, to a lesser extent, at the border of the SM and in the thickness of the circular muscle layer; the labelling distribution consistently overlapped with that of the three ICC subtypes, as confirmed by the c-Kit antibody labelled twin slices.

The reduction in Cx43 might be due to a reduced number of connexons and/or to altered protein composition of these channels. In both cases, the consequence could be an impairment in the electrical transmission to the smooth muscle. The ability of prebiotics to prevent Cx43 loss suggests the involvement of the microbiota. In this regard, it was reported, in humans and mice, that gut inflammatory processes of different genesis trigger a molecular cascade able to affect the ICC, causing ICC-pathy[272,273] and that fructans

prebiotic such as inulin, that represents the major component of our prebiotic mixture, has anti-inflammatory and antioxidant properties besides promoting Bifidobacterium increase[274,275].

The functional results in Cspl-treated mice showed a decrease in the amplitude of both TTX-insensitive spontaneous contractile activity and direct muscle contractile response to methacholine, which could suggest an impairment of the smooth muscle. It would be premature to conclude that the effect of Cspl on the response to methacholine is not mediated by the cholinergic pathways. However, since the number of ChAT-IR myenteric neurons was found to be unaltered in Cspl-treated animals, we put forward the hypothesis that the drug affects the contractility of smooth muscle cells both indirectly (due to the ICC-pathy), and directly damaging the muscarinic receptors. The prebiotics were not effective in preventing the reduction of the response to methacholine.

Unexpectedly, Cspl had no significant effects on SCFA concentrations in the feces. SCFA are implicated in the wellness of the microbiota and of the host. Among them, a particular emphasis has been placed on butyric, propionate and acetate acids[276, 277].

11.2 Research Study 1 - Conclusions

In summary, it can be concluded that Cspl causes injury to the mouse proximal and distal colon. In addition to the lack of weight gain due to systemic GI damage, the drug impairs mucin production and mucosa integrity responsible for mucositis and cause a significant decrease in the amplitude of spontaneous contractions, which is associated with constipation. It is reasonable to hypothesize that the latter manifestations are due to an ICC-pathy characterized by a significant decrease in Cx43 expression. Moreover, it is likely that the Cspl muscular changes are the result of postsynaptic muscarinic damage, as demonstrated by the deficit in the contractile response to the cholinergic agonist methacholine.

The prebiotic mixture, administered chronically during chemotherapy, appears to have a protective effect on the intestinal wall, preventing mucositis and the decrease in mucin secretion. Prebiotics also seem to counteract the loss of Cx43 and the impairment of spontaneous motility. However, the prebiotics have no effect on the alteration of postsynaptic muscarinic receptors.

Based on our results, we hypothesize that the beneficial effects of prebiotics on the intestinal wall may be the result of their protective action on the microbiota, particularly due to the preservation of the mucous layer integrity. Unlike the expectations, the study of SCFA did not show any significant variations either in Cspl or Cspl+Prebio treatment, suggesting that other mechanisms or metabolic ways might be implicated in the efficacy of the treatment in protecting the gut wall.

Nevertheless, we suggest that the proposed treatment, which is easy to take and free of side effects, deserves attention to help to maintain the effective dose of chemotherapy by preventing and/or reducing its toxicity and even improving its effectiveness.

11.3 RESEARCH STUDY 2 - DISCUSSION

The rWAS study shows that cholinergic neurotransmission in the rat distal colon is changed by daily exposure to a one-hour psychosocial stress for 10 days Specifically, rWAS produces: i) a significant increase in the mucus acidity in the epithelium without changes in total mucus secretion; ii) a significant increase in amplitude of the contractile responses to electrical stimulation that is counteracts by TTX and atropine treatment: iii) an increase in the number of ChAT-IR myenteric neurons. The treatment with OB prevents most of these changes. Mayer and Collins in 2002[255] lodged the criteria to evaluate animals' models for functional disorders and Traini et al[222] demonstrated that the currently used rWAS procedure with those criteria and that the colonic modifications overlap those observed in IBS patients. In particular, the increased fecal production in rWAS rats during the stress application is a clear sign of colonic hyperactivity [222,278,279].

In this research study, we observed a significant increase in acidic mucus secretion in rWAS rats. Mucus covers the entire gastrointestinal surface and plays a critical role in local homeostasis, influencing the bacterial population and luminal pH[280]. In IBS patients the mucus quality has never been evaluated, nevertheless dysbiosis was described in more than 70% of cases[281]. These microbial impairment causes changes in mucus quality, low-grade mucosal inflammation and alters the intestinal barrier[282,283]. Mucus composition modifications also induce dysbiosis, so a never-ending vicious cycle is established Literature data show that acetylcholine regulates mucus secretion, epithelial ion transport and the activity of colonic crypt; thus, we suppose that at the basis of the observed altered mucosal secretion in rWAS colon, there is an activation of cholinergic pathways (i.e. those located at the level of the submucosal plexus). If so, the ability of OB to prevent mucus secretion modification in rWAS+OB rats might be imputable to its antimuscarinic activity. In this regard, it has been reported that OB controls submucosal cholinergic activation by inhibiting the M3 receptors [284]. Zhou and collaborators have proven that OB also acts as an antibiotic killing pathogenic microbes such as the *Staphylococcus aureus*; therefore, the OB prevention of mucus changes in rWAS could also be mediated by its antimicrobial property.

.

In the functional experiments, the increased amplitude of electrically induced contractile responses in rWAS preparations compared to the Ctrl/Sham ones and the similar amplitude of the direct muscular response to methacholine between the two animal groups indicate that the rWAS animal model selectively involves the cholinergic output without affecting the post-synaptic muscular response. The observation that, in all animal groups, the EFS-induced contractile responses were abolished by TTX or atropine confirms their nervous and cholinergic origins, respectively. According with a main involvement of the cholinergic system in rWAS are the immunohistochemical results showed an increase in the number of ChAT-IR myenteric neurons in this group of rats. When OB was administrated (rWAS+OB) we observed no EFS-induced increase in the amplitude of neuronal contractions, opposite to what was recorded in rWAS preparations. However, the effect of OB on the colonic mechanical responses was more complex than expected. In fact, in the rWAS+OB preparations and in those of rats treated only with OB, the amplitude of neurally-induced contractile responses to EFS was significantly lower than that of Ctrl/Sham animals, suggesting the presence of an intrinsic antimuscarinic action of the drug [221], regardless of the application of stress. In favor of a direct antimuscarinic effect of OB is the observation that the amplitude of the muscular responses to methacholine was reduced in both OB and rWAS+OB preparations in comparison with Ctrl/Sham and rWAS rats. Thus, the functional data suggest that OB decreases the amplitude of EFS-induced contractile responses at least in part through an antimuscarinic activity. Whether this decrease in the EFS in rWAS+OB preparations comprises both, presynaptic and post-synaptic cholinergic structures cannot be inferred from these studies, as the neuronal effect could be masked by the direct antimuscarinic post-synaptic effects of the drug on smooth muscle.

Immunohistochemical experiments showed that rWAS have a significant increase in the number of ChAT-IR, indicating that stress activates the cholinergic system; OB prevented ChAT-IR increment.

In summary, a dual mechanism of action is at the bases of the OB effect on cholinergic transmission: on neurons (presynaptic) and on smooth muscle cells (postsynaptic); this statement is given based on the summa of immunohistochemical and functional data.

The main mediator of psychosocial stress in mammals is thought to be the hypothalamic corticotropin-releasing hormone (CRF)[285–288]. CRF injected centrally or peripherally, mimics responses that

are also produced by stress, including adverse gut responses[285,289,290]. CRF acts on CRF1 and CRF2 receptors. However, the response caused by the CRFR activation are significantly different. In particular, CRF1r only directly induces the adverse effects, whereas CRF2r blocks CRF1r activation; CRF2r seems to have no effect by itself. CRF has a higher affinity forCRF1r , than for CRF2r [285,288,291,292]. In the rat distal colon, 95% of myenteric neurons express CRF1r, and when CRF binds to CRF1r, 50% of these neurons show a significant increase in c-fos [285,292,293]. Up to 40% of cholinergic neurons express c-fos, as revealed by co-labelling experiments, and c-fos activation promotes transcription of choline acetyltransferase and other neurotransmitter biosynthetic enzymes (42) Krukoff and coll.(data) reported that c-fos activation augments defecation. We can conclude that, in rWAS rats, CRF1r-c-fos activation induces ChAT gene transcription and, sequentially, an increase in ChAT-IR myenteric neurons.

As previously stated, OB administration prevents the action of chronic stress on the cholinergic system. In fact, Traini et al. (data)[222] reported that rats subjected to wrap restrain stress, another type of psychosocial stress model, showed an increase in CRF1r and CRF2r expression in colonic myenteric neurons and that OB prevented the increase in CRF1r without affecting the increase in CRF2r.

11.4 Research Study 2- Conclusions

The present study, aimed to investigate the pathogenic mechanisms of IBS using an animal model(rWAS) and the treatment of OB, led us to draw a composite picture where the combination of morphological and functional experiments proved to be essential. Previously, our research group[222], using the same model and drug treatment, showed that a depression of spontaneous contractility was associated with a significant increase in the inhibitory nitrergic neurons. At present, we detect an increase in the electrically evoked responses of the colonic wall of rWAS rats associates with an increase in the excitatory cholinergic neurons. All together, these data allow us to state that psychosocial stress affects the two main mediators of enteric motility. Moreover, starting from the well-known role of CRF as a mediator of psychosocial stress [285,286] and based on the available data demonstrating that CRF receptors are highly expressed in both nitrergic and cholinergic neurons[291,292], we consider that CRF plays a major role in the pathogenesis of IBS and propose

that OB, by preventing CRF1r activation, is able to interrupt the cascade of events that cause the functional and immunohistochemical changes described in rWAS rats. Furthermore, the reduced response to methacholine in OB-treated rats indicates that OB exerts 'per se' a post-synaptic antimuscarinic effect, independently of stress, and confirms the complexity of its mechanism of action [221].

In this perspective, it will be interesting to evaluate blood and brain corticotropin levels during the application of stress to better understand the mechanisms of action of OB [221,294–296]. Finally, from a clinical point of view, our results strengthen the hypothesis formulated in some clinical studies[297,298] that cyclical or intermittent treatment with OB, regardless of the presence of IBS symptoms, may be an appropriate therapeutic strategy to manage the disease.

BIBLIOGRAPHY

1. Knoblaugh, S. E. & Randolph-Habecker, J. Necropsy and Histology. in *Comparative Anatomy and Histology* 23–51 (Elsevier, 2018). doi:10.1016/B978-0-12-802900-8.00003-8.
2. Padmanabhan, P., Grosse, J., Asad, A. B. M. A., Radda, G. K. & Golay, X. Gastrointestinal transit measurements in mice with 99mTc-DTPA-labeled activated charcoal using NanoSPECT-CT. *EJNMMI Res.* **3**, 60 (2013).
3. Hugenholtz, F. & de Vos, W. M. Mouse models for human intestinal microbiota research: a critical evaluation. *Cell. Mol. Life Sci. CMLS* **75**, 149–160 (2018).
4. Uysal, M. *et al.* Caecum location in laboratory rats and mice: an anatomical and radiological study. *Lab. Anim.* **51**, 245–255 (2017).
5. Snipes, R. L. Anatomy of the cecum of the laboratory mouse and rat. *Anat. Embryol. (Berl.)* **162**, 455–474 (1981).
6. Yip, J. L. K., Balasuriya, G. K., Spencer, S. J. & Hill-Yardin, E. L. Examining enteric nervous system function in rat and mouse: an interspecies comparison of colonic motility. *Am. J. Physiol.-Gastrointest. Liver Physiol.* **323**, G477–G487 (2022).
7. Theiler, K. *The House Mouse: Atlas of Embryonic Development*. (Springer Berlin Heidelberg, Berlin, Heidelberg, 1989). doi:10.1007/978-3-642-88418-4.
8. Furness, J. B. The enteric nervous system and neurogastroenterology. *Nat. Rev. Gastroenterol. Hepatol.* **9**, 286–294 (2012).
9. Donadon, M. & Santoro, M. M. The origin and mechanisms of smooth muscle cell development in vertebrates. *Development* **148**, dev197384 (2021).
10. Hill-Eubanks, D. C., Werner, M. E., Heppner, T. J. & Nelson, M. T. Calcium Signaling in Smooth Muscle. *Cold Spring Harb. Perspect. Biol.* **3**, a004549–a004549 (2011).
11. Guiu, J. *et al.* Tracing the origin of adult intestinal stem cells. *Nature* **570**, 107–111 (2019).

12. Of Journal ‘Morphologia’, E. O. Histology: A Text and Atlas: With Correlated Cell and Molecular Biology. Eighth Edition, 2018 Authors: Wojciech Pawlina; Michael H. Ross. *Morphologia* **13**, 76–89 (2019).
13. Litvak, Y., Byndloss, M. X. & Bäumler, A. J. Colonocyte metabolism shapes the gut microbiota. *Science* **362**, eaat9076 (2018).
14. Beumer, J. & Clevers, H. Cell fate specification and differentiation in the adult mammalian intestine. *Nat. Rev. Mol. Cell Biol.* **22**, 39–53 (2021).
15. Azzouz, L. L. & Sharma, S. Physiology, Large Intestine. in *StatPearls* (StatPearls Publishing, Treasure Island (FL), 2025).
16. Sorensen, M. V., Matos, J. E., Praetorius, H. A. & Leipziger, J. Colonic potassium handling. *Pflüg. Arch. - Eur. J. Physiol.* **459**, 645–656 (2010).
17. Sandle, G. I. & Hunter, M. Apical potassium (BK) channels and enhanced potassium secretion in human colon. *QJM* **103**, 85–89 (2010).
18. Hanukoglu, I. & Hanukoglu, A. Epithelial sodium channel (ENaC) family: Phylogeny, structure–function, tissue distribution, and associated inherited diseases. *Gene* **579**, 95–132 (2016).
19. Greger, R. Role of CFTR in the Colon. *Annu. Rev. Physiol.* **62**, 467–491 (2000).
20. Kiela, P. R. & Ghishan, F. K. Physiology of Intestinal Absorption and Secretion. *Best Pract. Res. Clin. Gastroenterol.* **30**, 145–159 (2016).
21. Costa, M. *et al.* Characterization of alternating neurogenic motor patterns in mouse colon. *Neurogastroenterol. Motil.* **33**, e14047 (2021).
22. Bywater, R. A., Small, R. C. & Taylor, G. S. Neurogenic slow depolarizations and rapid oscillations in the membrane potential of circular muscle of mouse colon. *J. Physiol.* **413**, 505–519 (1989).
23. Bush, G., Luu, P. & Posner, M. I. Cognitive and emotional influences in anterior cingulate cortex. *Trends Cogn. Sci.* **4**, 215–222 (2000).
24. Brierley, S. M., Nichols, K., Grasby, D. J. & Waterman, S. A. Neural mechanisms underlying migrating motor complex formation in mouse isolated colon. *Br. J. Pharmacol.* **132**, 507–517 (2001).

25. Bayguinov, P. O., Hennig, G. W. & Smith, T. K. Ca2+ imaging of activity in ICC-MY during local mucosal reflexes and the colonic migrating motor complex in the murine large intestine. *J. Physiol.* **588**, 4453–4474 (2010).
26. Beck, K., Friebe, A. & Voussen, B. Nitrergic signaling via interstitial cells of Cajal and smooth muscle cells influences circular smooth muscle contractility in murine colon. *Neurogastroenterol. Motil.* **30**, e13300 (2018).
27. Fung, C. & Vanden Berghe, P. Functional circuits and signal processing in the enteric nervous system. *Cell. Mol. Life Sci.* **77**, 4505–4522 (2020).
28. Spencer, N. J. & Hu, H. Enteric nervous system: sensory transduction, neural circuits and gastrointestinal motility. *Nat. Rev. Gastroenterol. Hepatol.* **17**, 338–351 (2020).
29. Furness, J. B. The enteric nervous system: normal functions and enteric neuropathies. *Neurogastroenterol. Motil.* **20**, 32–38 (2008).
30. Brehmer, A., Schrödl, F. & Neuhuber, W. Morphological classifications of enteric neurons -- 100 years after Dogiel. *Anat. Embryol. (Berl.)* **200**, 125–135 (1999).
31. Clerc, N., Furness, J. B., Bornstein, J. C. & Kunze, W. A. A. Correlation of electrophysiological and morphological characteristics of myenteric neurons of the duodenum in the guinea-pig. *Neuroscience* **82**, 899–914 (1997).
32. Nurgali, K., Stebbing, M. J. & Furness, J. B. Correlation of electrophysiological and morphological characteristics of enteric neurons in the mouse colon. *J. Comp. Neurol.* **468**, 112–124 (2004).
33. Fleming, M. A., Ehsan, L., Moore, S. R. & Levin, D. E. The Enteric Nervous System and Its Emerging Role as a Therapeutic Target. *Gastroenterol. Res. Pract.* **2020**, 1–13 (2020).
34. Kreulen, D. L. & Szurszewski, J. H. Reflex pathways in the abdominal prevertebral ganglia: evidence for a colo-colonic inhibitory reflex. *J. Physiol.* **295**, 21–32 (1979).
35. Hibberd, T. J., Zagorodnyuk, V. P., Spencer, N. J. & Brookes, S. J. H. Identification and mechanosensitivity of viscerofugal neurons. *Neuroscience* **225**, 118–129 (2012).
36. Furness, J. B. Novel gut afferents: Intrinsic afferent neurons and intestinofugal neurons. *Auton. Neurosci. Basic Clin.* **125**, 81–85 (2006).

37. Gulbransen, B. D. & Sharkey, K. A. Novel functional roles for enteric glia in the gastrointestinal tract. *Nat. Rev. Gastroenterol. Hepatol.* **9**, 625–632 (2012).

38. Mullen, R. J., Buck, C. R. & Smith, A. M. NeuN, a neuronal specific nuclear protein in vertebratesxs. *Development* **116**, 201–211 (1992).

39. Gusel'nikova, V. V. & Korzhevskiy, D. E. NeuN As a Neuronal Nuclear Antigen and Neuron Differentiation Marker. *Acta Naturae* **7**, 42–47 (2015).

40. Trowern, A. R., Laight, R., MacLean, N. & Mann, D. A. Detection of neuron-specific protein gene product (PGP) 9.5 in the rat and zebrafish using anti-human PGP9.5 antibodies. *Neurosci. Lett.* **210**, 21–24 (1996).

41. Jouhilahti, E.-M., Peltonen, S. & Peltonen, J. Class III β-Tubulin Is a Component of the Mitotic Spindle in Multiple Cell Types. *J. Histochem. Cytochem.* **56**, 1113–1119 (2008).

42. Boesmans, W., Hao, M. M. & Vanden Berghe, P. Optogenetic and chemogenetic techniques for neurogastroenterology. *Nat. Rev. Gastroenterol. Hepatol.* **15**, 21–38 (2018).

43. Zhai, P. *et al.* Regulating electronic states of nitride/hydroxide to accelerate kinetics for oxygen evolution at large current density. *Nat. Commun.* **14**, 1873 (2023).

44. Hussain, S. *et al.* A COMPREHENSIVE REVIEW ON NEUROTRANSMITTERS, ITS BIOLOGICAL IMPORTANCE AND METHODS OF ANALYSIS. *J. Microbiol. Mol. Genet.* **4**, 11–41 (2023).

45. Halder, N. & Lal, G. Cholinergic System and Its Therapeutic Importance in Inflammation and Autoimmunity. *Front. Immunol.* **12**, 660342 (2021).

46. Steinhoff, M. S., Von Mentzer, B., Geppetti, P., Pothoulakis, C. & Bunnett, N. W. Tachykinins and Their Receptors: Contributions to Physiological Control and the Mechanisms of Disease. *Physiol. Rev.* **94**, 265–301 (2014).

47. Swaminathan, M., Hill-Yardin, E. L., Bornstein, J. C. & Foong, J. P. P. Endogenous Glutamate Excites Myenteric Calbindin Neurons by Activating Group I Metabotropic Glutamate Receptors in the Mouse Colon. *Front. Neurosci.* **13**, 426 (2019).

48. Ekblad, E. & Bauer, A. J. Role of vasoactive intestinal peptide and inflammatory mediators in enteric neuronal plasticity. *Neurogastroenterol. Motil.* **16 Suppl 1**, 123–128 (2004).

49. Watkins, C. C. *et al.* Carbon monoxide mediates vasoactive intestinal polypeptide-associated nonadrenergic/noncholinergic neurotransmission. *Proc. Natl. Acad. Sci.* **101**, 2631–2635 (2004).
50. Koh, S. D., Dick, G. M. & Sanders, K. M. Small-conductance Ca2+-dependent K+ channels activated by ATP in murine colonic smooth muscle. *Am. J. Physiol.-Cell Physiol.* **273**, C2010–C2021 (1997).
51. Waseda, K. *et al.* Participation of ATP in Nonadrenergic, Noncholinergic Relaxation of Longitudinal Muscle of Wistar Rat Jejunum. *J. Pharmacol. Sci.* **97**, 91–100 (2005).
52. Matsuda, N. M. & Miller, S. M. Non-adrenergic non-cholinergic inhibition of gastrointestinal smooth muscle and its intracellular mechanism(s). *Fundam. Clin. Pharmacol.* **24**, 261–268 (2010).
53. O'Toole, T. J. & Sharma, S. Physiology, Somatostatin. in *StatPearls* (StatPearls Publishing, Treasure Island (FL), 2025).
54. Brookes, S. J. H., Steele, P. A. & Costa, M. Identification and immunohistochemistry of cholinergic and non-cholinergic circular muscle motor neurons in the guinea-pig small intestine. *Neuroscience* **42**, 863–878 (1991).
55. Holzer, P. & Holzer-Petsche, U. Tachykinins in the gut. Part I. Expression, release and motor function. *Pharmacol. Ther.* **73**, 173–217 (1997).
56. Grider, J. R. Neurotransmitters Mediating the Intestinal Peristaltic Reflex in the Mouse. *J. Pharmacol. Exp. Ther.* **307**, 460–467 (2003).
57. Fahrenkrug, J. *et al.* Nervous release of vasoactive intestinal polypeptide in the gastrointestinal tract of cats: possible physiological implications. *J. Physiol.* **284**, 291–305 (1978).
58. Costa, M. *et al.* Projections and chemical coding of neurons with immunoreactivity for nitric oxide synthase in the guinea-pig small intestine. *Neurosci. Lett.* **148**, 121–125 (1992).
59. Sanders, K. M. & Ward, S. M. Nitric oxide as a mediator of nonadrenergic noncholinergic neurotransmission. *Am. J. Physiol.-Gastrointest. Liver Physiol.* **262**, G379–G392 (1992).
60. Xue, L. *et al.* Carbon monoxide and nitric oxide as coneurotransmitters in the enteric nervous system: Evidence from genomic deletion of biosynthetic enzymes. *Proc. Natl. Acad. Sci.* **97**, 1851–1855 (2000).

61. Brookes, S. J. H., Steele, P. A. & Costa, M. Calretinin immunoreactivity in cholinergic motor neurones, interneurones and vasomotor neurones in the guinea-pig small intestine. *Cell Tissue Res.* **263**, 471–481 (1991).

62. Young, H. M., Furness, J. B. & Povey, J. M. Analysis of connections between nitric oxide synthase neurons in the myenteric plexus of the guinea-pig small intestine. *J. Neurocytol.* **24**, 257–263 (1995).

63. Brookes, S. J. H. Classes of enteric nerve cells in the guinea-pig small intestine. *Anat. Rec.* **262**, 58–70 (2001).

64. Furness, J. B. & Costa, M. Neurons with 5-hydroxytryptamine-like immunoreactivity in the enteric nervous system: Their projections in the guinea-pig small intestine. *Neuroscience* **7**, 341–349 (1982).

65. Monro, R. L., Bertrand, P. P. & Bornstein, J. C. ATP and 5-HT are the principal neurotransmitters in the descending excitatory reflex pathway of the guinea-pig ileum. *Neurogastroenterol. Motil.* **14**, 255–264 (2002).

66. Gwynne, R. & Bornstein, J. Synaptic Transmission at Functionally Identified Synapses in the Enteric Nervous System: Roles for Both Ionotropic and Metabotropic Receptors. *Curr. Neuropharmacol.* **5**, 1–17 (2007).

67. Portbury, A. L. *et al.* Cholinergic, somatostatin-immunoreactive interneurons in the guinea pig intestine: morphology, ultrastructure, connections and projections. *J. Anat.* **187 (Pt 2)**, 303–321 (1995).

68. Li, Z. S. & Furness, J. B. Immunohistochemical localisation of cholinergic markers in putative intrinsic primary afferent neurons of the guinea-pig small intestine. *Cell Tissue Res.* **294**, 35–43 (1998).

69. Johnson, P. J. & Bornstein, J. C. Neurokinin-1 and -3 receptor blockade inhibits slow excitatory synaptic transmission in myenteric neurons and reveals slow inhibitory input. *Neuroscience* **126**, 137–147 (2004).

70. Surprenant, A. Slow excitatory synaptic potentials recorded from neurones of guinea-pig submucous plexus. *J. Physiol.* **351**, 343–361 (1984).

71. Monro, R. L., Bertrand, P. P. & Bornstein, J. C. ATP participates in three excitatory postsynaptic potentials in the submucous plexus of the guinea pig ileum. *J. Physiol.* **556**, 571–584 (2004).

72. Cassuto, J., Fahrenkrug, J., Jodal, M., Tuttle, R. & Lundgren, O. Release of vasoactive intestinal polypeptide from the cat small intestine exposed to cholera toxin. *Gut* **22**, 958–963 (1981).

73. Banks, M. R., Farthing, M. J. G., Robberecht, P. & Burleigh, D. E. Antisecretory actions of a novel vasoactive intestinal polypeptide (VIP) antagonist in human and rat small intestine. *Br. J. Pharmacol.* **144**, 994–1001 (2005).

74. Keast, J. R., Furness, J. B. & Costa, M. Investigations of nerve populations influencing ion transport that can be stimulated electrically, by serotonin and by a nicotinic agonist. *Naunyn. Schmiedebergs Arch. Pharmacol.* **331**, 260–266 (1985).

75. Holst, J. J. *et al.* GRP nerves in pig antrum: role of GRP in vagal control of gastrin secretion. *Am. J. Physiol.-Gastrointest. Liver Physiol.* **253**, G643–G649 (1987).

76. Weigert, N. *et al.* Role of vagal fibers and bombesin/gastrin-releasing peptide-neurons in distention-induced gastrin release in rats. *Regul. Pept.* **69**, 33–40 (1997).

77. Nilsson, G., Simon, J., Yalow, R. S. & Berson, S. A. Plasma gastrin and gastric acid responses to sham feeding and feeding in dogs. *Gastroenterology* **63**, 51–59 (1972).

78. Feldman, M., Richardson, C. T., Taylor, I. L. & Walsh, J. H. Effect of Atropine on Vagal Release of Gastrin and Pancreatic Polypeptide. *J. Clin. Invest.* **63**, 294–298 (1979).

79. Finkleman, B. On the nature of inhibition in the intestine. *J. Physiol.* **70**, 145–157 (1930).

80. Macrae, I. M., Furness, J. B. & Costa, M. Distribution of subgroups of noradrenaline neurons in the coeliac ganglion of the guinea-pig. *Cell Tissue Res.* **244**, (1986).

81. Costa, M. & Furness, J. B. Somatostatin is present in a subpopulation of noradrenergic nerve fibres supplying the intestine. *Neuroscience* **13**, 911–919 (1984).

82. Dresel, P. & Wallentin, I. Effects of Sympathetic Vasoconstrictor Fibres, Noradrenaline and Vasopressin on the Intestinal Vascular Resistance during Constant Blood Flow or Blood Pressure. *Acta Physiol. Scand.* **66**, 427–436 (1966).

83. Furness, J. B. The adrenergic innervation of the vessels supplying and draining the gastrointestinal tract. *Z. F**r Zellforsch. Mikrosk. Anat.* **113**, 67–82 (1971).

84. Furness, J. B. *et al.* Distribution, pathways and reactions to drug treatment of nerves with neuropeptide Y- and pancreatic polypeptide-like immunoreactivity in the guinea-pig digestive tract. *Cell Tissue Res.* **234**, (1983).

85. Crowcroft, P. J., Holman, M. E. & Szurszewski, J. H. Excitatory input from the distal colon to the inferior mesenteric ganglion in the guinea-pig. *J. Physiol.* **219**, 443–461 (1971).

86. Dalsgaard, C.-J. *et al.* Origin of peptide-containing fibers in the inferior mesenteric ganglion of the guinea-pig: Immunohistochemical studies with antisera to substance P, enkephalin, vasoactive intestinal polypeptide, cholecystokinin and bombesin. *Neuroscience* **9**, 191–211 (1983).

87. Love, J. A. & Szurszewski, J. H. The electrophysiological effects of vasoactive intestinal polypeptide in the guinea-pig inferior mesenteric ganglion. *J. Physiol.* **394**, 67–84 (1987).

88. Ramón Y Cajal, S. *Histologie Du Système Nerveux de l'homme & Des Vertébrés*. (Maloine, Paris, 1909). doi:10.5962/bhl.title.48637.

89. Vannucchi, M. G. & Traini, C. Interstitial cells of Cajal and telocytes in the gut: twins, related or simply neighbor cells? *Biomol. Concepts* **7**, 93–102 (2016).

90. Radenkovic, G., Radenkovic, D. & Velickov, A. Development of interstitial cells of Cajal in the human digestive tract as the result of reciprocal induction of mesenchymal and neural crest cells. *J. Cell. Mol. Med.* **22**, 778–785 (2018).

91. Thuneberg, L. Interstitial cells of Cajal: intestinal pacemaker cells? *Adv. Anat. Embryol. Cell Biol.* **71**, 1–130 (1982).

92. Al-Shboul, O. A. The importance of interstitial cells of cajal in the gastrointestinal tract. *Saudi J. Gastroenterol. Off. J. Saudi Gastroenterol. Assoc.* **19**, 3–15 (2013).

93. Vannucchi, M. G. Receptors in interstitial cells of Cajal: identification and possible physiological roles. *Microsc. Res. Tech.* **47**, 325–335 (1999).

94. Hulzinga, J. D. *et al.* W/kit gene required for interstitial cells of Cajal and for intestinal pacemaker activity. *Nature* **373**, 347–349 (1995).

95. Huizinga, J. D., Hussain, A. & Chen, J.-H. Interstitial cells of Cajal and human colon motility in health and disease. *Am. J. Physiol. Gastrointest. Liver Physiol.* **321**, G552–G575 (2021).

96. Faussone-Pellegrini, M. S. & Thuneberg, L. Guide to the identification of interstitial cells of Cajal. *Microsc. Res. Tech.* **47**, 248–266 (1999).

97. Faussone-Pellegrini, M.-S., Vannucchi, M.-G., Ledder, O., Huang, T.-Y. & Hanani, M. Plasticity of interstitial cells of Cajal: a study of mouse colon. *Cell Tissue Res.* **325**, 211–217 (2006).

98. Komuro, T. Comparative morphology of interstitial cells of Cajal: ultrastructural characterization. *Microsc. Res. Tech.* **47**, 267–285 (1999).

99. Gomez-Pinilla, P. J. *et al.* Ano1 is a selective marker of interstitial cells of Cajal in the human and mouse gastrointestinal tract. *Am. J. Physiol.-Gastrointest. Liver Physiol.* **296**, G1370–G1381 (2009).

100. Yoneda, S., Takano, H., Takaki, M. & Suzuki, H. Properties of spontaneously active cells distributed in the submucosal layer of mouse proximal colon. *J. Physiol.* **542**, 887–897 (2002).

101. Koh, S. D., Sanders, K. M. & Ward, S. M. Spontaneous electrical rhythmicity in cultured interstitial cells of cajal from the murine small intestine. *J. Physiol.* **513 (Pt 1)**, 203–213 (1998).

102. Thomson, L. *et al.* Interstitial cells of Cajal generate a rhythmic pacemaker current. *Nat. Med.* **4**, 848–851 (1998).

103. Huizinga, J. D., Zhu, Y., Ye, J. & Molleman, A. High-conductance chloride channels generate pacemaker currents in interstitial cells of Cajal. *Gastroenterology* **123**, 1627–1636 (2002).

104. Zhu, M. H. *et al.* A Ca(2+)-activated Cl(-) conductance in interstitial cells of Cajal linked to slow wave currents and pacemaker activity. *J. Physiol.* **587**, 4905–4918 (2009).

105. Yang, Y. D. *et al.* TMEM16A confers receptor-activated calcium-dependent chloride conductance. *Nature* **455**, 1210–1215 (2008).

106. Hwang, S. J. *et al.* Expression of anoctamin 1/TMEM16A by interstitial cells of Cajal is fundamental for slow wave activity in gastrointestinal muscles. *J. Physiol.* **587**, 4887–4904 (2009).

107. Plujà, L. *et al.* Evidence supporting presence of two pacemakers in rat colon. *Am. J. Physiol. Gastrointest. Liver Physiol.* **281**, G255-266 (2001).

108. Wright, G. W. J. *et al.* Cholinergic signalling-regulated KV7.5 currents are expressed in colonic ICC-IM but not ICC-MP. *Pflugers Arch.* **466**, 1805–1818 (2014).

109. Yoneda, S., Fukui, H. & Takaki, M. Pacemaker activity from submucosal interstitial cells of Cajal drives high-frequency and low-amplitude circular muscle contractions in the mouse proximal colon. *Neurogastroenterol. Motil.* **16**, 621–627 (2004).

110. Lies, B. *et al.* Nitrergic signalling via interstitial cells of Cajal regulates motor activity in murine colon. *J. Physiol.* **593**, 4589–4601 (2015).

111. Yang, S. *et al.* Persistent distention of colon damages interstitial cells of Cajal through Ca2+ -ERK-AP-1-miR-34c-SCF deregulation. *J. Cell. Mol. Med.* **21**, 1881–1892 (2017).

112. Bhat, A. A. *et al.* Tight Junction Proteins and Signaling Pathways in Cancer and Inflammation: A Functional Crosstalk. *Front. Physiol.* **9**, 1942 (2018).

113. Revel, J. P. & Karnovsky, M. J. HEXAGONAL ARRAY OF SUBUNITS IN INTERCELLULAR JUNCTIONS OF THE MOUSE HEART AND LIVER. *J. Cell Biol.* **33**, C7-12 (1967).

114. Goodenough, D. A. Bulk isolation of mouse hepatocyte gap junctions. Characterization of the principal protein, connexin. *J. Cell Biol.* **61**, 557–563 (1974).

115. Hansson, E. & Skiöldebrand, E. Low-grade inflammation causes gap junction-coupled cell dysfunction throughout the body, which can lead to the spread of systemic inflammation. *Scand. J. Pain* **19**, 639–649 (2019).

116. Totland, M. Z., Rasmussen, N. L., Knudsen, L. M. & Leithe, E. Regulation of gap junction intercellular communication by connexin ubiquitination: physiological and pathophysiological implications. *Cell. Mol. Life Sci. CMLS* **77**, 573–591 (2020).

117. Loewenstein, W. R. Junctional intercellular communication: the cell-to-cell membrane channel. *Physiol. Rev.* **61**, 829–913 (1981).

118. Lauf, U. *et al.* Dynamic trafficking and delivery of connexons to the plasma membrane and accretion to gap junctions in living cells. *Proc. Natl. Acad. Sci. U. S. A.* **99**, 10446–10451 (2002).

119. Wong, J. *et al.* The Role of Connexins in Gastrointestinal Diseases. *J. Mol. Biol.* **431**, 643–652 (2019).

120. Garfield, R. E., Sims, S. & Daniel, E. E. Gap Junctions: Their Presence and Necessity in Myometrium During Parturition. *Science* **198**, 958–960 (1977).

121. Garfield, R. E., Sims, S. M., Kannan, M. S. & Daniel, E. E. Possible role of gap junctions in activation of myometrium during parturition. *Am. J. Physiol.-Cell Physiol.* **235**, C168–C179 (1978).

122. Willebrords, J. *et al.* Connexins and their channels in inflammation. *Crit. Rev. Biochem. Mol. Biol.* **51**, 413–439 (2016).

123. Nielsen, M. S. *et al.* Gap Junctions. in *Comprehensive Physiology* (ed. Prakash, Y. S.) 1981–2035 (Wiley, 2012). doi:10.1002/cphy.c110051.

124. Leithe, E., Mesnil, M. & Aasen, T. The connexin 43 C-terminus: A tail of many tales. *Biochim. Biophys. Acta BBA - Biomembr.* **1860**, 48–64 (2018).

125. Liu, L. W. C., Farraway, L., Berezin, I. & Huizinga, J. D. Interstitial cells of Cajal: mediators of communication between circular and longitudinal muscle layers of canine colon. *Cell Tissue Res.* **294**, 69–79 (1998).

126. Katturajan, R. & Evan Prince, S. A role of connexin 43 on the drug-induced liver, kidney, and gastrointestinal tract toxicity with associated signaling pathways. *Life Sci.* **280**, 119629 (2021).

127. Döring, B. *et al.* Ablation of connexin43 in smooth muscle cells of the mouse intestine: functional insights into physiology and morphology. *Cell Tissue Res.* **327**, 333–342 (2007).

128. Matsuuchi, L. & Naus, C. C. Gap junction proteins on the move: Connexins, the cytoskeleton and migration. *Biochim. Biophys. Acta BBA - Biomembr.* **1828**, 94–108 (2013).

129. Francis, R. *et al.* Connexin43 modulates cell polarity and directional cell migration by regulating microtubule dynamics. *PloS One* **6**, e26379 (2011).

130. Maes, M., Cogliati, B., Crespo Yanguas, S., Willebrords, J. & Vinken, M. Roles of connexins and pannexins in digestive homeostasis. *Cell. Mol. Life Sci. CMLS* **72**, 2809–2821 (2015).

131. Giaroni, C., De Ponti, F., Cosentino, M., Lecchini, S. & Frigo, G. Plasticity in the enteric nervous system. *Gastroenterology* **117**, 1438–1458 (1999).

132. Lomax, A. E., Fernández, E. & Sharkey, K. A. Plasticity of the enteric nervous system during intestinal inflammation. *Neurogastroenterol. Motil.* **17**, 4–15 (2005).

133. Leithe, E., Mesnil, M. & Aasen, T. The connexin 43 C-terminus: A tail of many tales. *Biochim. Biophys. Acta BBA - Biomembr.* **1860**, 48–64 (2018).

134. User, S. Chemioterapia. *ISSalute* https://www.issalute.it/index.php/la-salute-dalla-a-alla-z-menu/c/chemioterapia (2018).

135. Makin, G. Principles of chemotherapy. *Paediatr. Child Health* **28**, 183–188 (2018).

136. Carelle, N. *et al.* Changing patient perceptions of the side effects of cancer chemotherapy. *Cancer* **95**, 155–163 (2002).

137. Di Fiore, F. & Van Cutsem, E. Acute and long-term gastrointestinal consequences of chemotherapy. *Best Pract. Res. Clin. Gastroenterol.* **23**, 113–124 (2009).

138. Vasko, M. R., Shariati, B. & Zanville, N. The role of DNA damage and repair in toxicity to postmitotic cells caused by cancer therapies. in *DNA Repair in Cancer Therapy* 383–428 (Elsevier, 2016). doi:10.1016/B978-0-12-803582-5.00013-9.

139. Rosenberg, B., Vancamp, L., Trosko, J. E. & Mansour, V. H. Platinum Compounds: a New Class of Potent Antitumour Agents. *Nature* **222**, 385–386 (1969).

140. Rosenberg, B. & VanCamp, L. The successful regression of large solid sarcoma 180 tumors by platinum compounds. *Cancer Res.* **30**, 1799–1802 (1970).

141. Rosenberg, B. Platinum coordination complexes in cancer chemotherapy. *Naturwissenschaften* **60**, 399–406 (1973).

142. Varbanov, H. P., Kuttler, F., Banfi, D., Turcatti, G. & Dyson, P. J. Screening-based approach to discover effective platinum-based chemotherapies for cancers with poor prognosis. *PLOS ONE* **14**, e0211268 (2019).

143. Valentová, J. & Lintnerová, L. Chirality in Anticancer Agents. in *Current Topics in Chirality - From Chemistry to Biology* (ed. Akitsu, T.) (IntechOpen, 2021). doi:10.5772/intechopen.98977.

144. Tsvetkova, D. & Ivanova, S. Application of Approved Cisplatin Derivatives in Combination Therapy against Different Cancer Diseases. *Mol. Basel Switz.* **27**, 2466 (2022).

145. Wang, Z. & Zhu, G. DNA Damage Repair Pathways and Repair of Cisplatin-Induced DNA Damage. in *Reference Module in Chemistry, Molecular Sciences and Chemical Engineering* B9780124095472142519 (Elsevier, 2018). doi:10.1016/B978-0-12-409547-2.14251-9.

146. Zhang, C., Xu, C., Gao, X. & Yao, Q. Platinum-based drugs for cancer therapy and anti-tumor strategies. *Theranostics* **12**, 2115–2132 (2022).

147. Dasari, S. & Bernard Tchounwou, P. Cisplatin in cancer therapy: Molecular mechanisms of action. *Eur. J. Pharmacol.* **740**, 364–378 (2014).

148. Shen, D.-W., Pouliot, L. M., Hall, M. D. & Gottesman, M. M. Cisplatin Resistance: A Cellular Self-Defense Mechanism Resulting from Multiple Epigenetic and Genetic Changes. *Pharmacol. Rev.* **64**, 706–721 (2012).

149. Florea, A.-M. & Büsselberg, D. Cisplatin as an Anti-Tumor Drug: Cellular Mechanisms of Activity, Drug Resistance and Induced Side Effects. *Cancers* **3**, 1351–1371 (2011).

150. Wang, D. & Lippard, S. J. Cellular processing of platinum anticancer drugs. *Nat. Rev. Drug Discov.* **4**, 307–320 (2005).

151. Fuertes, M., Castilla, J., Alonso, C. & Pérez, J. Cisplatin Biochemical Mechanism of Action: From Cytotoxicity to Induction of Cell Death Through Interconnections Between Apoptotic and Necrotic Pathways. *Curr. Med. Chem.* **10**, 257–266 (2003).

152. Kanat, O., Ertas, H. & Caner, B. Platinum-induced neurotoxicity: A review of possible mechanisms. *World J. Clin. Oncol.* **8**, 329 (2017).

153. Chen, H. H. W. & Kuo, M. T. Role of Glutathione in the Regulation of Cisplatin Resistance in Cancer Chemotherapy. *Met.-Based Drugs* **2010**, 1–7 (2010).

154. Chirino, Y. I. & Pedraza-Chaverri, J. Role of oxidative and nitrosative stress in cisplatin-induced nephrotoxicity. *Exp. Toxicol. Pathol.* **61**, 223–242 (2009).

155. Galanski, M. S. Recent Developments in the Field of Anticancer Platinum Complexes. *Recent Patents Anticancer Drug Discov.* **1**, 285–295 (2006).

156. Ciarimboli, G. Anticancer Platinum Drugs Update. *Biomolecules* **11**, 1637 (2021).

157. Santosa, D. *et al.* Serotonin Levels and Chemotherapy-Induced Nausea and Vomiting in Cancer Patients: A Cross-Sectional Study. *Asian Pac. J. Cancer Prev.* **25**, 3263–3267 (2024).

158. McQuade, R. M., Bornstein, J. C. & Nurgali, K. Anti-Colorectal Cancer Chemotherapy-Induced Diarrhoea: Current Treatments and Side-Effects. *Int. J. Clin. Med.* **05**, 393–406 (2014).

159. Stojanovska, V., Sakkal, S. & Nurgali, K. Platinum-based chemotherapy: gastrointestinal immunomodulation and enteric nervous system toxicity. *Am. J. Physiol.-Gastrointest. Liver Physiol.* **308**, G223–G232 (2015).

160. Yamamoto, H., Ishihara, K., Takeda, Y., Koizumi, W. & Ichikawa, T. Changes in the Mucus Barrier during Cisplatin-Induced Intestinal Mucositis in Rats. *BioMed Res. Int.* **2013**, 1–8 (2013).

161. Cabezos, P. A., Vera, G., Martín-fontelles, M. I., Fernández-pujol, R. & Abalo, R. Cisplatin-induced gastrointestinal dysmotility is aggravated after chronic administration in the rat. Comparison with pica: Chronic cisplatin and gastrointestinal motility. *Neurogastroenterol. Motil.* **22**, 797-e225 (2010).

162. Vera, G. *et al.* Enteric neuropathy evoked by repeated cisplatin in the rat: Cisplatin and enteric neuropathy. *Neurogastroenterol. Motil.* **23**, 370-e163 (2011).

163. Wafai, L. *et al.* Effects of oxaliplatin on mouse myenteric neurons and colonic motility. *Front. Neurosci.* **7**, (2013).

164. Uranga, J. A. *et al.* Alterations in the small intestinal wall and motor function after repeated cisplatin in rat. *Neurogastroenterol. Motil.* **29**, e13047 (2017).

165. Stojanovska, V., McQuade, R. M., Miller, S. & Nurgali, K. Effects of Oxaliplatin Treatment on the Myenteric Plexus Innervation and Glia in the Murine Distal Colon. *J. Histochem. Cytochem.* **66**, 723–736 (2018).

166. McQuade, R. M., Stojanovska, V., Bornstein, J. C. & Nurgali, K. PARP inhibition in platinum-based chemotherapy: Chemopotentiation and neuroprotection. *Pharmacol. Res.* **137**, 104–113 (2018).

167. Pini, A. *et al.* Glucagon-like peptide 2 counteracts the mucosal damage and the neuropathy induced by chronic treatment with cisplatin in the mouse gastric fundus. *Neurogastroenterol. Motil.* **28**, 206–216 (2016).

168. Nardini, P. *et al.* GLP-2 Prevents Neuronal and Glial Changes in the Distal Colon of Mice Chronically Treated with Cisplatin. *Int. J. Mol. Sci.* **21**, 8875 (2020).

169. Perše, M. Cisplatin Mouse Models: Treatment, Toxicity and Translatability. *Biomedicines* **9**, 1406 (2021).

170. Brestoff, J. R. & Artis, D. Commensal bacteria at the interface of host metabolism and the immune system. *Nat. Immunol.* **14**, 676–684 (2013).

171. Zheng, D., Liwinski, T. & Elinav, E. Interaction between microbiota and immunity in health and disease. *Cell Res.* **30**, 492–506 (2020).

172. Rinninella, E. *et al.* What is the Healthy Gut Microbiota Composition? A Changing Ecosystem across Age, Environment, Diet, and Diseases. *Microorganisms* **7**, 14 (2019).

173. Clemente, J. C., Ursell, L. K., Parfrey, L. W. & Knight, R. The impact of the gut microbiota on human health: an integrative view. *Cell* **148**, 1258–1270 (2012).

174. Jandhyala, S. M. *et al.* Role of the normal gut microbiota. *World J. Gastroenterol.* **21**, 8787–8803 (2015).

175. Ridaura, V. K. *et al.* Gut microbiota from twins discordant for obesity modulate metabolism in mice. *Science* **341**, 1241214 (2013).

176. Ley, R. E. *et al.* Obesity alters gut microbial ecology. *Proc. Natl. Acad. Sci.* **102**, 11070–11075 (2005).

177. Fu, J., Zheng, Y., Gao, Y. & Xu, W. Dietary Fiber Intake and Gut Microbiota in Human Health. *Microorganisms* **10**, 2507 (2022).

178. Cummings, J. H., Pomare, E. W., Branch, W. J., Naylor, C. P. & Macfarlane, G. T. Short chain fatty acids in human large intestine, portal, hepatic and venous blood. *Gut* **28**, 1221–1227 (1987).

179. Du, Y. *et al.* The Role of Short Chain Fatty Acids in Inflammation and Body Health. *Int. J. Mol. Sci.* **25**, 7379 (2024).

180. Agranyoni, O. *et al.* Gut microbiota determines the social behavior of mice and induces metabolic and inflammatory changes in their adipose tissue. *Npj Biofilms Microbiomes* **7**, 28 (2021).

181. Dempsey, E. & Corr, S. C. Lactobacillus spp. for Gastrointestinal Health: Current and Future Perspectives. *Front. Immunol.* **13**, 840245 (2022).

182. Mu, Q. *et al.* Control of lupus nephritis by changes of gut microbiota. *Microbiome* **5**, 73 (2017).

183. Sokol, H. *et al.* Faecalibacterium prausnitzii is an anti-inflammatory commensal bacterium identified by gut microbiota analysis of Crohn disease patients. *Proc. Natl. Acad. Sci. U. S. A.* **105**, 16731–16736 (2008).

184. Stanaszek, P. M., Snell, J. F. & O'Neill, J. J. Isolation, extraction, and measurement of acetylcholine from Lactobacillus plantarum. *Appl. Environ. Microbiol.* **34**, 237–239 (1977).

185. Mazmanian, S. K., Round, J. L. & Kasper, D. L. A microbial symbiosis factor prevents intestinal inflammatory disease. *Nature* **453**, 620–625 (2008).

186. Tan, S. *et al.* Interaction between the gut microbiota and colonic enteroendocrine cells regulates host metabolism. *Nat. Metab.* **6**, 1076–1091 (2024).

187. Stojanov, S., Berlec, A. & Štrukelj, B. The Influence of Probiotics on the Firmicutes/Bacteroidetes Ratio in the Treatment of Obesity and Inflammatory Bowel disease. *Microorganisms* **8**, 1715 (2020).

188. Guo, J. *et al.* Characteristics of gut microbiota in representative mice strains: Implications for biological research. *Anim. Models Exp. Med.* **5**, 337–349 (2022).

189. Montassier, E. *et al.* 16S rRNA Gene Pyrosequencing Reveals Shift in Patient Faecal Microbiota During High-Dose Chemotherapy as Conditioning Regimen for Bone Marrow Transplantation. *Microb. Ecol.* **67**, 690–699 (2014).

190. Alsholi, D. M. *et al.* Lactobacillus rhamnosus Attenuates Cisplatin-Induced Intestinal Mucositis in Mice via Modulating the Gut Microbiota and Improving Intestinal Inflammation. *Pathogens* **12**, 1340 (2023).

191. Gong, S. *et al.* Gut microbiota accelerates cisplatin-induced acute liver injury associated with robust inflammation and oxidative stress in mice. *J. Transl. Med.* **19**, 147 (2021).

192. Hsiao, Y.-P. *et al.* Administration of Lactobacillus reuteri Combined with Clostridium butyricum Attenuates Cisplatin-Induced Renal Damage by Gut Microbiota Reconstitution, Increasing Butyric Acid Production, and Suppressing Renal Inflammation. *Nutrients* **13**, 2792 (2021).

193. Chambers, L. M. *et al.* Disruption of the Gut Microbiota Confers Cisplatin Resistance in Epithelial Ovarian Cancer. *Cancer Res.* **82**, 4654–4669 (2022).

194. Myhrstad, M. C. W., Tunsjø, H., Charnock, C. & Telle-Hansen, V. H. Dietary Fiber, Gut Microbiota, and Metabolic Regulation-Current Status in Human Randomized Trials. *Nutrients* **12**, 859 (2020).

195. Gibson, G. R. & Roberfroid, M. B. Dietary modulation of the human colonic microbiota: introducing the concept of prebiotics. *J. Nutr.* **125**, 1401–1412 (1995).

196. World Gastroenterology Organisation (WGO). *World Gastroenterology Organisation (WGO)* https://www.worldgastroenterology.org.

197. Mishra, P. *et al.* Prebiotics: Ignored player in the fight against cancer. *Cancer Rep.* **6**, e1870 (2023).

198. Li, Y. *et al.* Prebiotic-Induced Anti-tumor Immunity Attenuates Tumor Growth. *Cell Rep.* **30**, 1753-1766.e6 (2020).

199. Hamilton, A. M. *et al.* Diet-microbiome interactions promote enteric nervous system resilience following spinal cord injury. *Npj Biofilms Microbiomes* **10**, 75 (2024).

200. Nicholson, J. K. *et al.* Host-gut microbiota metabolic interactions. *Science* **336**, 1262–1267 (2012).

201. Heaney, L. M. Applying mass spectrometry-based assays to explore gut microbial metabolism and associations with disease. *Clin. Chem. Lab. Med. CCLM* **58**, 719–732 (2020).

202. Dalile, B., Van Oudenhove, L., Vervliet, B. & Verbeke, K. The role of short-chain fatty acids in microbiota–gut–brain communication. *Nat. Rev. Gastroenterol. Hepatol.* **16**, 461–478 (2019).

203. Mirzaei, R. *et al.* Role of microbiota-derived short-chain fatty acids in nervous system disorders. *Biomed. Pharmacother.* **139**, 111661 (2021).

204. Nøhr, M. K. *et al.* GPR41/FFAR3 and GPR43/FFAR2 as Cosensors for Short-Chain Fatty Acids in Enteroendocrine Cells vs FFAR3 in Enteric Neurons and FFAR2 in Enteric Leukocytes. *Endocrinology* **154**, 3552–3564 (2013).

205. Reigstad, C. S. *et al.* Gut microbes promote colonic serotonin production through an effect of short-chain fatty acids on enterochromaffin cells. *FASEB J.* **29**, 1395–1403 (2015).

206. Yano, J. M. *et al.* Indigenous Bacteria from the Gut Microbiota Regulate Host Serotonin Biosynthesis. *Cell* **161**, 264–276 (2015).

207. Tang, Y., Chen, Y., Jiang, H., Robbins, G. T. & Nie, D. G-protein-coupled receptor for short-chain fatty acids suppresses colon cancer. *Int. J. Cancer* **128**, 847–856 (2011).

208. Kobayashi, M. *et al.* A short-chain fatty acid, propionate, enhances the cytotoxic effect of cisplatin by modulating GPR41 signaling pathways in HepG2 cells. *Oncotarget* **9**, 31342–31354 (2018).

209. Oka, P. *et al.* Global prevalence of irritable bowel syndrome according to Rome III or IV criteria: a systematic review and meta-analysis. *Lancet Gastroenterol. Hepatol.* **5**, 908–917 (2020).

210. Barbara, G. *et al.* Italian guidelines for the management of irritable bowel syndrome. *Dig. Liver Dis.* **55**, 187–207 (2023).

211. Drossman, D. A. Functional Gastrointestinal Disorders: History, Pathophysiology, Clinical Features, and Rome IV. *Gastroenterology* **150**, 1262-1279.e2 (2016).

212. Moloney, R. D., O'Mahony, S. M., Dinan, T. G. & Cryan, J. F. Stress-induced visceral pain: toward animal models of irritable-bowel syndrome and associated comorbidities. *Front. Psychiatry* **6**, 15 (2015).

213. Zhang, Y.-Z. & Li, Y.-Y. Inflammatory bowel disease: pathogenesis. *World J. Gastroenterol.* **20**, 91–99 (2014).

214. Moloney, R. D., Desbonnet, L., Clarke, G., Dinan, T. G. & Cryan, J. F. The microbiome: stress, health and disease. *Mamm. Genome* **25**, 49–74 (2014).

215. Zhuang, X., Xiong, L., Li, L., Li, M. & Chen, M. Alterations of gut microbiota in patients with irritable bowel syndrome: A systematic review and meta-analysis. *J. Gastroenterol. Hepatol.* **32**, 28–38 (2017).

216. Fond, G. *et al.* Anxiety and depression comorbidities in irritable bowel syndrome (IBS): a systematic review and meta-analysis. *Eur. Arch. Psychiatry Clin. Neurosci.* **264**, 651–660 (2014).

217. Evangelista, S., Cochet, P., Bromet, N., Criscuoli, M. & Maggi, C. A. A distribution study with (14)C-otilonium bromide in the rat: evidence for selective tropism for large intestine after oral administration. *Drug Metab. Dispos. Biol. Fate Chem.* **28**, 643–647 (2000).

218. Annaházi, A., Róka, R., Rosztóczy, A. & Wittmann, T. Role of antispasmodics in the treatment of irritable bowel syndrome. *World J. Gastroenterol.* **20**, 6031–6043 (2014).

219. Traini, C. *et al.* Chronic treatment with otilonium bromide induces changes in L-type Ca^{2+} channel, tachykinins, and nitric oxide synthase expression in rat colon muscle coat. *Neurogastroenterol. Motil.* **25**, (2013).

220. Traini, C., Evangelista, S., Girod, V., Faussone-Pellegrini, M. S. & Vannucchi, M. G. Changes of excitatory and inhibitory neurotransmitters in the colon of rats underwent to the wrap partial restraint stress. *Neurogastroenterol. Motil.* **28**, 1172–1185 (2016).

221. Evangelista, S., Traini, C. & Vannucchi, M. G. Otilonium Bromide: A Drug with a Complex Mechanism of Action. *Curr. Pharm. Des.* **24**, 1772–1779 (2018).

222. Traini, C. *et al.* Otilonium Bromide treatment prevents nitrergic functional and morphological changes caused by chronic stress in the distal colon of a rat IBS model. *J. Cell. Mol. Med.* **25**, 6988–7000 (2021).

223. Cipriani, G. *et al.* Changes in nitrergic and tachykininergic pathways in rat proximal colon in response to chronic treatment with otilonium bromide. *Neurogastroenterol. Motil.* **27**, 997–1009 (2015).

224. Traini, C., Evangelista, S., Girod, V., Faussone-Pellegrini, M. S. & Vannucchi, M. G. Repeated otilonium bromide administration prevents neurotransmitter changes in colon of rats underwent to wrap restraint stress. *J. Cell. Mol. Med.* **21**, 735–745 (2017).

225. Zhou, L. *et al.* Repurposing Antispasmodic Agent Otilonium Bromide for Treatment of Staphylococcus aureus Infections. *Front. Microbiol.* **11**, 1720 (2020).

226. Vannucchi, M. & Evangelista, S. Experimental Models of Irritable Bowel Syndrome and the Role of the Enteric Neurotransmission. *J. Clin. Med.* **7**, 4 (2018).

227. Catalioto, R.-M. *et al.* Increased paracellular absorption by bile salts and P-glycoprotein stimulated efflux of otilonium bromide in Caco-2 cells monolayers as a model of intestinal barrier. *J. Pharm. Sci.* **97**, 4087–4100 (2008).

228. Schneider, K. M. *et al.* The enteric nervous system relays psychological stress to intestinal inflammation. *Cell* **186**, 2823-2838.e20 (2023).

229. Godoy, L. D., Rossignoli, M. T., Delfino-Pereira, P., Garcia-Cairasco, N. & De Lima Umeoka, E. H. A Comprehensive Overview on Stress Neurobiology: Basic Concepts and Clinical Implications. *Front. Behav. Neurosci.* **12**, 127 (2018).

230. Goldstein, D. S. Stress and the “extended” autonomic system. *Auton. Neurosci.* **236**, 102889 (2021).

231. Cohen, S., Kessler, R. C. & Gordon, L. U. Strategies for Measuring Stress in Studies of Psychiatric and Physical Disorders. in *Measuring Stress: A Guide for Health and Social Scientists* (eds. Cohen, S., Kessler, R. C. & Gordon, L. U.) 0 (Oxford University Press, 1995). doi:10.1093/oso/9780195086416.003.0001.

232. Goldstein, D. S. & Kopin, I. J. Evolution of concepts of stress. *Stress Amst. Neth.* **10**, 109–120 (2007).

233. Joyner, M. J. & Casey, D. P. Regulation of increased blood flow (hyperemia) to muscles during exercise: a hierarchy of competing physiological needs. *Physiol. Rev.* **95**, 549–601 (2015).

234. Bruno, D., Nierenberg, J. J., Ritchie, J. C., Lutz, M. W. & Pomara, N. Cerebrospinal fluid cortisol concentrations in healthy elderly are affected by both APOE and TOMM40 variants. *Psychoneuroendocrinology* **37**, 366–371 (2012).

235. Goldstein, D. S. Clinical assessment of sympathetic responses to stress. *Ann. N. Y. Acad. Sci.* **771**, 570–593 (1995).

236. Hendry, E. *et al.* Validity of mental and physical stress models. *Neurosci. Biobehav. Rev.* **158**, 105566 (2024).

237. Gao, X. *et al.* Chronic stress promotes colitis by disturbing the gut microbiota and triggering immune system response. *Proc. Natl. Acad. Sci.* **115**, (2018).

238. Simrén, M. *et al.* Cumulative Effects of Psychologic Distress, Visceral Hypersensitivity, and Abnormal Transit on Patient-reported Outcomes in Irritable Bowel Syndrome. *Gastroenterology* **157**, 391-402.e2 (2019).

239. Larauche, M., Mulak, A. & Taché, Y. Stress and visceral pain: from animal models to clinical therapies. *Exp. Neurol.* **233**, 49–67 (2012).

240. Barreau, F., Cartier, C., Ferrier, L., Fioramonti, J. & Bueno, L. Nerve growth factor mediates alterations of colonic sensitivity and mucosal barrier induced by neonatal stress in rats. *Gastroenterology* **127**, 524–534 (2004).

241. Cenac, N. *et al.* Role for protease activity in visceral pain in irritable bowel syndrome. *J. Clin. Invest.* **117**, 636–647 (2007).

242. Gold, M. S., Zhang, L., Wrigley, D. L. & Traub, R. J. Prostaglandin E_2 Modulates TTX-R I_{Na} in Rat Colonic Sensory Neurons. *J. Neurophysiol.* **88**, 1512–1522 (2002).

243. Balestra, B. *et al.* Colonic mucosal mediators from patients with irritable bowel syndrome excite enteric cholinergic motor neurons. *Neurogastroenterol. Motil.* **24**, 1118 (2012).

244. Meng, X., Bao, B. & Yue, G. Global research trends on maternal separation paradigms as an early life stress model: A bibliometric analysis. *Heliyon* **9**, e18469 (2023).

245. Bradesi, S. *et al.* Repeated exposure to water avoidance stress in rats: a new model for sustained visceral hyperalgesia. *Am. J. Physiol.-Gastrointest. Liver Physiol.* **289**, G42–G53 (2005).

246. Mulak, A., Larauche, M. & Taché, Y. Psychological Stress Induces Visceral Analgesic or Hyperalgesic Response in Rodents: A Role of Preconditions. in *Frontiers of Gastrointestinal Research* (eds. Filaretova, L. P. & Takeuchi, K.) vol. 30 106–114 (S. Karger AG, 2012).

247. Million, M. *et al.* CRF2 receptor activation prevents colorectal distension induced visceral pain and spinal ERK1/2 phosphorylation in rats. *Gut* **55**, 172–181 (2006).

248. Fukudo, S. Role of corticotropin-releasing hormone in irritable bowel syndrome and intestinal inflammation. *J. Gastroenterol.* **42 Suppl 17**, 48–51 (2007).

249. Taché, Y. & Brunnhuber, S. From Hans Selye's discovery of biological stress to the identification of corticotropin-releasing factor signaling pathways: implication in stress-related functional bowel diseases. *Ann. N. Y. Acad. Sci.* **1148**, 29–41 (2008).

250. Atkinson, W., Lockhart, S., Whorwell, P. J., Keevil, B. & Houghton, L. A. Altered 5-Hydroxytryptamine Signaling in Patients With Constipation- and Diarrhea-Predominant Irritable Bowel Syndrome. *Gastroenterology* **130**, 34–43 (2006).

251. Taguchi, R. *et al.* Selective corticotropin-releasing factor 1 receptor antagonist E2508 reduces restraint stress-induced defecation and visceral pain in rat models. *Psychoneuroendocrinology* **75**, 110–115 (2017).

252. Belkind-Gerson, J., Graeme-Cook, F. & Winter, H. Enteric Nervous System Disease and Recovery, Plasticity, and Regeneration. *J. Pediatr. Gastroenterol. Nutr.* **42**, 343–350 (2006).

253. Holland, A. M., Bon-Frauches, A. C., Keszthelyi, D., Melotte, V. & Boesmans, W. The enteric nervous system in gastrointestinal disease etiology. *Cell. Mol. Life Sci.* **78**, 4713–4733 (2021).

254. Gori, S. *et al.* Gut microbiota and cancer: How gut microbiota modulates activity, efficacy and toxicity of antitumoral therapy. *Crit. Rev. Oncol. Hematol.* **143**, 139–147 (2019).

255. Mayer, E. A. & Collins, S. M. Evolving pathophysiologic models of functional gastrointestinal disorders. *Gastroenterology* **122**, 2032–2048 (2002).

256. Crona, D. J. *et al.* A Systematic Review of Strategies to Prevent Cisplatin-Induced Nephrotoxicity. *The Oncologist* **22**, 609–619 (2017).

257. Mao, B. *et al.* In vitro fermentation of fructooligosaccharides with human gut bacteria. *Food Funct.* **6**, 947–954 (2015).

258. Kuo, S.-M., Chan, W.-C. & Hu, Z. Wild-Type and IL10-Null Mice Have Differential Colonic Epithelial Gene Expression Responses to Dietary Supplementation with Synbiotic Bifidobacterium animalis Subspecies lactis and Inulin. *J. Nutr.* **144**, 245–251 (2014).

259. Yamamoto, K., Matsunaga, S., Matsui, M., Takeda, N., & Yamatodani, A. Pica in mice as a new model for the study of emesis. *Methods Find. Exp. Clin. Pharmacol.* **24**, 135 (2002).

260. Squecco, R. *et al.* Relaxin Affects Smooth Muscle Biophysical Properties and Mechanical Activity of the Female Mouse Colon. *Endocrinology* **156**, 4398–4410 (2015).

261. O'Flaherty, S., Saulnier, D. M., Pot, B. & Versalovic, J. How can probiotics and prebiotics impact mucosal immunity? *Gut Microbes* **1**, 293–300 (2010).

262. Hardy, H., Harris, J., Lyon, E., Beal, J. & Foey, A. D. Probiotics, prebiotics and immunomodulation of gut mucosal defences: homeostasis and immunopathology. *Nutrients* **5**, 1869–1912 (2013).

263. Basnet, J., Eissa, M. A., Yanes Cardozo, L. L., Romero, D. G. & Rezq, S. Impact of Probiotics and Prebiotics on Gut Microbiome and Hormonal Regulation. *Gastrointest. Disord.* **6**, 801–815 (2024).

264. Traserra, S. *et al.* The asymmetric innervation of the circular and longitudinal muscle of the mouse colon differently modulates myogenic slow phasic contractions. *Neurogastroenterol. Motil.* **32**, e13778 (2020).

265. Costa, M. *et al.* Motor patterns in the proximal and distal mouse colon which underlie formation and propulsion of feces. *Neurogastroenterol. Motil.* **33**, e14098 (2021).

266. Chen, J.-H. *et al.* Neurogenic and Myogenic Properties of Pan-Colonic Motor Patterns and Their Spatiotemporal Organization in Rats. *PLoS ONE* **8**, e60474 (2013).

267. Hibberd, T. J. *et al.* Neurogenic and myogenic patterns of electrical activity in isolated intact mouse colon. *Neurogastroenterol. Motil.* **29**, 1–12 (2017).

268. Tu, L. *et al.* Insights Into Acute and Delayed Cisplatin-Induced Emesis From a Microelectrode Array, Radiotelemetry and Whole-Body Plethysmography Study of Suncus murinus (House Musk Shrew). *Front. Pharmacol.* **12**, 746053 (2021).

269. Nemeth, L., Maddur, S. & Puri, P. Immunolocalization of the gap junction protein Connexin43 in the interstitial cells of Cajal in the normal and Hirschsprung's disease bowel. *J. Pediatr. Surg.* **35**, 823–828 (2000).

270. Coyle, D. *et al.* Expression of connexin 26 and connexin 43 is reduced in Hirschsprung's disease. *J. Surg. Res.* **206**, 242–251 (2016).

271. Sun, T. *et al.* Aging-dependent decrease in the numbers of enteric neurons, interstitial cells of Cajal and expression of connexin43 in various regions of gastrointestinal tract. *Aging* **10**, 3851–3865 (2018).

272. Wei, J. *et al.* Effects of lipopolysaccharide-induced inflammation on the interstitial cells of Cajal. *Cell Tissue Res.* **356**, 29–37 (2014).

273. An, J. *et al.* Electroacupuncture reduces blood glucose by regulating intestinal flora in type 2 diabetic mice. *J. Diabetes* **14**, 695–710 (2022).

274. Guarino, M. *et al.* Mechanisms of Action of Prebiotics and Their Effects on Gastro-Intestinal Disorders in Adults. *Nutrients* **12**, 1037 (2020).

275. Pasqualetti, V. *et al.* Antioxidant Activity of Inulin and Its Role in the Prevention of Human Colonic Muscle Cell Impairment Induced by Lipopolysaccharide Mucosal Exposure. *PLoS ONE* **9**, e98031 (2014).

276. Hays, K. E., Pfaffinger, J. M. & Ryznar, R. The interplay between gut microbiota, short-chain fatty acids, and implications for host health and disease. *Gut Microbes* **16**, 2393270 (2024).

277. Ney, L.-M. *et al.* Short chain fatty acids: key regulators of the local and systemic immune response in inflammatory diseases and infections. *Open Biol.* **13**, 230014 (2023).

278. Mukhtar, K., Nawaz, H. & Abid, S. Functional gastrointestinal disorders and gut-brain axis: What does the future hold? *World J. Gastroenterol.* **25**, 552–566 (2019).

279. Bercik, P. The Brain-Gut-Microbiome Axis and Irritable Bowel Syndrome. *Gastroenterol. Hepatol.* **16**, 322–324 (2020).

280. He, C. *et al.* View from the Biological Property: Insight into the Functional Diversity and Complexity of the Gut Mucus. *Int. J. Mol. Sci.* **24**, 4227 (2023).

281. Casén, C. *et al.* Deviations in human gut microbiota: a novel diagnostic test for determining dysbiosis in patients with IBS or IBD. *Aliment. Pharmacol. Ther.* **42**, 71–83 (2015).

282. Simrén, M. *et al.* Intestinal microbiota in functional bowel disorders: a Rome foundation report. *Gut* **62**, 159–176 (2013).

283. Juge, N. Relationship between mucosa-associated gut microbiota and human diseases. *Biochem. Soc. Trans.* **50**, 1225–1236 (2022).

284. Lindqvist, S. *et al.* The colon-selective spasmolytic otilonium bromide inhibits muscarinic M_3 receptor-coupled calcium signals in isolated human colonic crypts. *Br. J. Pharmacol.* **137**, 1134–1142 (2002).

285. Gourcerol, G. *et al.* Activation of Corticotropin-Releasing Factor Receptor 2 Mediates the Colonic Motor Coping Response to Acute Stress in Rodents. *Gastroenterology* **140**, 1586-1596.e6 (2011).

286. Kim, K.-J. *et al.* Corticotropin-releasing factor stimulates colonic motility *via* muscarinic receptors in the rat. *World J. Gastroenterol.* **23**, 3825 (2017).

287. Bale, T. L. & Vale, W. W. CRF and CRF Receptors: Role in Stress Responsivity and Other Behaviors. *Annu. Rev. Pharmacol. Toxicol.* **44**, 525–557 (2004).

288. Buckley, M. M., O'Halloran, K. D., Rae, M. G., Dinan, T. G. & O'Malley, D. Modulation of enteric neurons by interleukin-6 and corticotropin-releasing factor contributes to visceral hypersensitivity and altered colonic motility in a rat model of irritable bowel syndrome. *J. Physiol.* **592**, 5235–5250 (2014).

289. Maillot, C., Million, M., Wei, J. Y., Gauthier, A. & Taché, Y. Peripheral corticotropin-releasing factor and stress-stimulated colonic motor activity involve type 1 receptor in rats. *Gastroenterology* **119**, 1569–1579 (2000).

290. Larauche, M. *et al.* Cortagine, a CRF_1 agonist, induces stresslike alterations of colonic function and visceral hypersensitivity in rodents primarily through peripheral pathways. *Am. J. Physiol.-Gastrointest. Liver Physiol.* **297**, G215–G227 (2009).

291. Liu, S. *et al.* Differential actions of urocortins on neurons of the myenteric division of the enteric nervous system in guinea pig distal colon. *Br. J. Pharmacol.* **159**, 222–236 (2010).

292. Yuan, P. -q., Million, M., Wu, S. V., Rivier, J. & Taché, Y. Peripheral corticotropin releasing factor (CRF) and a novel CRF_1 receptor agonist, $stressin_1$ -A activate CRF_1 receptor expressing cholinergic and nitrergic

myenteric neurons selectively in the colon of conscious rats. *Neurogastroenterol. Motil.* **19**, 923–936 (2007).

293. Krukoff, T. L. Expression of c-fos in studies of central autonomic and sensory systems. *Mol. Neurobiol.* **7**, 247–263 (1993).

294. Triantafillidis, J. & Malgarinos, G. Long-term efficacy and safety of otilonium bromide in the management of irritable bowel syndrome: a literature review. *Clin. Exp. Gastroenterol.* 75 (2014) doi:10.2147/CEG.S46291.

295. Xu, C. *et al.* Otilonium bromide boosts antimicrobial activities of colistin against Gram-negative pathogens and their persisters. *Commun. Biol.* **5**, 613 (2022).

296. Rychter, J. *et al.* Colonic smooth muscle cells and colonic motility patterns as a target for irritable bowel syndrome therapy: mechanisms of action of otilonium bromide. *Ther. Adv. Gastroenterol.* **7**, 156–166 (2014).

297. Evangelista, S. Benefits from Long-Term Treatment in Irritable Bowel Syndrome. *Gastroenterol. Res. Pract.* **2012**, 1–6 (2012).

298. Boeckxstaens, G., Clavé, P., Corazziari, E. S. & Tack, J. Irritable bowel syndrome: focus on otilonium bromide. *Expert Rev. Gastroenterol. Hepatol.* **8**, 131–137 (2014).